

APPENDIX B – LABORATORY TESTS AND INJECTION MATERIAL RECOMMENDATION

B.1 Summary

This Appendix presents all laboratory experiments on samples of fly ash and crushed dusty sand supplied by both Swanbank River Power Plant and Keller Batching plant at the Ipswich Motor Way Construction Site. Also included in this document are some relevant experimental results from previous CSIRO experience.

Factors influencing properties of slurry fills are: viscosity and consistency (flow-ability, inject-ability) determining pumping power, stiffness and strength (both under undrained and drained and consolidated conditions) determining material deformation over time and under different loading conditions, long term stability of deposited material, cohesive and non-cohesive behaviour when used with or without cement, liquefaction, sedimentation and deposition rate, erosion and dispersion due to water and dynamic loads, chemical reactions and interactions with other surrounding substances.

Theoretically, CSIRO have developed several models to back up and predict experimental results relevant to ground subsidence. In particular, predictive analytical models have been developed to calculate the required pump pressure both in the pipeline and in the mining induced void structure to be filled with slurry from a borehole. The backup theories corresponding to mine subsidence, fracture of strata and mechanics of grout slurries for backfilling mining voids and cracks are discussed extensively in Alehossein, et al. 2010, Alehossein, 2009a, 2009b. Known as the CSIRO optimum mine slurry mix, CSIRO Sample 6 represents a specific, optimum mix with small proportions of natural soil such as sand and clay in combination with small amount of cement and a significant proportions of either mine coal washery wastes, or fly ash and crushed dusts, as nominated here at Collingwood Park as the most economical materials to be used. There are comprehensive research reports containing detailed site investigations, monitoring, laboratory and field tests results together with design solutions pertinent to CSIRO's previous experience on slurry backfilling from a number of ACARP and industrial mining research projects by Shen et al, 2006, 2007, 2010 and Gua et al, 2005a,b, 2007.

To characterise and assess suitability of fly ash together with other mix materials for grout injection and backfilling design, the following laboratory tests were conducted at CSIRO laboratories on selected samples taken from the Swanbank River Power Plant and Ipswich Motor Way Site deposits.

- Size distribution for maximum, average and minimum sizes of solid particles
- Sedimentation for deposition time and velocity of floating particles
- Viscosity for grout flow-ability and pump pressure determination
- Grout test for simulation of field grout test at smaller scale
- Consolidation for grout compressibility and deformation measurement

- Strength for grout load bearing capacity measurement
- Pipe test for grout resistance in transportation pipelines
- Flow erosion test for grout resistance to water flow and erosion
- Mix designs for optimum grout design from a mixture of materials
- Grout model for grout fluid mechanical behaviour
- Chemical analysis for presence of toxic and hazardous elements
- UQ basic soil mechanics and flume flow tests (**Appendix C**)

B.2 Size Distribution by Hydrometer (UQ)

Size distribution tests were carried out to determine proportions of different sizes including the maximum, average and minimum sizes of solid particles of fly ash, crush dust, cement and cohesive mixtures. Two different, independent methods were used.

From CSIRO laser tests, size of fly ash particles at 50% passing, d_{50} , was measured to be about 30-40 μm , and from hydrometry, the UQ measurements showed a $d_{50} = 15 \mu\text{m}$, suggesting a banded curve envelope, rather than a single S curve of size distribution. Figure B-1 shows the range of particle size distribution curves obtained for the three drums of Swanbank fly ash initially sampled. The addition of dispersant (in accordance with the AS 1289 standard method) prior to sieving is seen to increase the fines content (silt and clay-size) by about 5% by mass. This is due to the washing of fines off the coarser particles. Dispersant was also added to the fines prior to hydrometer analysis, and this analysis indicated a higher fines content still (by about a further 5%), although some of this apparent increase may be due to hindered settling. Emerson crumb testing of all three replicates of all three drum samples gave an Emerson Class No. of 6 for all tests, indicating a medium potential for erosion. See **Appendix C** for complete UQ test report.

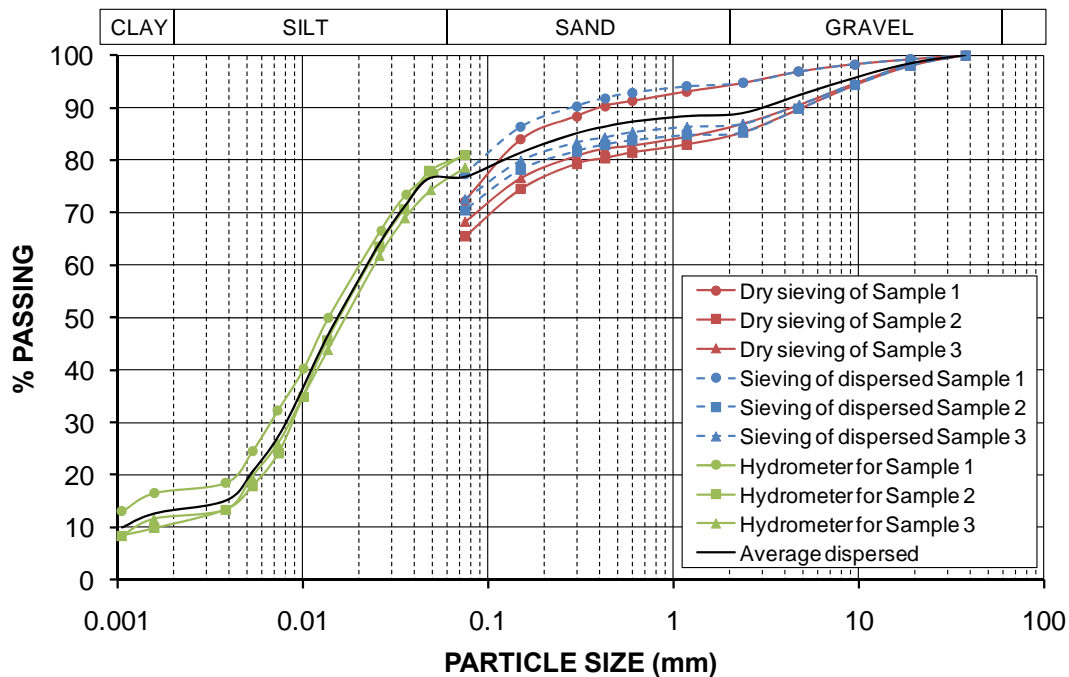


Figure B-1 Particle size distribution curves for Swanbank fly ash

B.3 Size Distribution by Laser

Particle size distribution tests were conducted on all possible components of non-cohesive (without cement) and cohesive (with cement) backfill slurry. A material behaves similar to silt when its size distribution is in the range of 2 – 60 μ , and it behaves similar to sand, when its size distribution is between 60 to 300 μ . In Australia the average size of fly ash particles at 50% passing, d_{50} , is about 30-40 μ . Similar to both silt and sand, fly ash has only friction without cohesion, and its friction angle in dry conditions is relatively large and approximately 40 degrees. Therefore, a mix of fly ash and water results in non-cohesive slurry.

Particle size distribution tests were conducted on all possible components of non-cohesive (without cement) and cohesive (with cement) backfill slurry. A material behaves similar to silt when its size distribution is in the range of 2 – 60 μ , and it behaves similar to sand, when its size distribution is between 60 to 300 μ . In Australia the average size of fly ash particles at 50% passing, d_{50} , is about 30-40 μ . Similar to both silt and sand, fly ash has only friction without cohesion, and its friction angle in dry conditions is relatively large and approximately 40 degrees. Therefore, a mix of fly ash and water results in non-cohesive slurry.

Mine coal waste rejects can be compared with fly ash and soils, which are categorised based on the size of their constituent particles or grains. In terms of size they are dominantly comparable with silt and sand. As shown in the table below, fly

ash is coarser than most of the coal waste fine particles, but smaller than sand and within comparable with the silt particle size.

- Gravel 2-60mm
- Sand 0.06-2mm Fly Ash (0.06-0.3mm); Coal Wash (0.06-1mm)
- Silt 0.002-0.06mm Fly Ash; Coal Wash (CW)
- Clay < 0.002mm Ultrafine Coal Wash (0.0005-0.002mm)
- Cement 0.0001-0.2 mm

At any given flow pressure and velocity, the flow resistance of a slurry depends highly on the shear or viscosity parameters of the slurry, which depend on the size distribution of the solid particles. All slurry component materials have been tested for both standard sieve and advanced Malvern laser diffraction particle size distribution analysis. General conclusions are listed below:

- The finer the slurry particles are, the less effort is normally required to pump such slurries through the pipeline and/or small holes and voids and gaps of the rock mass.
- The finer the slurry, the more compressible and deformable and the less is its bearing capacity to carry overburden load.
- As an exception, however, the Swanbank Fly Ash (FA) has the least compressibility among all the tested coal washery rejects, which has made it the most suitable slurry among all the individual fine and ultra fine slurries. In the absence of fly ash, any slurry solution has to be a multi-component mix design for a successful permanent grout injection operation.

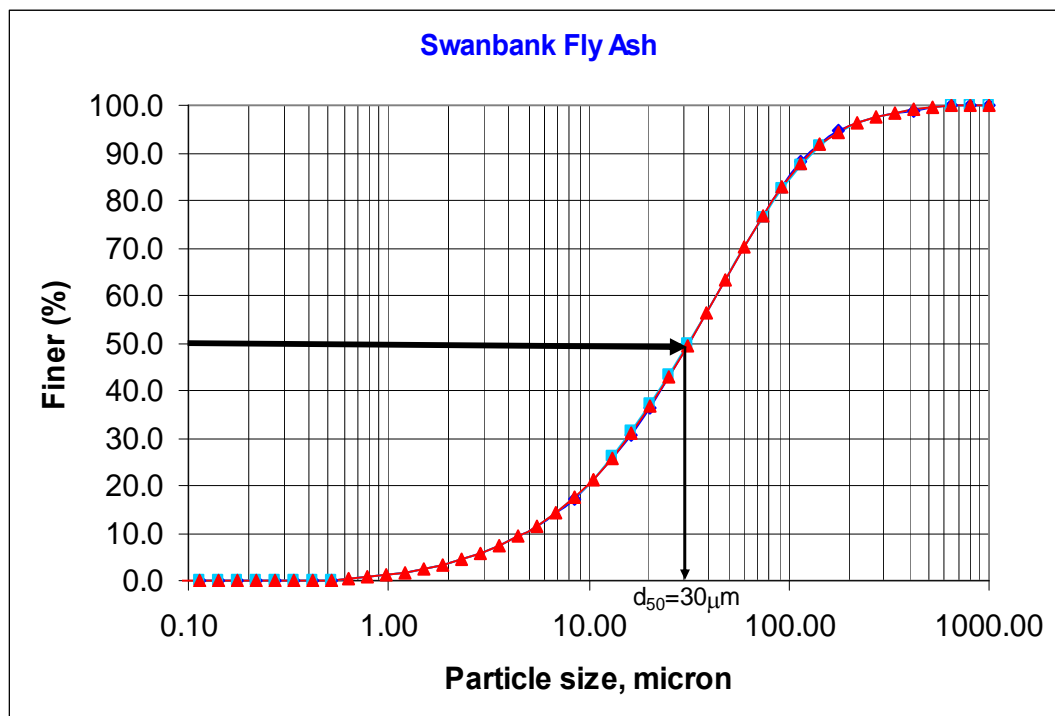


Figure B-2 Fly ash size distribution (% finer on vertical axis and size in micron on horizontal axis)

Figure B-2 presents size distribution of a typical sample of Swanbank fly-ash, conducted at the CSIRO minerals laboratory where $d_{50} = 30 \mu$. In these tests, a few representative samples, called sub samples, were taken from the initial representative sample and analysed. The resulting figure presents two almost identical size distribution graphs for the two sub samples and one for their average values.

Figure B-3 presents size distribution of a typical sample of Portland cement particles; Figure B-4 shows crushed dust size distribution and Figure B-5 presents size distribution of one of Keller's grout mixes used in the Ipswich Motor Way project. As shown in the figures, the average size, d_{50} , is 30 micron for FA, 20 for cement, 200 for crush dust which ahs dramatically reduced in the mix to 22 micron due to the dominant proportion of the fly ash and cement solution effect.

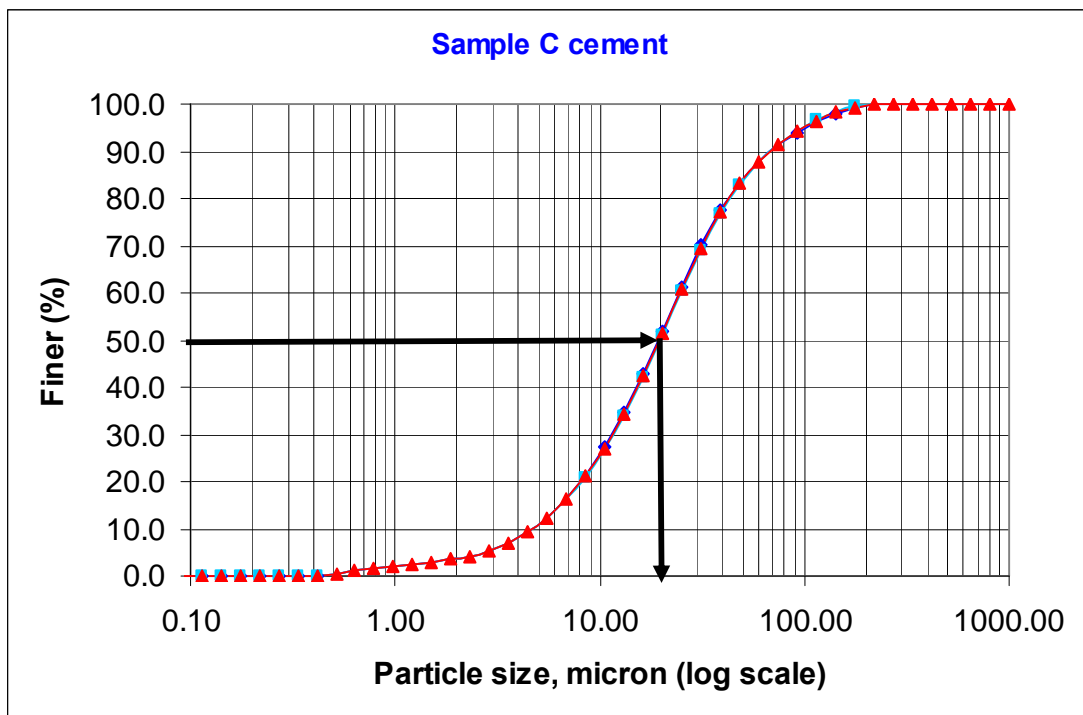


Figure B-3 Cement size distribution (% finer on vertical axis and size in micron on horizontal axis)

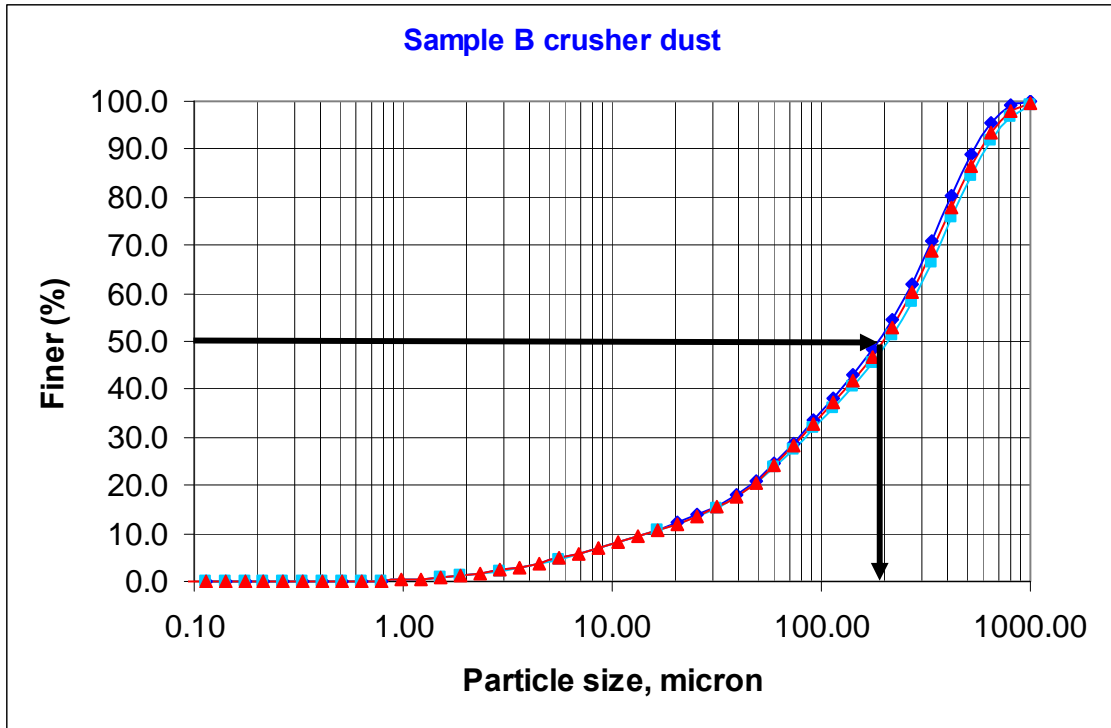


Figure B-4 Crusher dust size distribution (% finer on vertical axis and size in micron on horizontal axis)

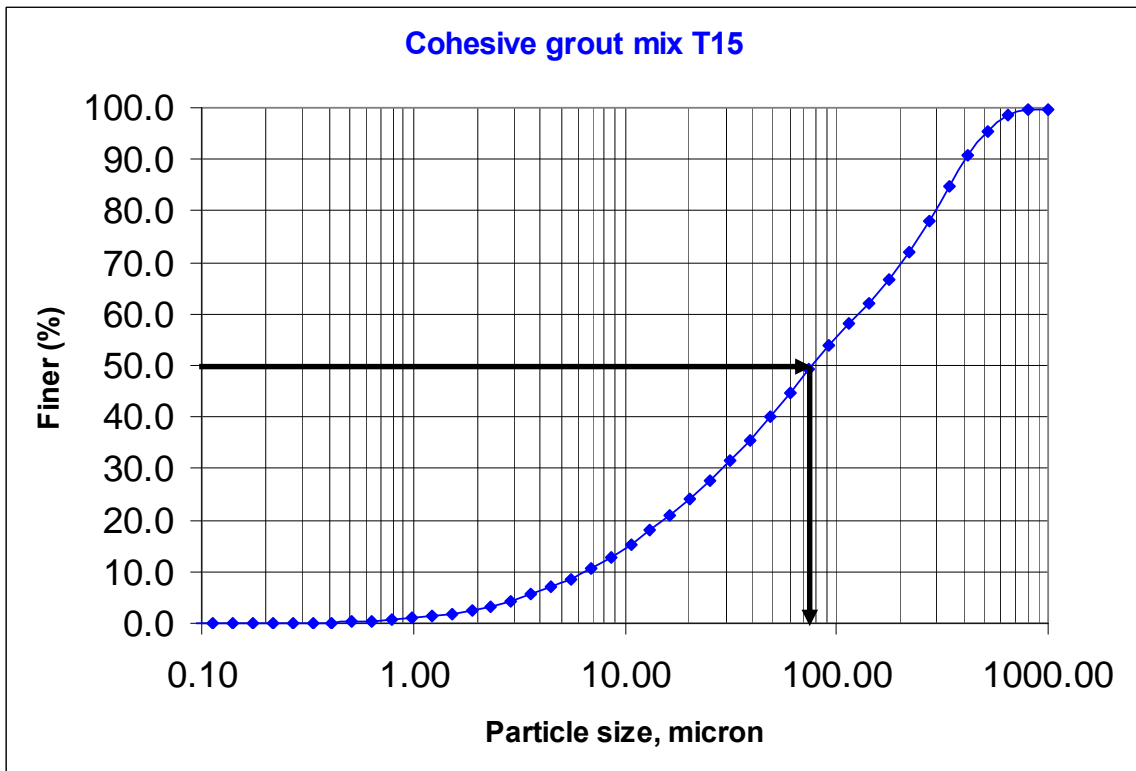


Figure B-5 Mix size distribution (% finer on vertical axis and size in micron on horizontal axis)

B.4 Sedimentation Tests by Glass Cups

Sedimentation or particle settlement tests are used to measure the rate of sedimentation or settlement of separately moving submerged solid particles filling the mining induced cracks to reduce further subsidence. A series of laboratory settlement experiments in normal glass cups were conducted to compare the rate of settlement for various material samples taken at different solids weight concentration. The theory behind the sedimentation or settlement of particles is illustrated in Figure B-6.

There are four distinct values of slurry velocity in relation to grout injection in the mining induced bed separated gaps. These are transportation pipe velocity, gap radial velocity, deposition velocity threshold, below which the solid particles separate from the carrier water and start to fall down under submerged gravity, and finally the terminal velocity. In the terminal velocity, the depositing particles reach their constant terminal velocity, as shown in Figure B-7. It is, however, of note that the future success of grout injection operation relies on the stiffness, strength, frictional integrity, durability and sustainability of these solid particles (Alehossein, 2009, Alehossein et al, 2010, Shen et al, 2010).

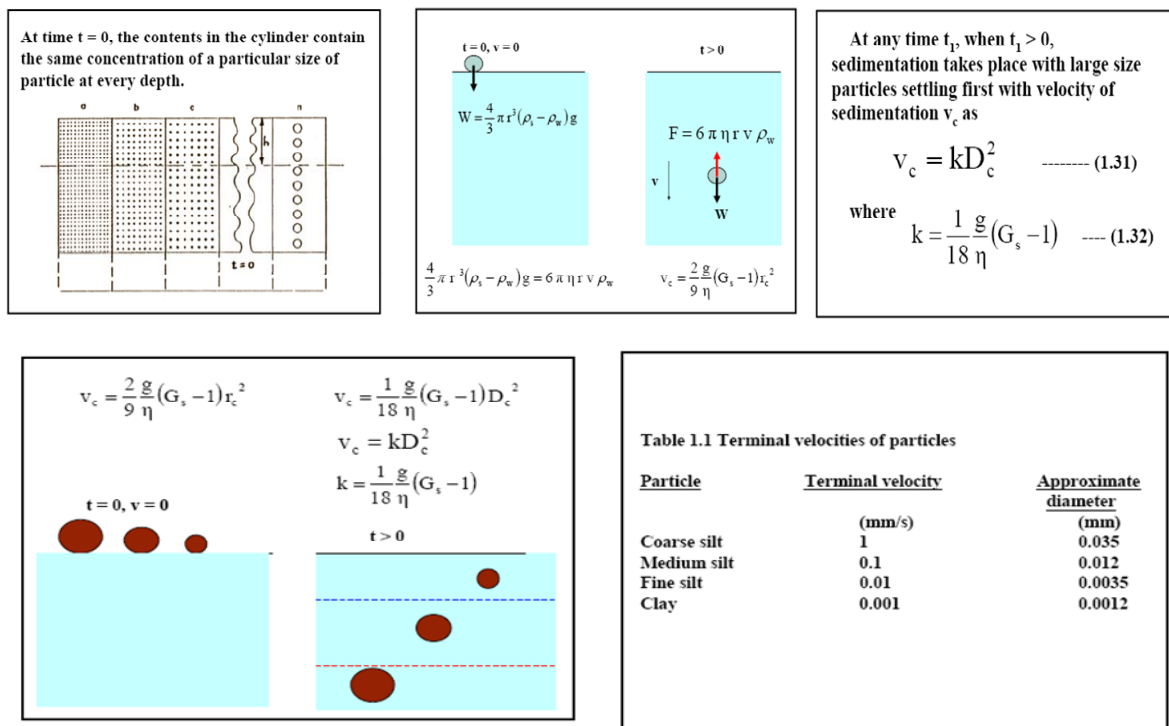


Figure B-6 Floating soil and coal wash/ash particles sediment due to gravity law and fluid limit speed principles (after Briaud, 2009). The terminal limit speed of most fine coal washery particles is in the range of 0.01-1mm/s

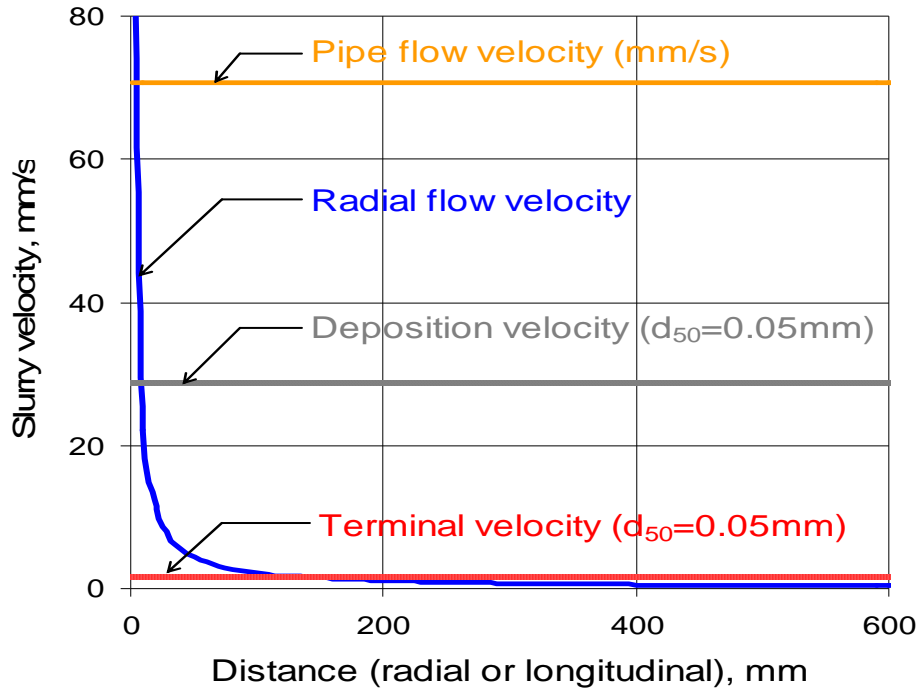


Figure B-7 An example of various velocities a grout is subjected to. Terminal (minimum), deposition, radial and pipe flow velocities for particles of average size of 50 μ .

Figure B-8 compares the total settlement and deposition of fly ash particles with other coal reject slurries just after 4 minutes at 50% solids weight concentration.

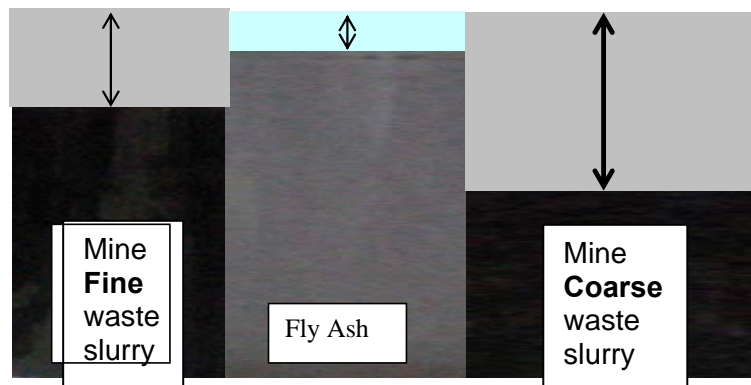


Figure B-8 Relative sedimentation or settlement comparisons of a fine mix (left), fly ash (middle) and a coarse mix (right) at 50% concentration - after 4 minutes

Figure B-9 shows glass cup settlement tests of fly ash samples at 50% (natural solids weight concentration), after few hours, and Figure B-10 shows the corresponding variation of settlement with time.

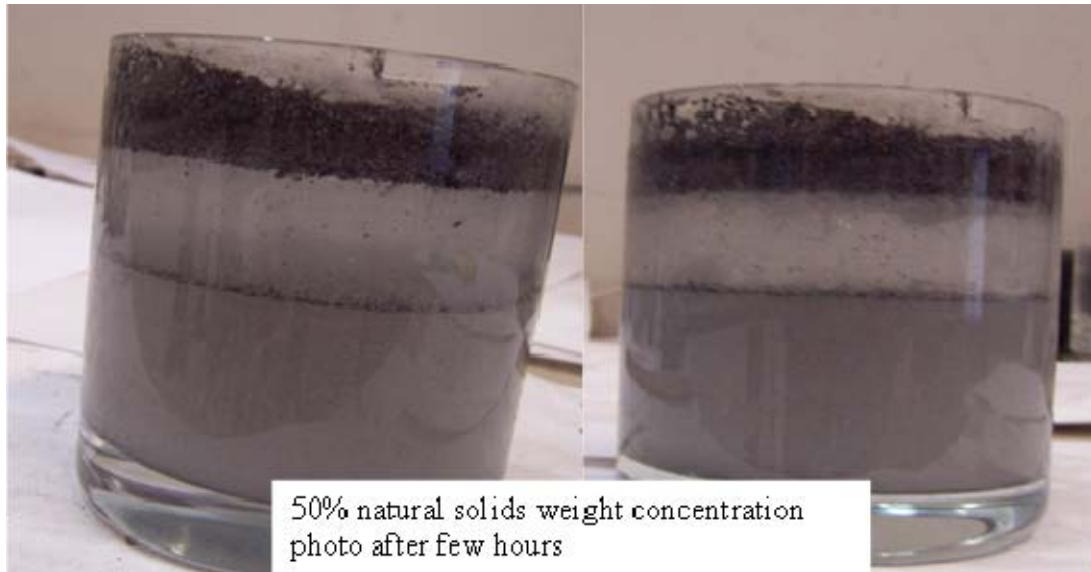


Figure B-9 Settlement test of Swanbank fly ash at 50% concentration after few hours

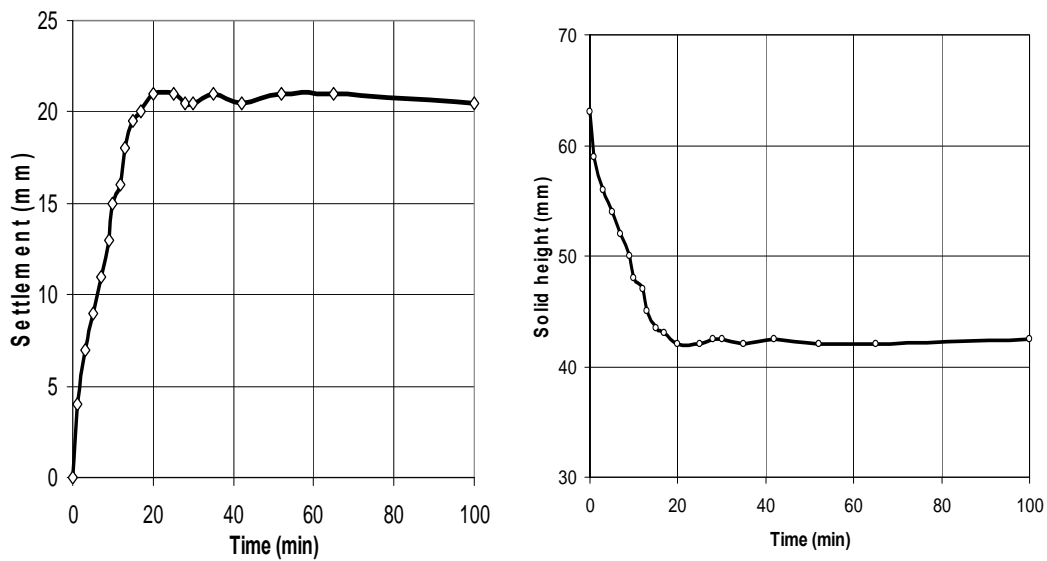


Figure B-10 Variation with time of the settlement or clear water height (left), or solid height (right) of the Swanbank fly ash at 50% natural solid concentration

B.5 Sedimentation Tests by Graded Buret (UQ)

The results of the settling column tests are presented in the form of Time and Log_{10} (Time) plots of height of solids, average % solids, average gravimetric moisture content, and average dry density, in Figure B-11 to Figure B-18, and the results are summarised in Table B-1.

Table B-1 Initial and final average % solids, gravimetric moisture content, dry density, and wet density on column settling of Swanbank fly ash from a slurry

% SOLIDS		GRAVIMETRIC MOISTURE CONTENT (%)		DRY DENSITY (g/cm ³)		WET DENSITY (g/cm ³)	
Initial	Final	Initial	Final	Initial	Final	Initial	Final
55	64.9	81.8	54.2	0.771	0.980	1.402	1.511
50	66.7	100.0	50.0	0.676	1.022	1.352	1.533
45	68.0	122.2	47.1	0.588	1.053	1.307	1.549
35	72.2	185.7	38.6	0.428	1.157	1.223	1.604

For all % solids tested (55%, 50%, 45%, and 35%), settling is complete within 150 to 300 minutes. The final % solids increases with decreasing initial % solids (64.9% solids from 55% solids initially to 72.2% solids from 35% solids initially), as does the dry density, while the gravimetric moisture content decreases with decreasing initial % solids. The initial and final wet densities (which drive settling) vary least with initial % solids.

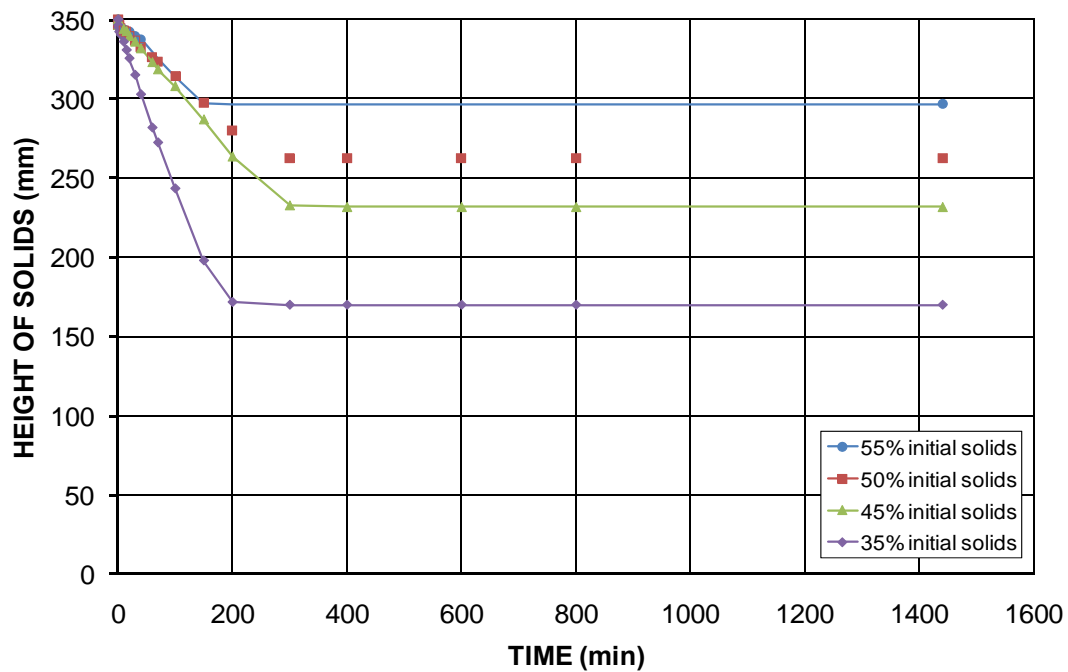


Figure B-11 Settlement of Swanbank fly ash solids vs. Time for various initial % solids

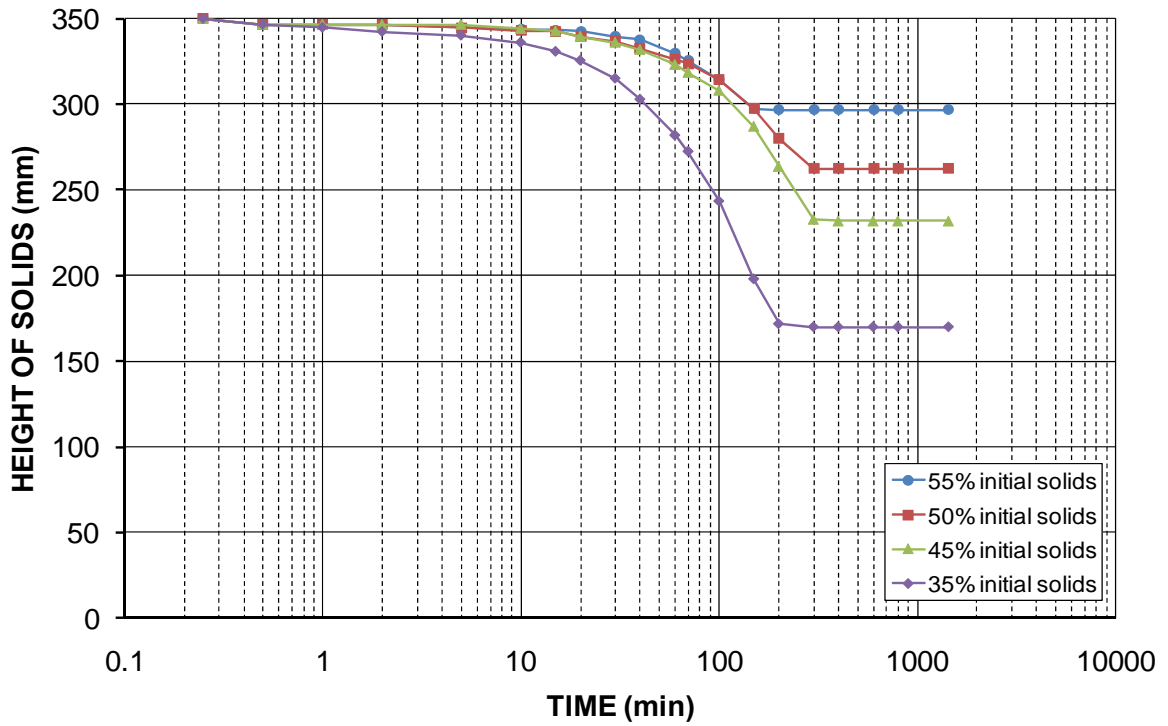


Figure B-12 Settlement of Swanbank fly ash solids vs. $\text{Log}_{10}(\text{Time})$ for various initial % solids

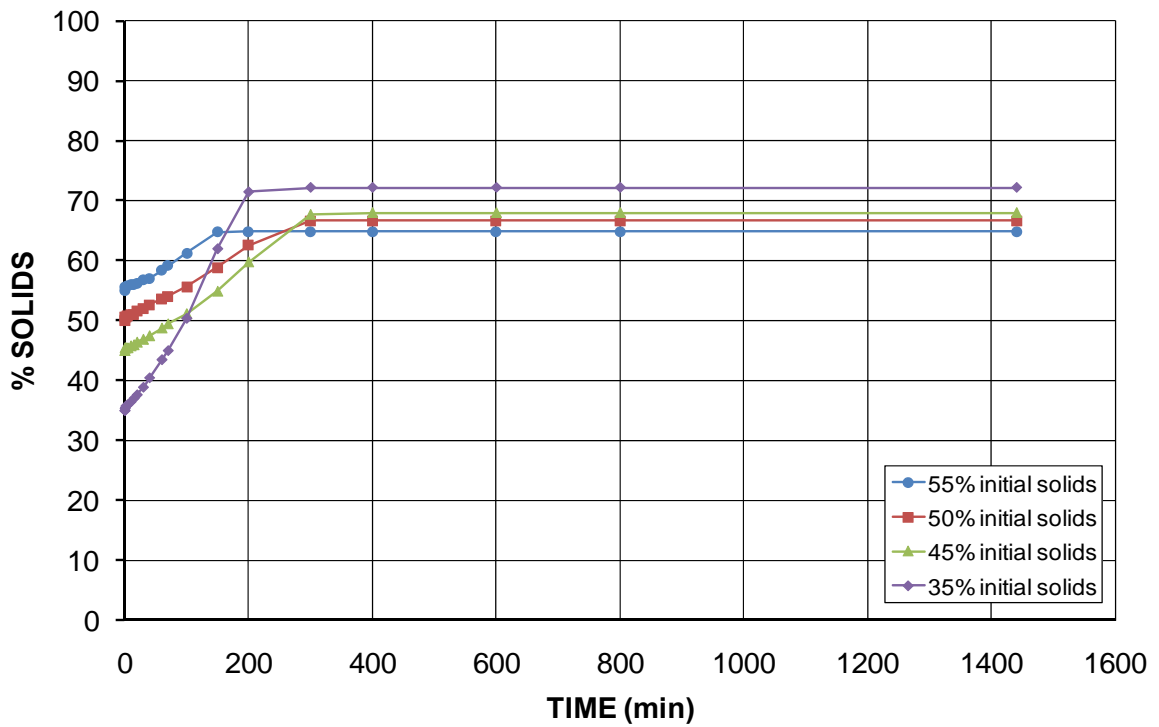


Figure B-13 Average % Solids of settling Swanbank fly ash solids vs. Time for various initial % solids

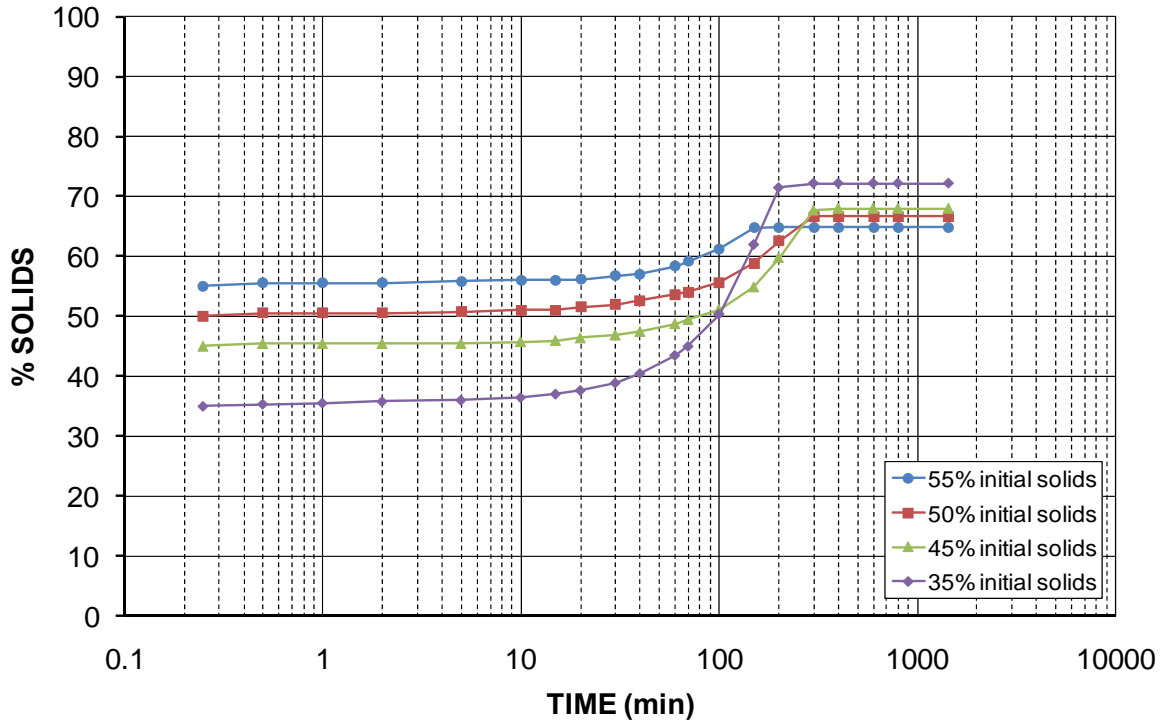


Figure B-14 Average % Solids of settling Swanbank fly ash solids vs. Log_{10} (Time) for various initial % solids

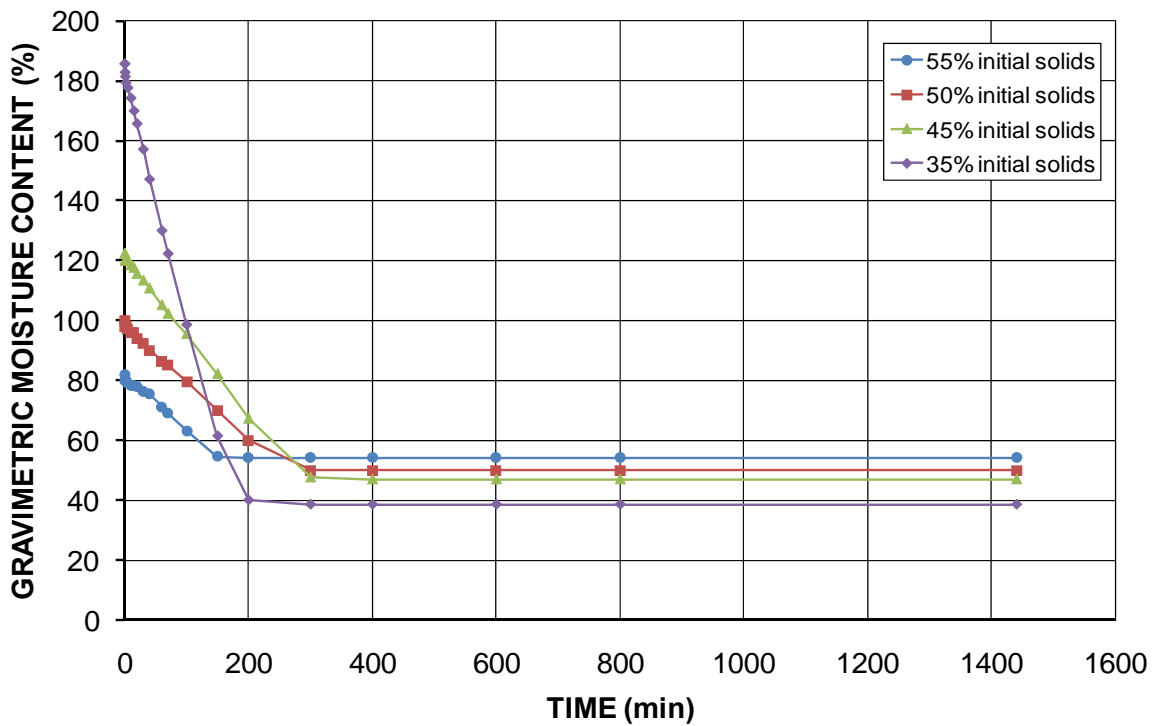


Figure B-15 Average gravimetric moisture content of settling Swanbank fly ash solids vs. Time for various initial % solids

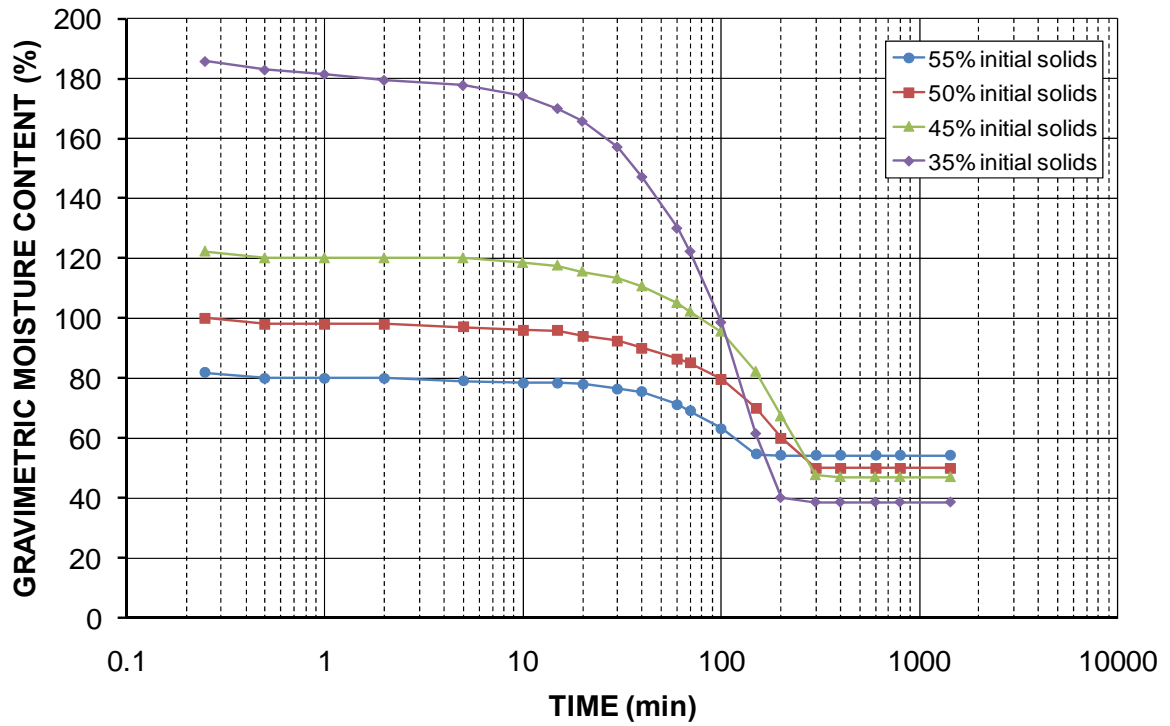


Figure B-16 Average gravimetric moisture content of settling Swanbank fly ash solids vs. Log₁₀ (Time) for various initial % solids

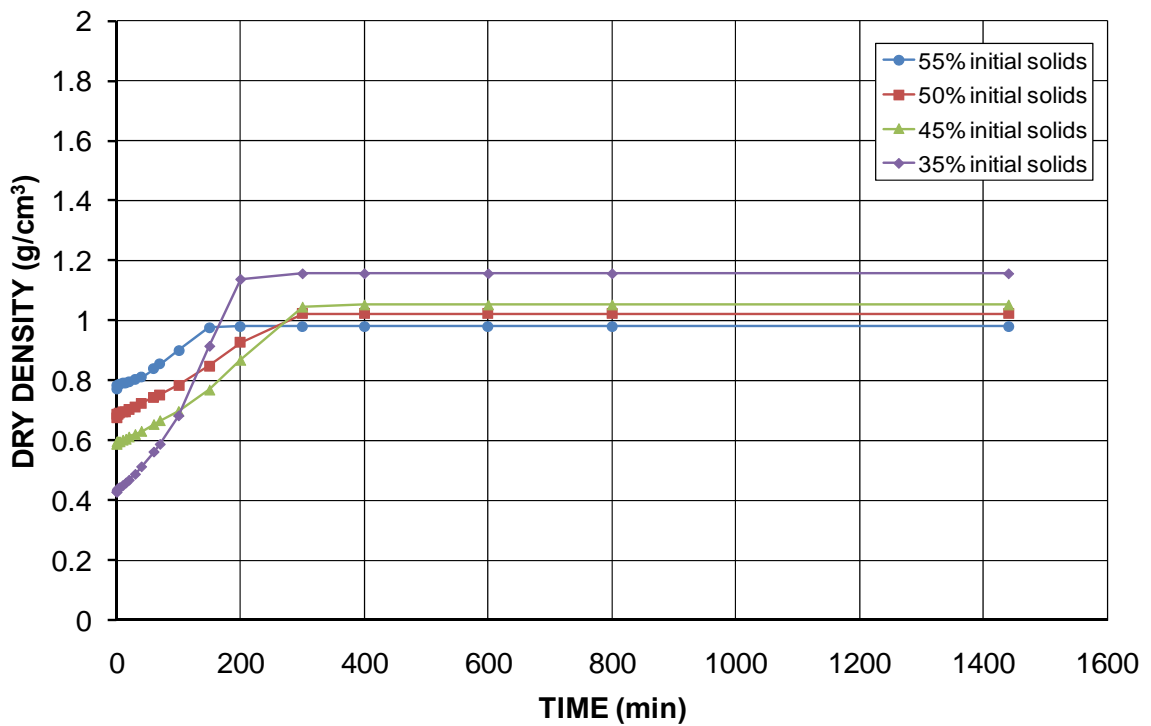


Figure B-17 Average dry density of settling Swanbank fly ash solids vs. Time for various initial % solids

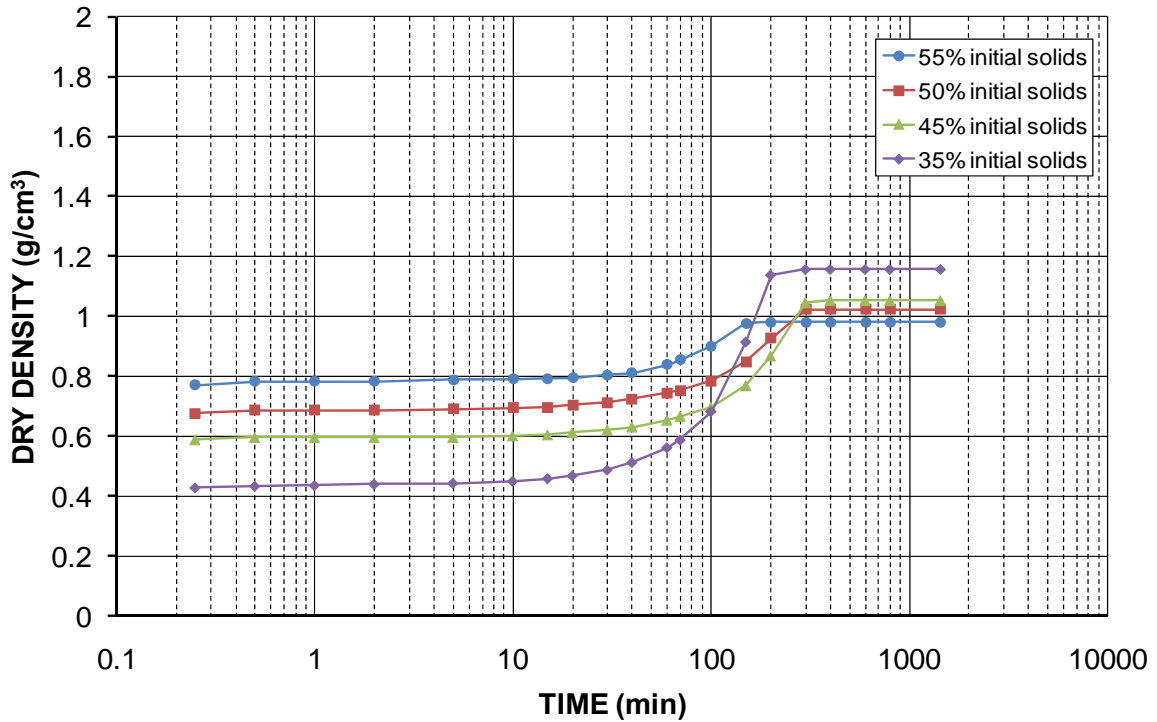


Figure B-18 Average dry density of settling Swanbank fly ash solids vs. Log_{10} (Time) for various initial % solids

B.6 Viscosity Tests

Slurry resistance to flow, shearing and pumping power, is measured by a viscosity test, which should be determined before any field trials in the grout injection system design. Figure B-19 shows the viscometer used in the lab. In the laboratory viscosity test, the shear resistance of a small sample of slurry is poured in a cylindrical container of a viscosity instrument in which a submerged solid cylinder rotates at a pre-set speed against the slurry shear flow resistance measured by the torque recorded in the instrument software. The measured torque resistance of the slurry depends on the viscosity of the slurry and the rpm of the rotating cylinder, which is a measure of the slurry shear strain rate. If the function representing the relation between the shear stress (τ) and the shear strain rate ($\dot{\gamma}$) is a line with a zero intercept, then the slurry is called Newtonian and the constant slope is called viscosity (μ); otherwise it is categorised as non-Newtonian fluid (Alehossein 2009, Alehossein et al 2010). It is called a Bingham plastic slurry (Alehossein, 2009) when the intercept is nonzero (τ_0) and a line with a slope of (μ_0) can represent the shear stress function. Slurry samples tested at CSIRO laboratory can be characterised either by an approximate single line or generally by several lines or so called multi-linear Bingham plastic model ($\tau = \tau_0 + \mu_0 \dot{\gamma}$). Depending on the range of shear rate and degree of solid concentration, viscosity test data can be approximated by either a line, or more accurately by several lines, so called multi-linear models. A single line model is generally sufficient enough for low solid concentration slurries, particularly at low shear rates or fluid speed.

Linear Bingham model

In the single linear Bingham model (Alehossein, 2009, Alehossein et al 2010), we normally fit only one single line into our test data. The line is represented by the following equation:

$$\tau = \tau_0 + \mu_0 \dot{\gamma}, \quad (1)$$

where $\dot{\gamma}$ and τ are the x and y parameters of the line, τ_0 is the line intercept parameter and μ_0 is line the slope. The line intercept parameter, τ_0 , is also called the Bingham plastic yield or cohesion and the line slope parameter, μ_0 , represents the linear constant viscosity.

Since the slope μ_0 is constant and doesn't change with shear rate, the slurry or fluid is categorised as Newtonian. When the slope is not constant, however, the fluid is called Non-Newtonian. In a viscosity test we measure how the shear stress, τ , varies with the variation of shear rate, $\dot{\gamma}$. Usually the measured data is not in the form of a nice regular shape, hence, we try to simplify them by curve fitting. The simplest curves are obviously multiple lines, as explained below.



Figure B-19 Variation with time of the settlement or clear water height (left), or solid height (right) of the Swanbank fly ash at 50% natural solid concentration

Multi-linear Bingham model

Depending on slurry viscosity, solid concentration and range of shear rate, if we intend to mimic more accurately the viscosity experimental data, we need to use more than one line to fit into our experimental data (multi-linear model), particularly when we want a more accurate model for a wide range of shear rate. We consider here only bilinear models, although the method can be extended to more than two lines. While our laboratory viscometer is limited to a maximum shear rate of 700 /s (or shear strain per second), we normally consider two range of shear rates, 0 to 100/s and 100/s to 700/s.

In the bilinear model, the shear stress shear rate is fit into two distinct lines (e.g. one line in the range 0 to 100 /s and another for the range 100 to 700 /s). As in the case of single line modelling shown by the equation (1) above, each line can be identified by its two main parameters, namely the yield intercept, τ_0 , and the viscosity slope, μ_0 . This is illustrated in Figure B-20 and by two distinct linear equations (2a) and (2b).

As shown in the equations, the major difference between the linear and bilinear equations is the shear rate term in the second line, which must be measured with respect to the end of the first line, rather than from its zero value at the x-axis origin.

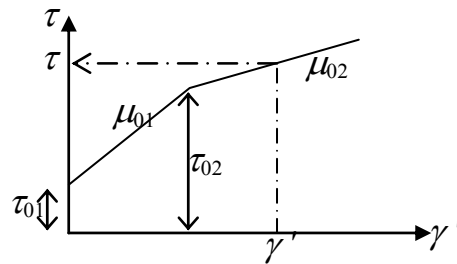


Figure B-20 Bingham bilinear plastic model

$$\tau_1 = \tau_{01} + \mu_{01}(\gamma' - \gamma'_{01}) \quad (2a)$$

$$\tau_2 = \tau_{02} + \mu_{02}(\gamma' - \gamma'_{02}) \quad (2b)$$

B.7 Viscosity Tests on Non-Cohesive Slurry

The results of viscosity tests on slurry grouts at various solid weight concentrations on Swanbank fly ash are shown in Figure B-21 and Figure B-22. Figure B-23 compares viscosity of fly ash compared to other coal reject slurries at solids weight concentration of 40%. Table B-2 provides a list of solids weight concentrations considered for viscosity tests. The higher the solids concentration, the higher is both the plastic yield, or cohesion intercept, and the viscosity (slope of the shear stress – shear strain rate curve).

Table B-2 Viscosity test (under ground water no cement)

Sample No.	Concentration of FA (%)
1	20
2	40
3	50
4	60
5	70
6	75

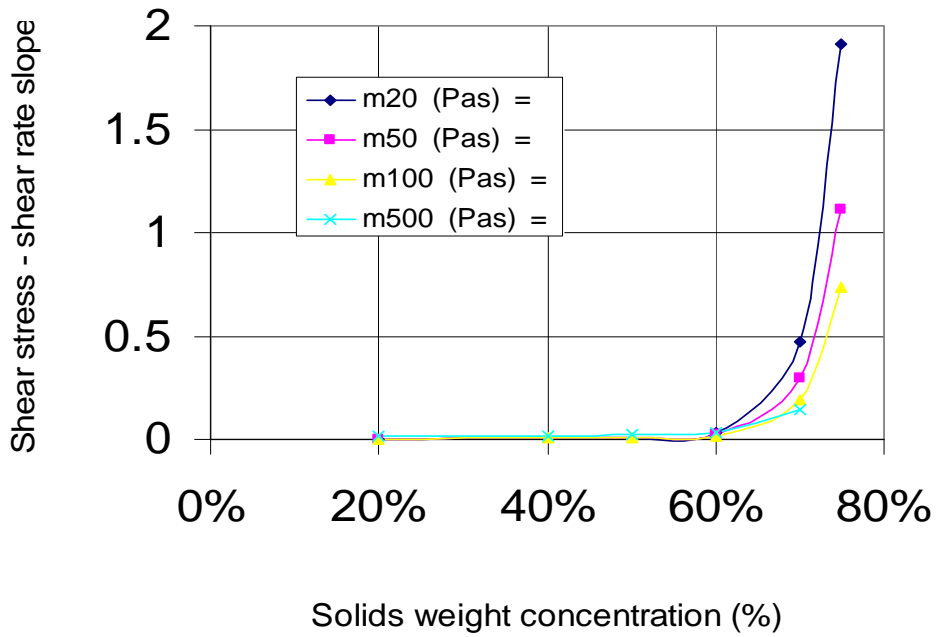


Figure B-21 Viscosity (slope) of shear stress versus shear strain rate curve obtained in viscosity tests of Swanbank fly ash at different solids weight concentrations for shear rate values of 20, 50, 100 and 500 /s.

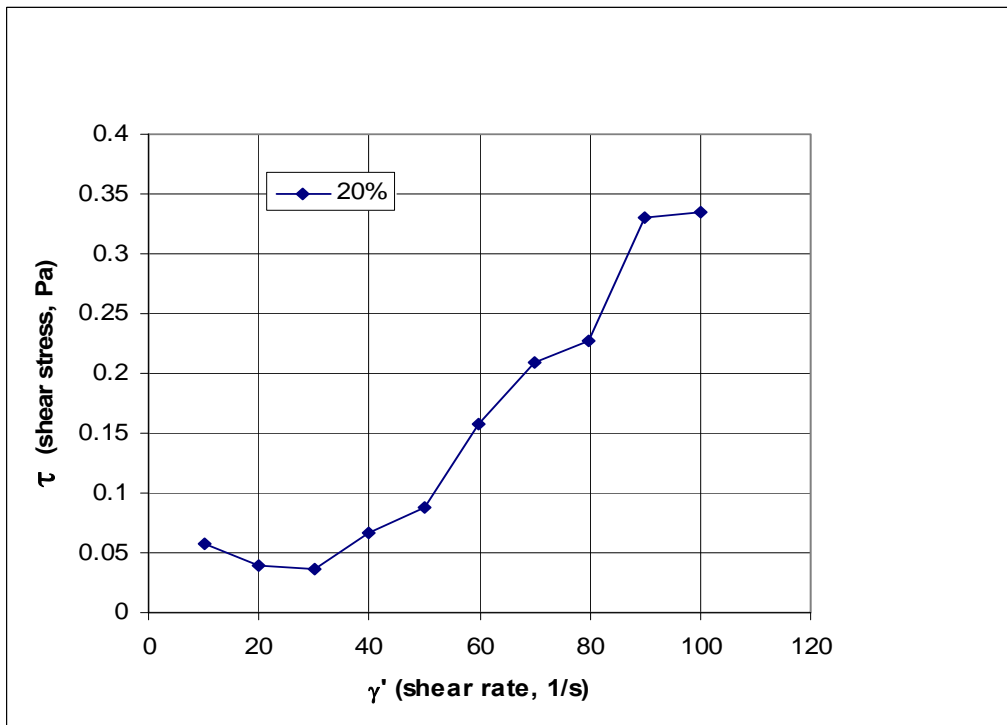


Figure B-22a Viscosity test results - Shear stress versus shear strain rate of Swanbank fly ash at 20% solids weight concentration for shear rate range of 0-100 /s.

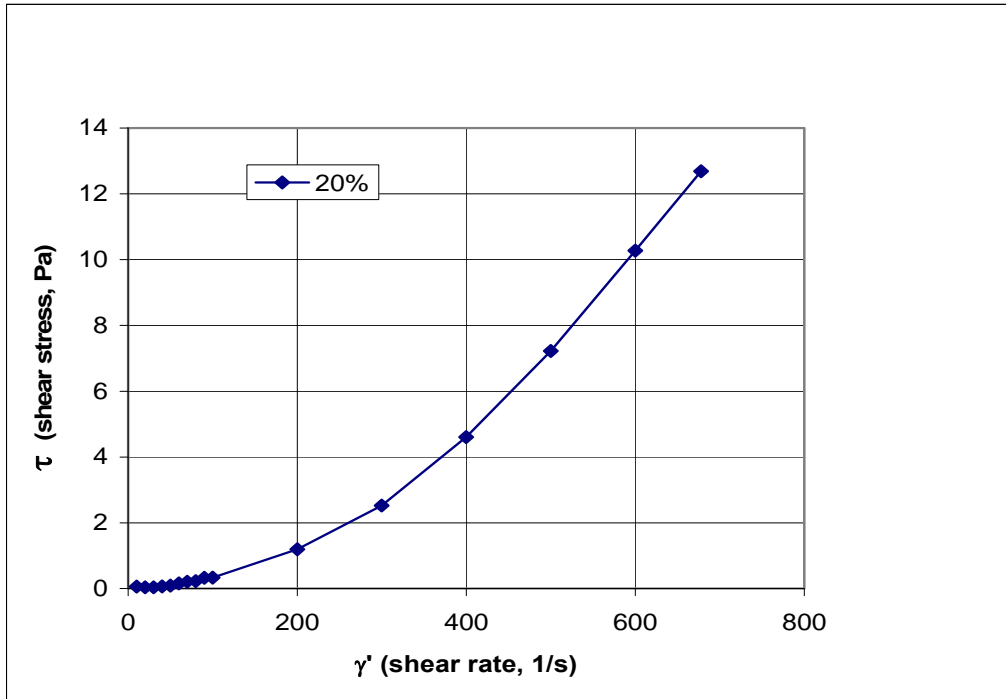


Figure B-22b Viscosity test results - Shear stress versus shear strain rate of Swanbank fly ash at 20% solids weight concentration for shear rate range of 0-700 /s.

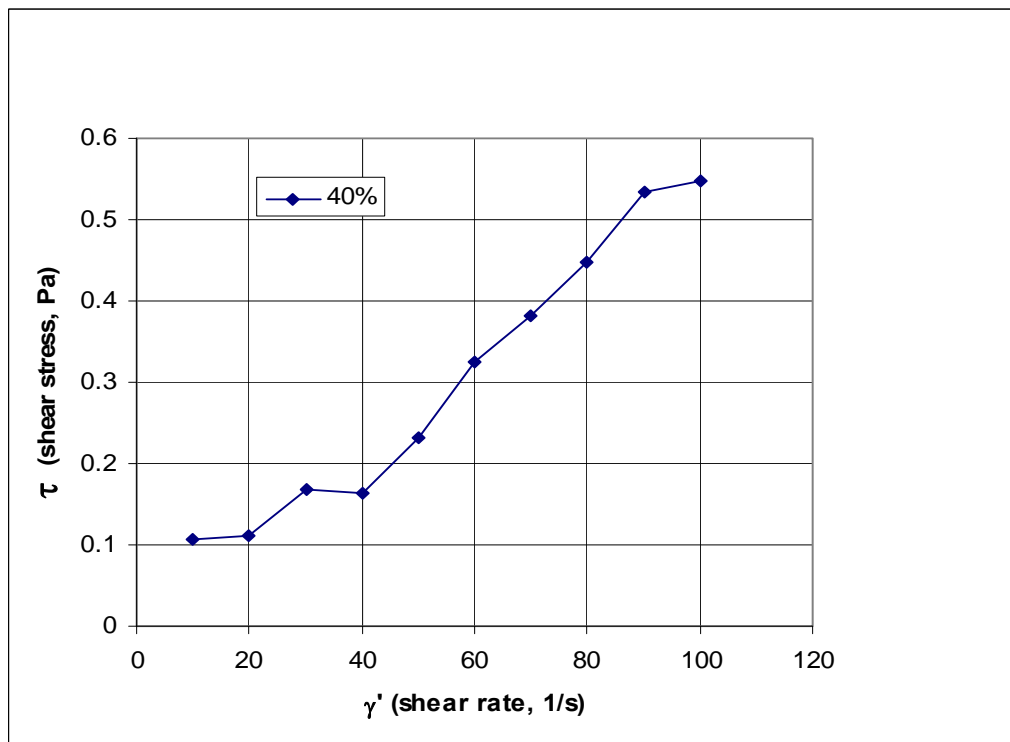


Figure B-22c Viscosity test results - Shear stress versus shear strain rate of Swanbank fly ash at 40% solids weight concentration for shear rate range of 0-100 /s.

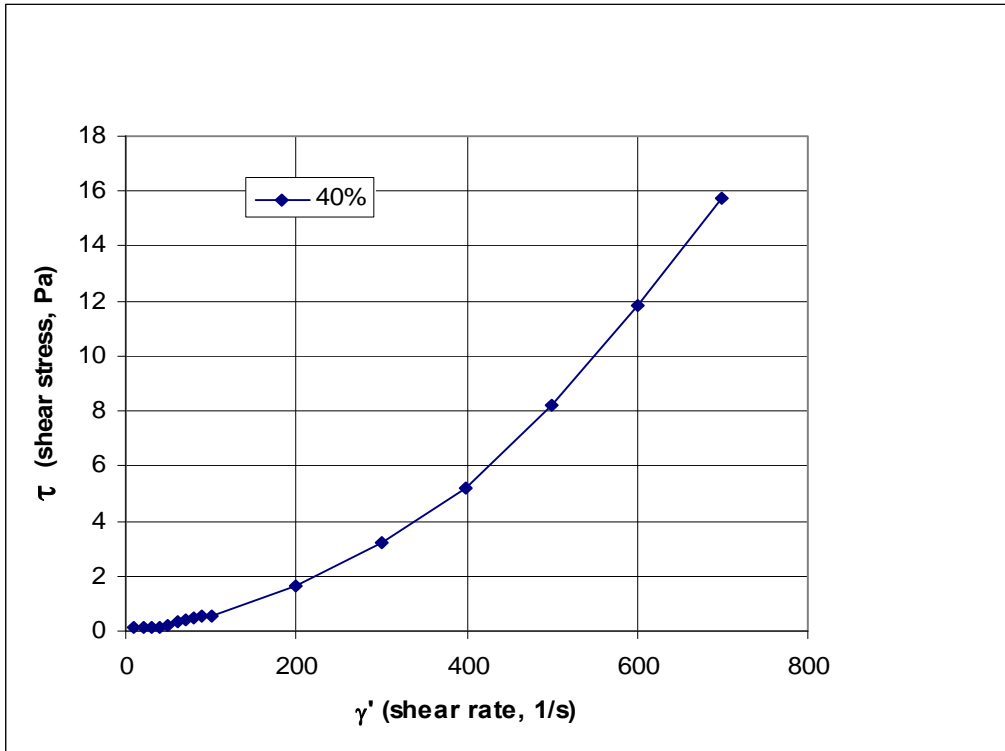


Figure B-22d Viscosity test results - Shear stress versus shear strain rate of Swanbank fly ash at 40% solids weight concentration for shear rate range of 0-700 /s.

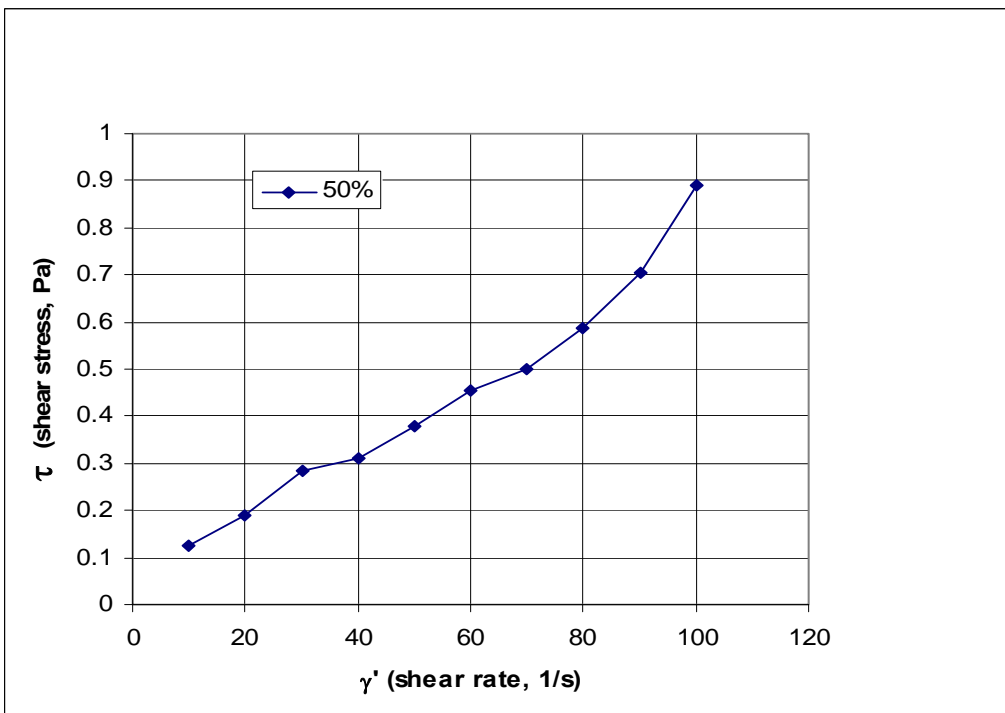


Figure B-22e Viscosity test results - Shear stress versus shear strain rate of Swanbank fly ash at 50% solids weight concentration for shear rate range of 0-100 /s.

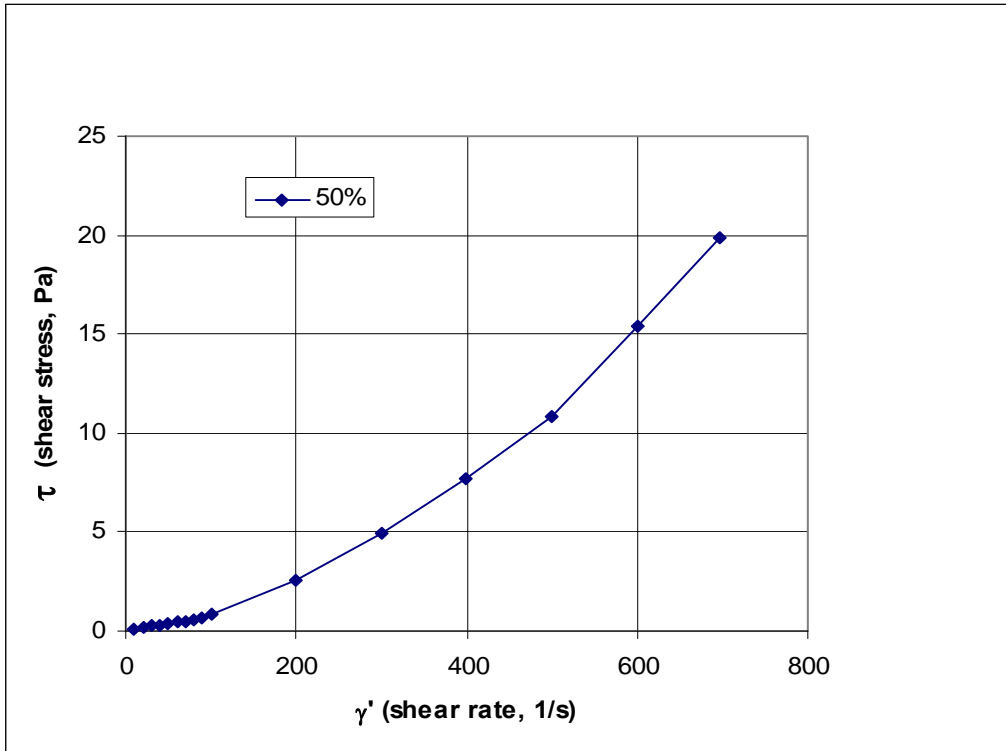


Figure B-22f Viscosity test results - Shear stress versus shear strain rate of Swanbank fly ash at 50% solids weight concentration for shear rate range of 0-100 /s.

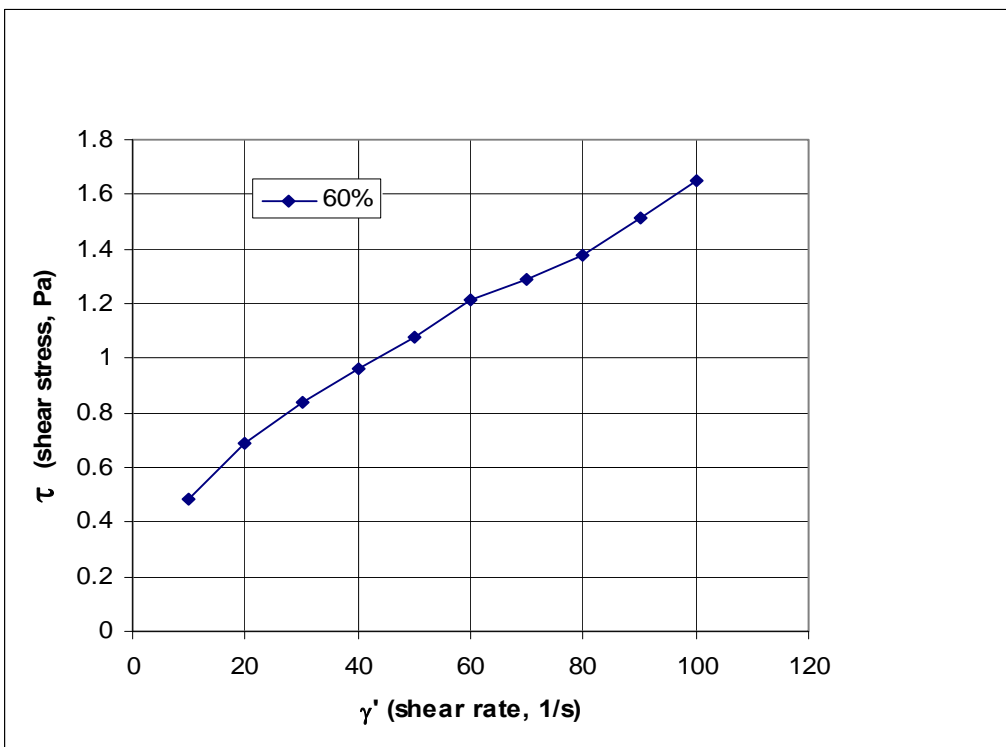


Figure B-22g Viscosity test results - Shear stress versus shear strain rate of Swanbank fly ash at 60% solids weight concentration for shear rate range of 0-100 /s.

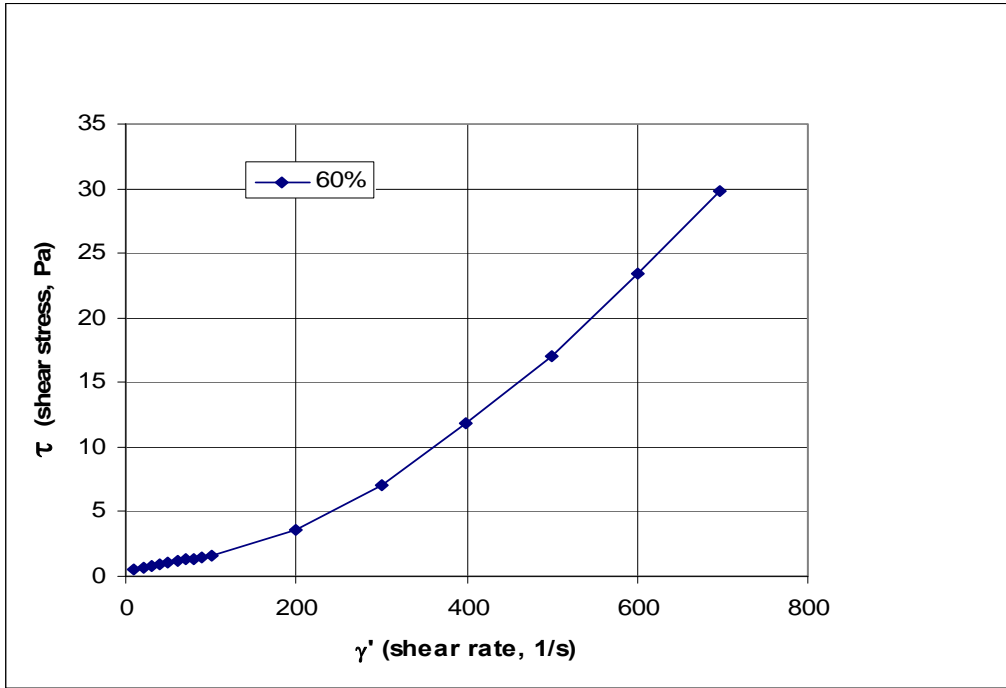


Figure B-22h Viscosity test results - Shear stress versus shear strain rate of Swanbank fly ash at 60% solids weight concentration for shear rate range of 0-700 /s.

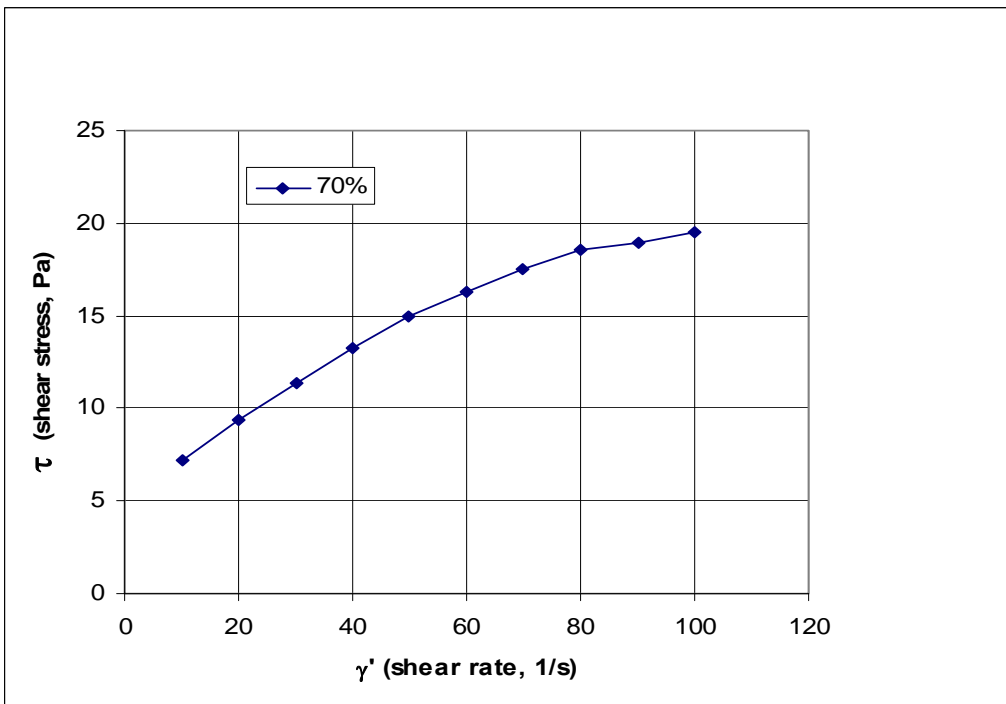


Figure B-22i Viscosity test results - Shear stress versus shear strain rate of Swanbank fly ash at 70% solids weight concentration for shear rate range of 0-100 /s.

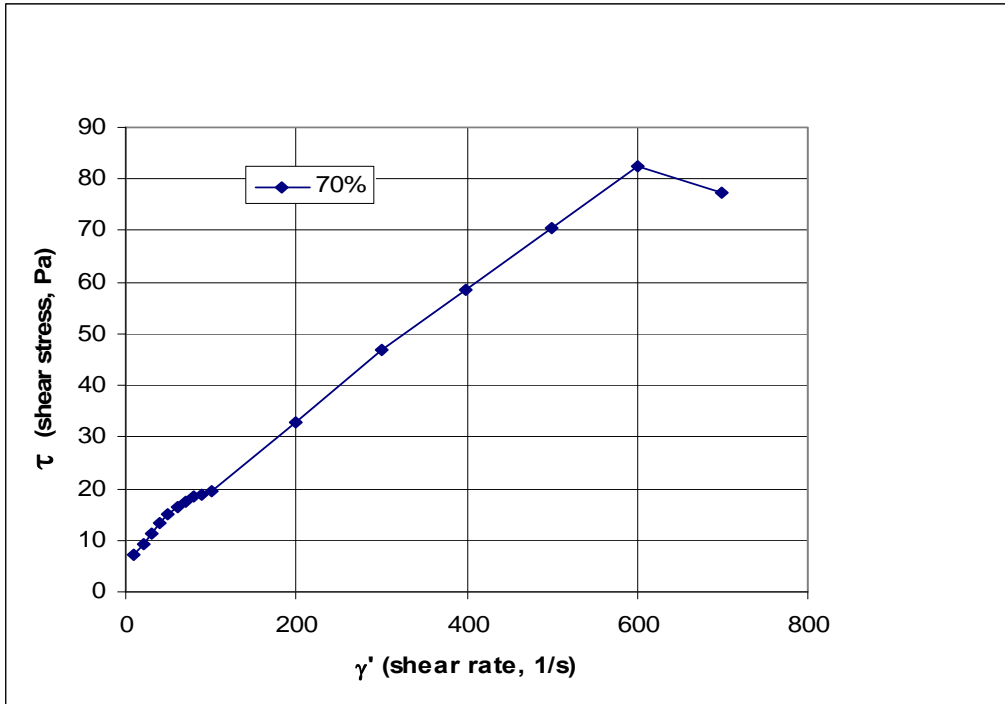


Figure B-22j Viscosity test results - Shear stress versus shear strain rate of Swanbank fly ash at 70% solids weight concentration for shear rate range of 0-700 /s.

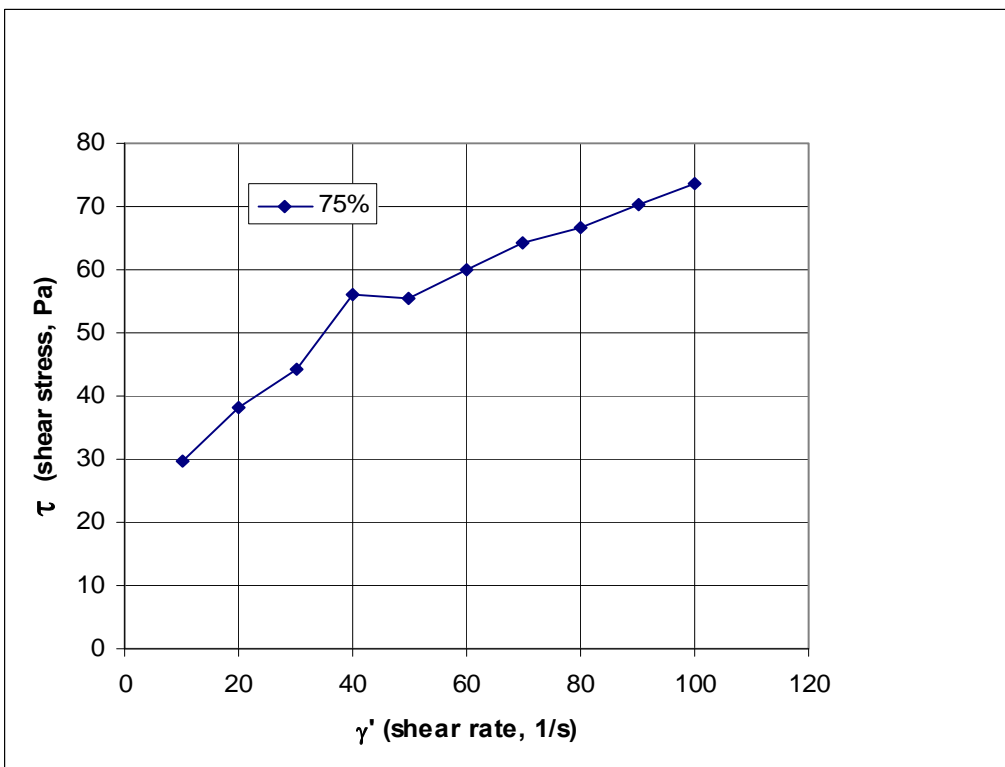


Figure B-22k Viscosity test results - Shear stress versus shear strain rate of Swanbank fly ash at 75% solids weight concentration for shear rate range of 0-100 /s.

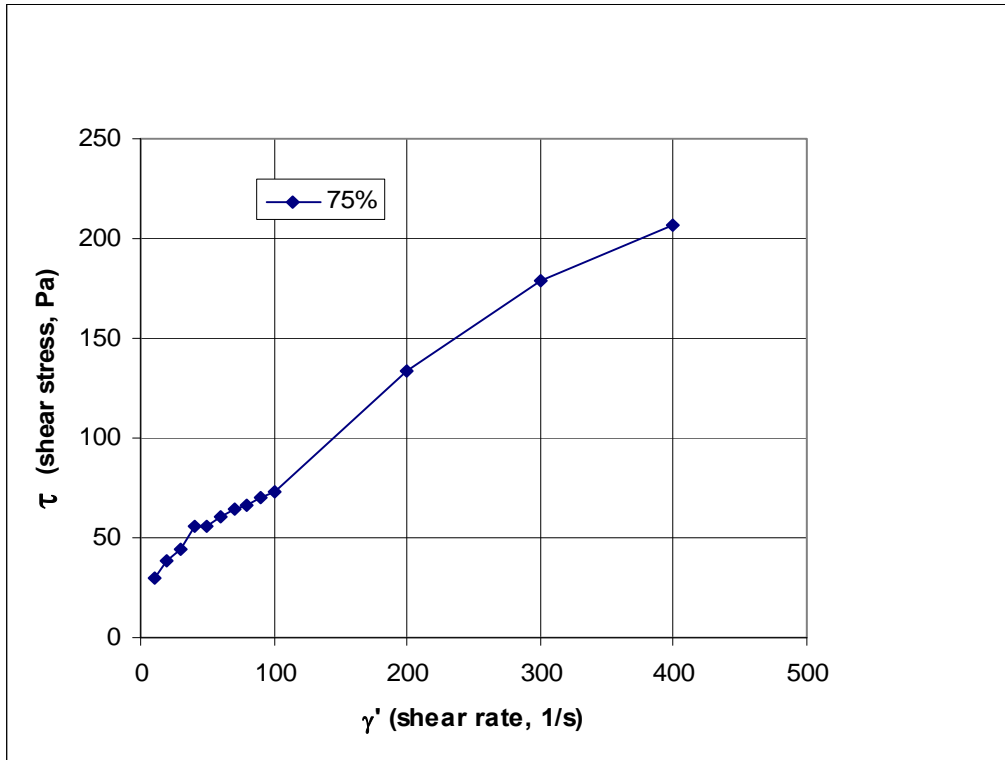


Figure B-22 Viscosity test results - Shear stress versus shear strain rate of Swanbank fly ash at 75% solids weight concentration for shear rate range of 0-400 /s.

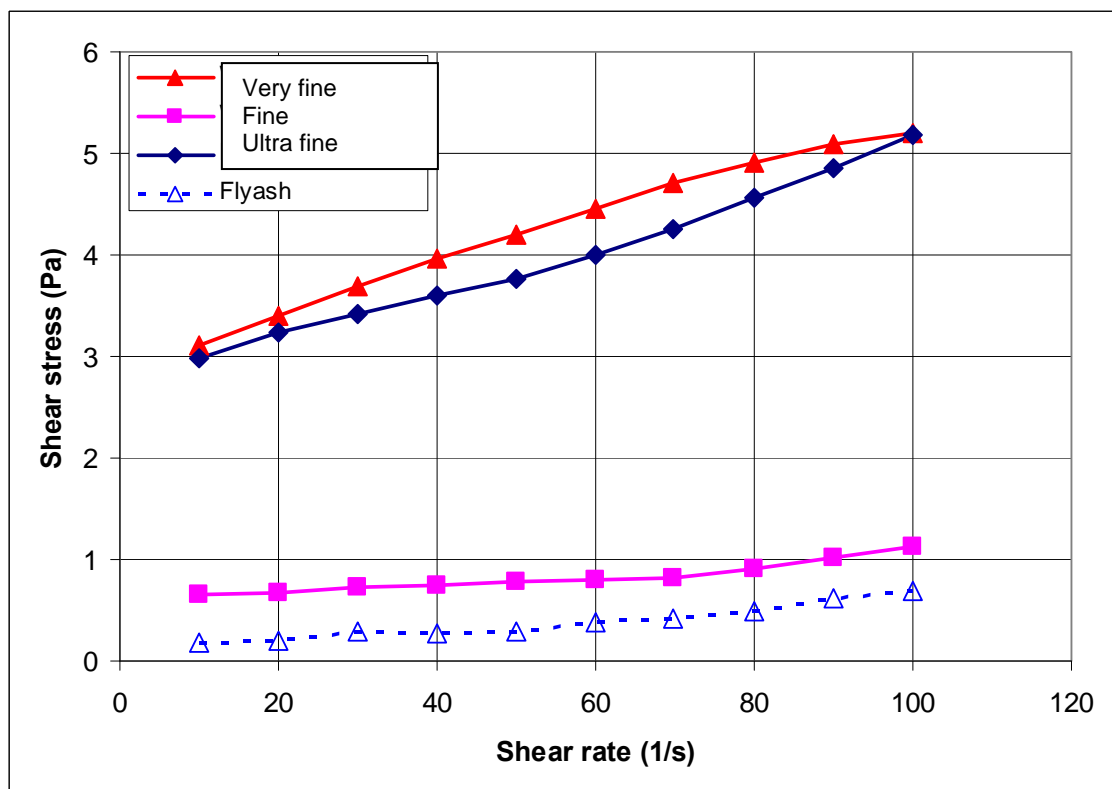


Figure B-23 Comparison of shear stress versus shear rate viscosity test results of fly ash slurry and other mine coal washery wastes at solid concentration of 40%.

B.8 Viscosity Tests on Cohesive Slurry

A series of viscosity tests at different time intervals were conducted on fly ash slurries at %40 and 60% solids weight concentration, in which 5% of the solids are replaced with cement. Their material component proportions are given in Table B-3 and Table B-4. The slope or viscosity variation with time is given in Figure B-24 and Figure B-26, respectively, while the viscosity tests results at the two different solids weight concentration of 40% and 60%, in terms of shear stress function against shear strain rate, are provided in Figure B-25 and Figure B-27, respectively. Only at high flow velocities the viscous effects reduce slightly as shown in these figures. As expected, both plastic yield (cohesion intercept) and viscosity (slope) of cohesive slurries increase with time due to cement hardening effect.

Table B-3 Material proportions for 40% solids weight concentration

Swanbank fly ash	35g
Cement	5g
Water	60g
Time interval	15 min
Solids weight concentration	40%

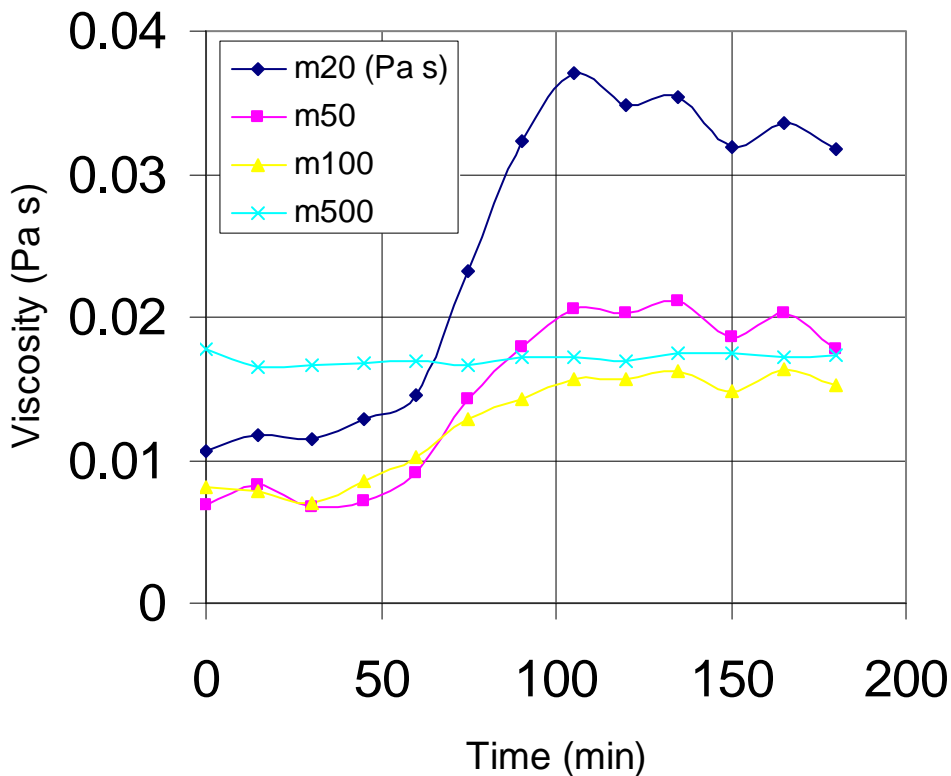


Figure B-24 Variation of viscosity (slope) of shear stress versus shear strain rate curve, obtained in viscosity tests of cohesive Swanbank fly ash slurry at 40% solids weight concentration, with time for shear rate values of 20, 50, 100 and 500 /s.

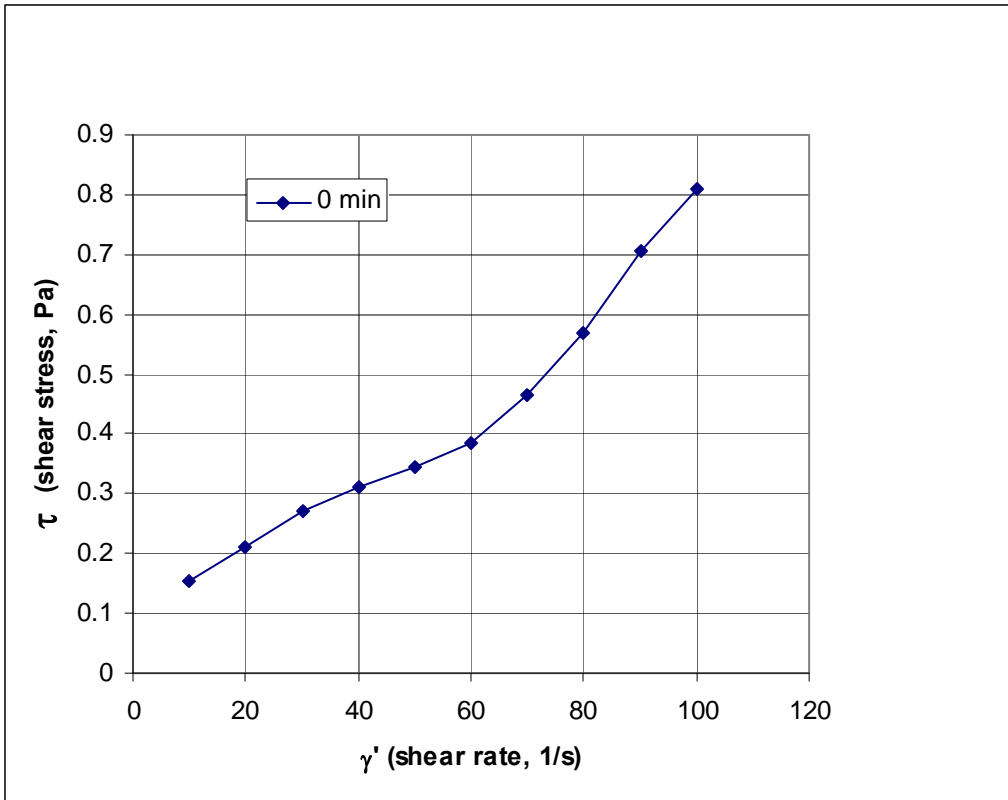


Figure B-25a Shear stress versus shear strain rate tests of cohesive Swanbank fly ash slurry at 40% solids weight concentration at time zero for shear rate range of 0-100 /s.

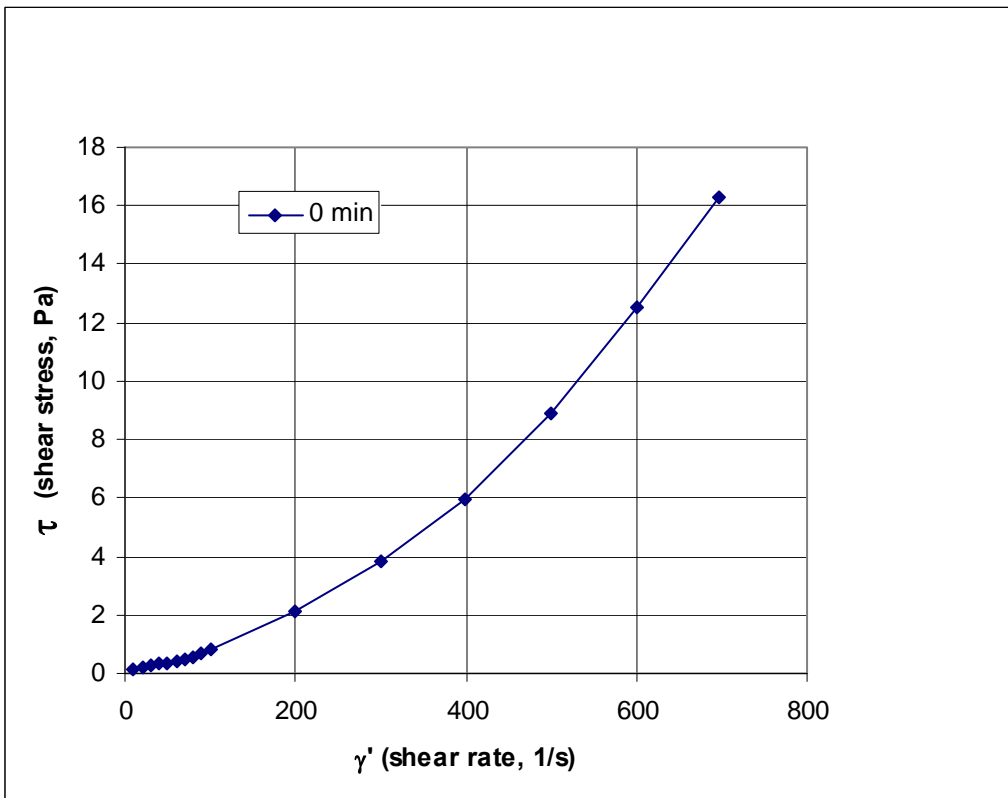


Figure B-25b Shear stress versus shear strain rate tests of cohesive Swanbank fly ash slurry at 40% solids weight concentration at time zero for shear rate range of 0-700 /s.

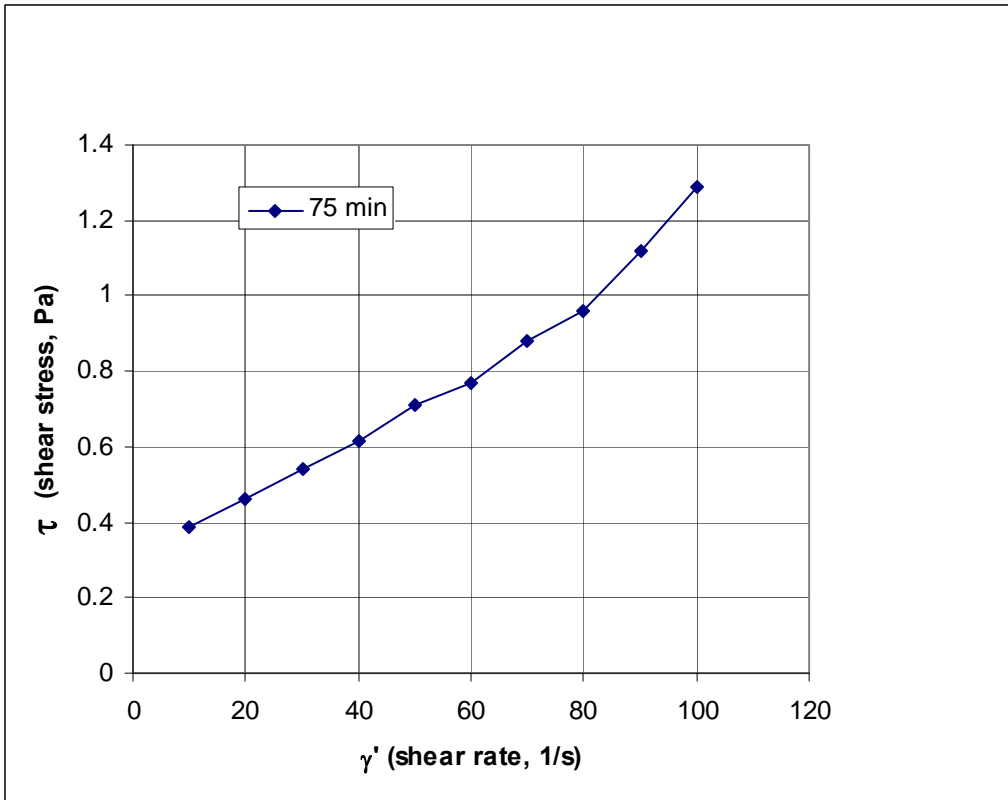


Figure B-25c Shear stress versus shear strain rate tests of cohesive Swanbank fly ash slurry at 40% solids weight concentration after 75 minutes for shear rate range of 0-100 /s.

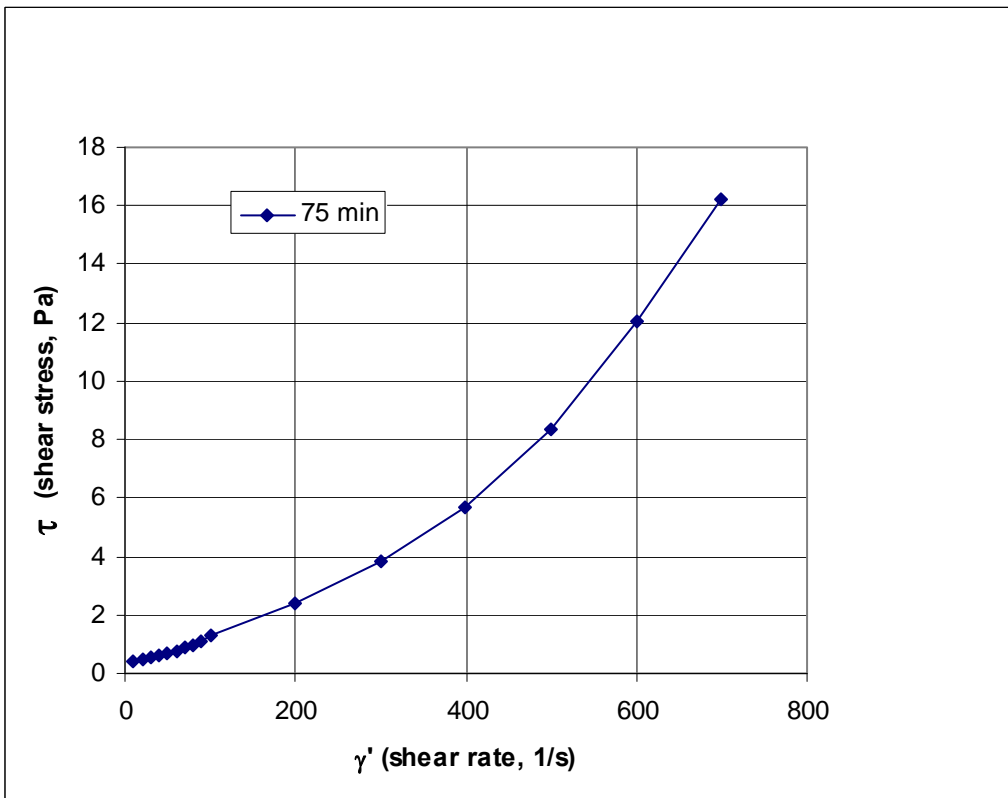


Figure B-25d Shear stress versus shear strain rate tests of cohesive Swanbank fly ash slurry at 40% solids weight concentration after 75 minutes for shear rate range of 0-700 /s.

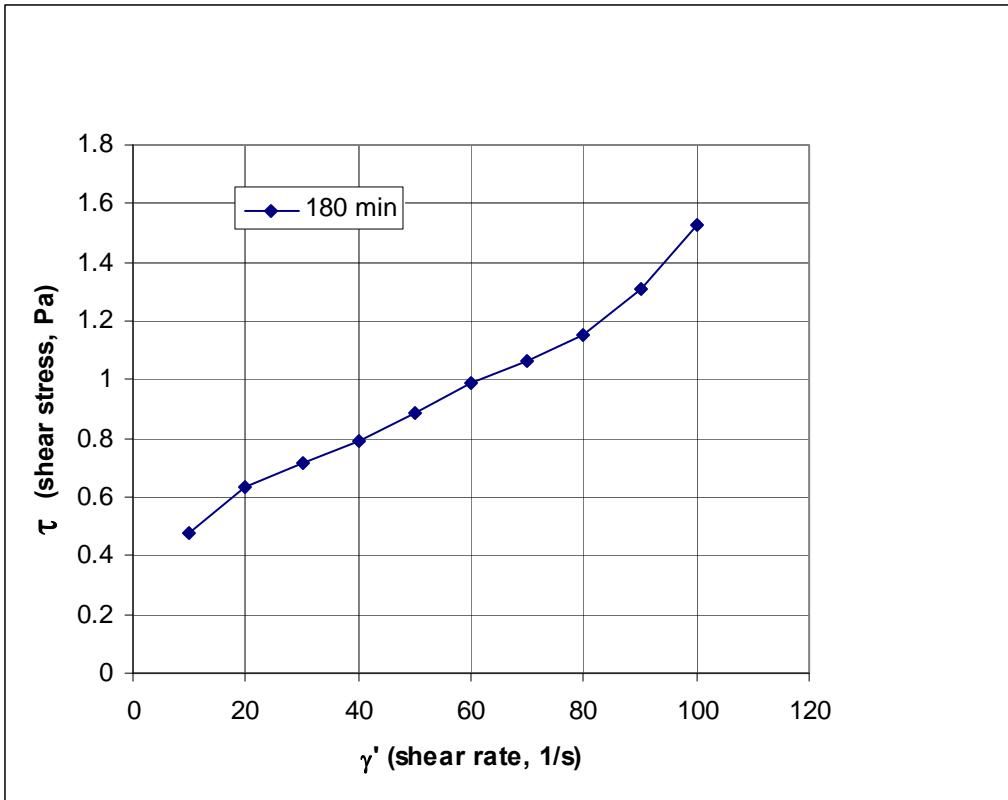


Figure B-25e Shear stress versus shear strain rate tests of cohesive Swanbank fly ash slurry at 40% solids weight concentration after 180 minutes for shear rate range of 0-100 /s.

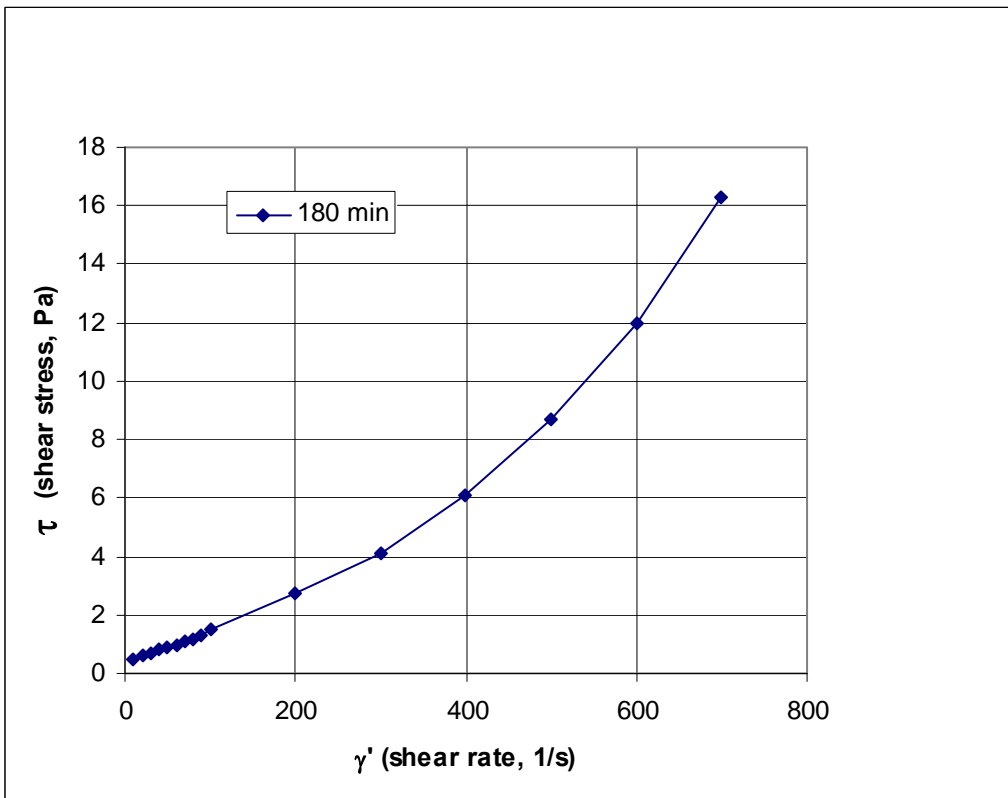


Figure B-25f Shear stress versus shear strain rate tests of cohesive Swanbank fly ash slurry at 40% solids weight concentration after 180 minutes for shear rate range of 0-700 /s.

Table B-4 Material proportions for 60% solids weight concentration

Swanbank fly ash	55g
Cement	5g
Water	40g
Time interval	15 min

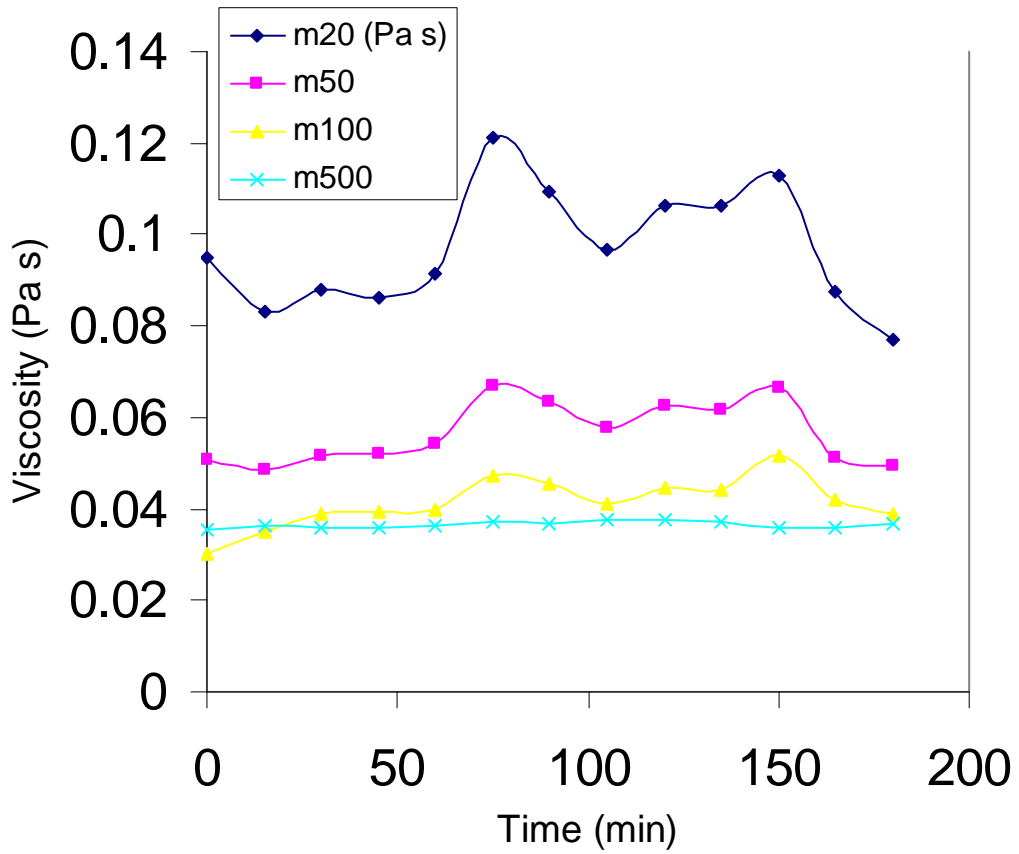


Figure B-26 Variation of viscosity (slope) of shear stress versus shear strain rate curve, obtained in viscosity tests of cohesive Swanbank fly ash slurry at 60% solids weight concentration, with time for shear rate values of 20, 50, 100 and 500 /s.

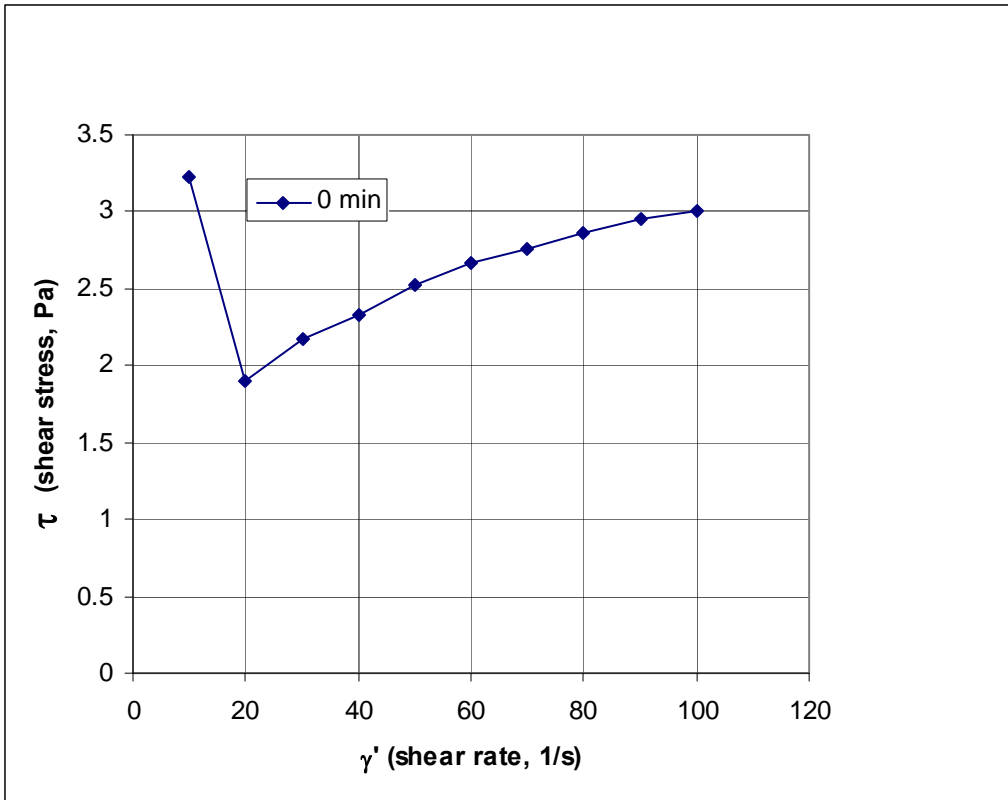


Figure B-27a Shear stress versus shear strain rate tests of cohesive Swanbank fly ash slurry at 60% solids weight concentration at zero time for shear rate range of 0-100 /s.

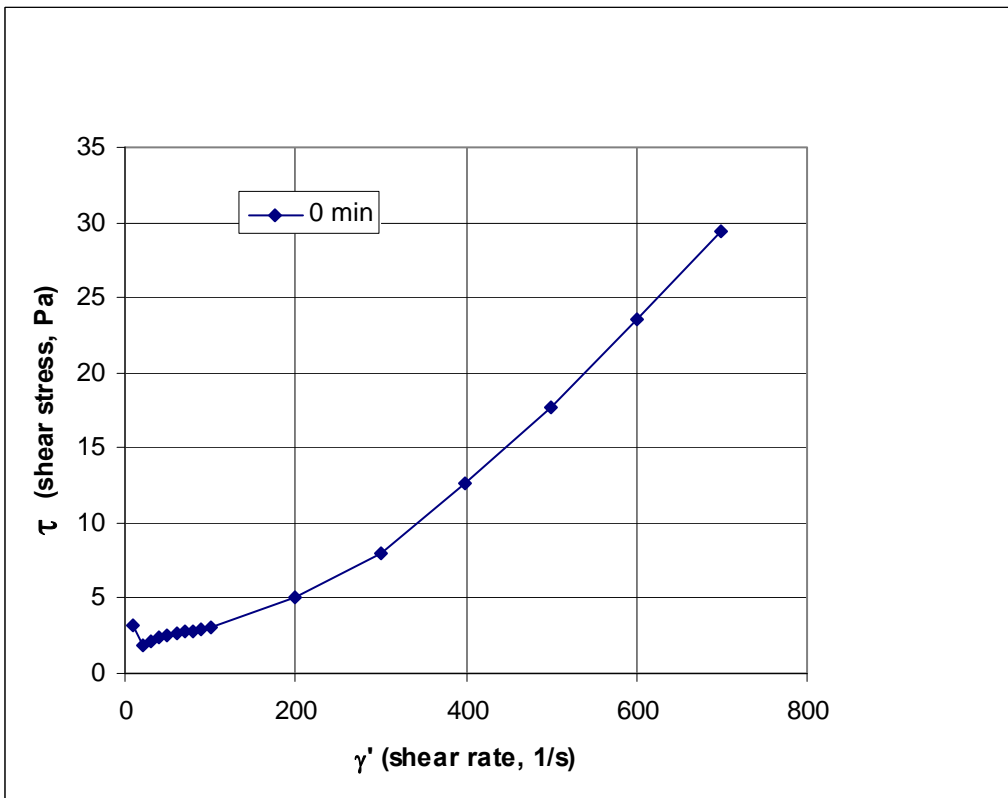


Figure B-27b Shear stress versus shear strain rate tests of cohesive Swanbank fly ash slurry at 60% solids weight concentration at zero time for shear rate range of 0-700 /s.

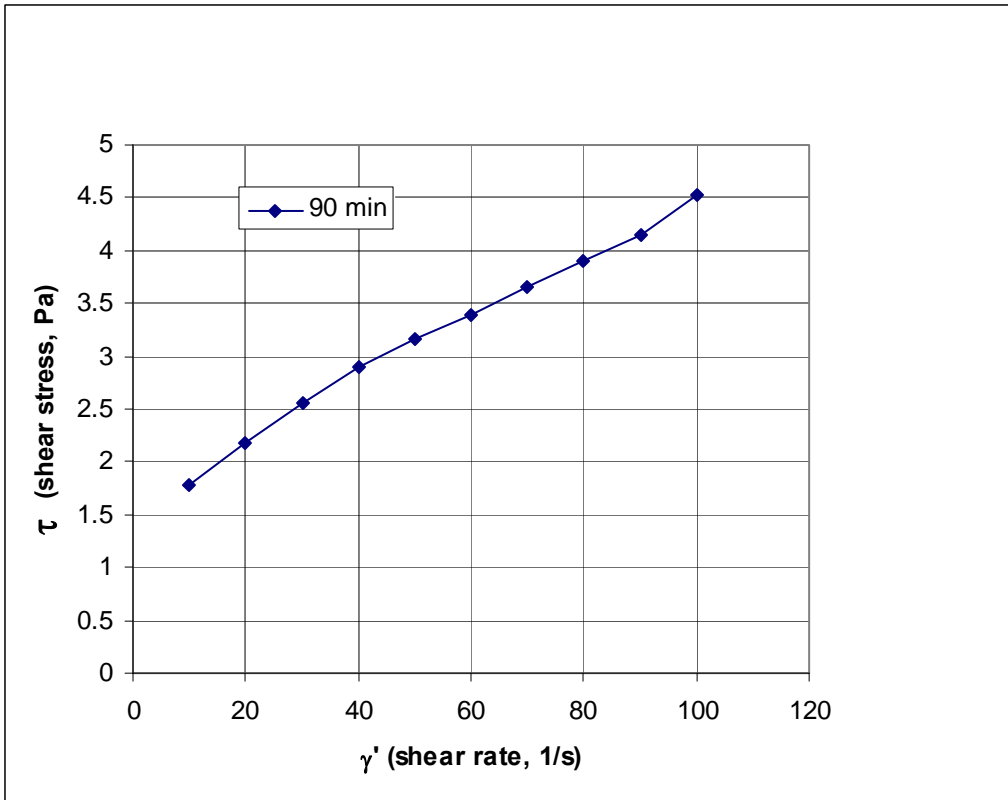


Figure B-27c Shear stress versus shear strain rate tests of cohesive Swanbank fly ash slurry at 60% solids weight concentration after 90 minutes for shear rate range of 0-100 /s.

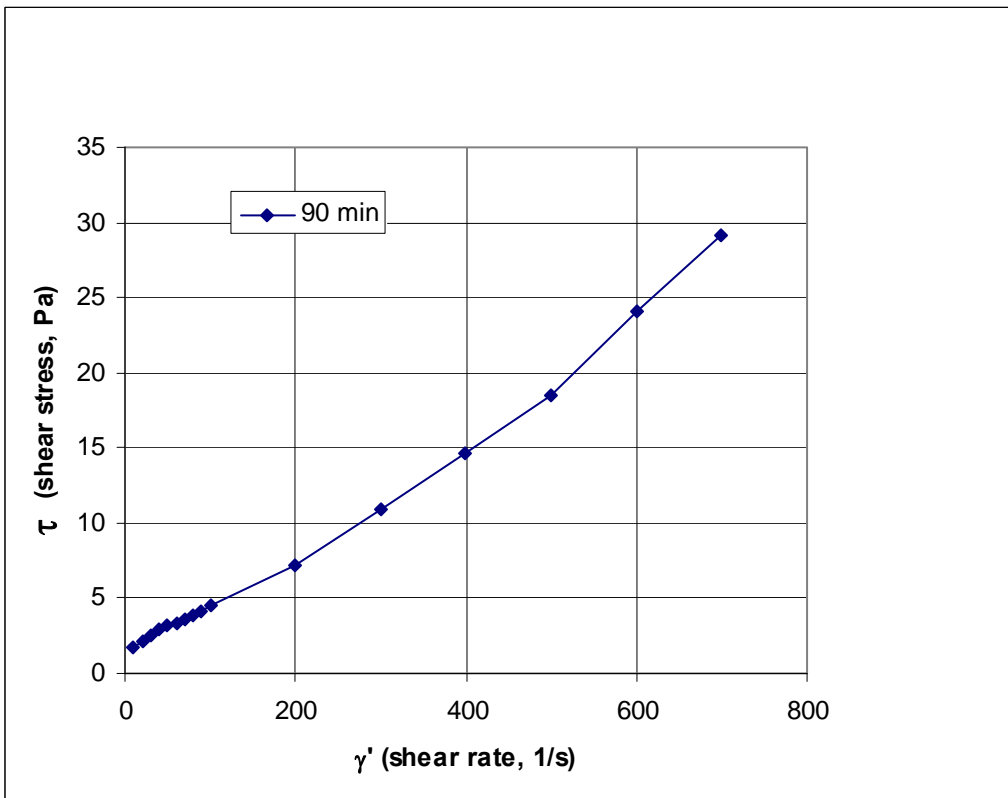


Figure B-27d Shear stress versus shear strain rate tests of cohesive Swanbank fly ash slurry at 60% solids weight concentration after 90 minutes for shear rate range of 0-700 /s.

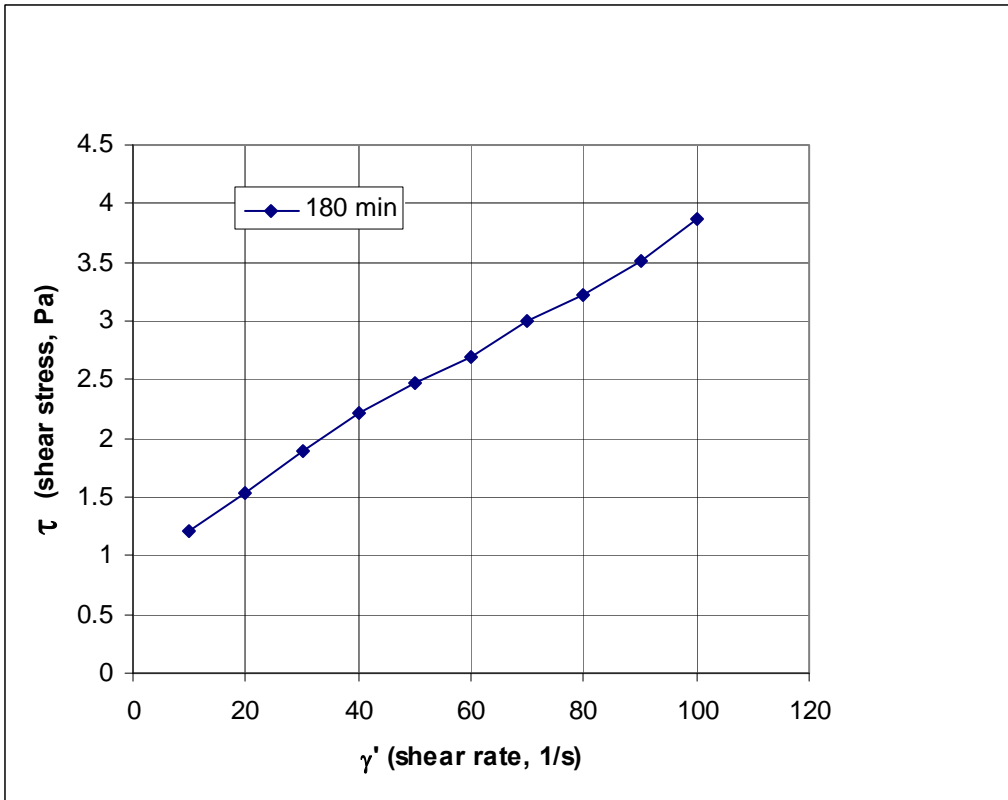


Figure B-27e Shear stress versus shear strain rate tests of cohesive Swanbank fly ash slurry at 60% solids weight concentration after 180 minutes for shear rate range of 0-100 /s.

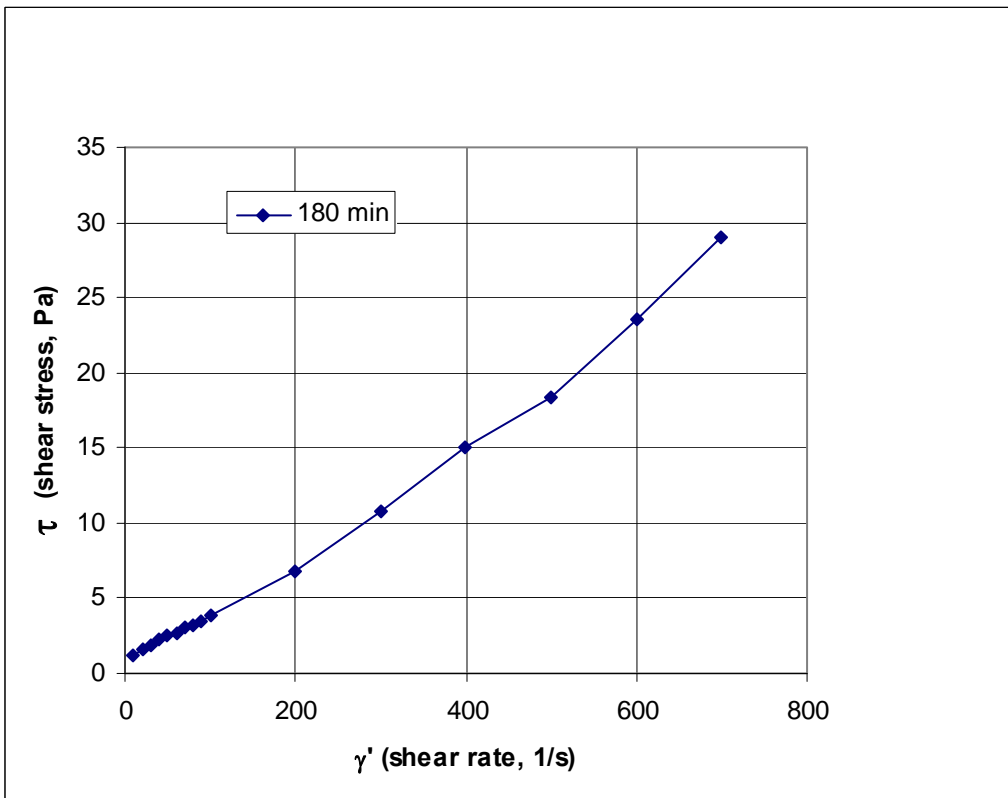


Figure B-27f Shear stress versus shear strain rate tests of cohesive Swanbank fly ash slurry at 60% solids weight concentration after 90 minutes for shear rate range of 0-100 /s.

B.9 Ipswich Motorway T14 and T15 Mix viscosity tests

CSIRO conducted viscosity test on the T14 and T15 Mix designs for Ipswich motorway grout project. We used the same underground water which Keller supplied us with, and we had to sieve the crusher dust to remove the particles greater than 1.00 mm sieve size.

The T14 mix consists of 55.5% crusher dust, 19% fly ash or pond-ash, 6.3% cement and 19.1% water. These test results are shown in Figure B-28.

The T15 mix consists of 52.4% crusher dusts, 18% fly ash or pond-ash, 6.0% cement and 23.7% underground water. These test results are shown in Figure B-29.

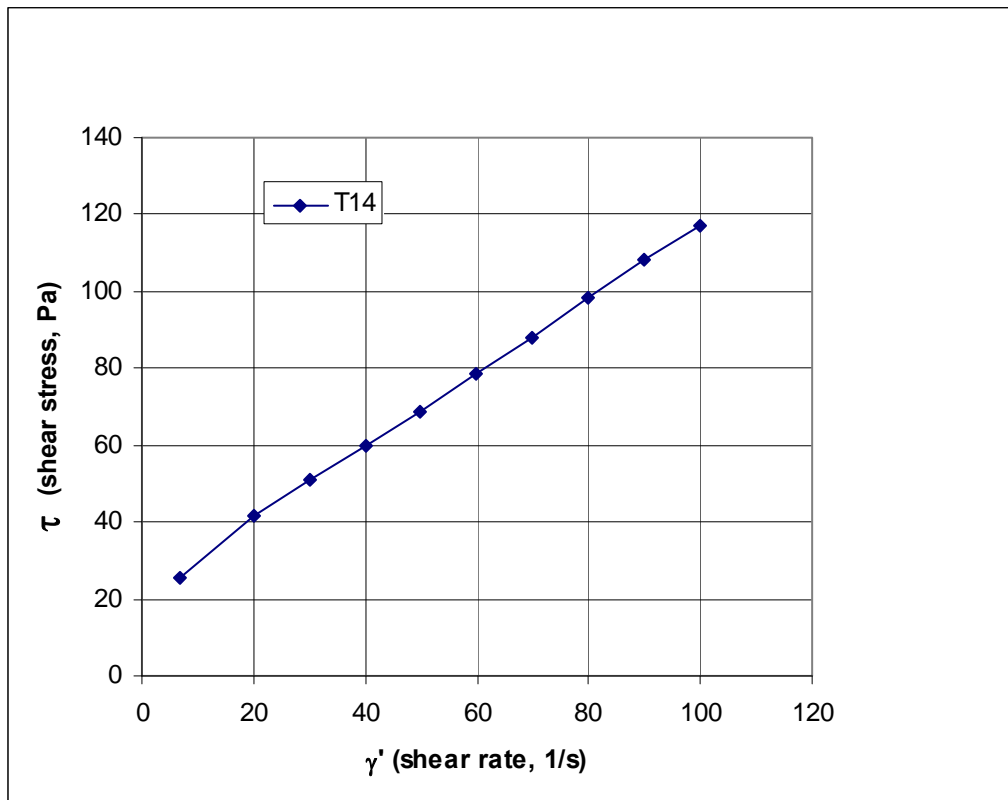


Figure B-28a Shear stress versus shear strain rate tests of T14 mix for shear rate range of 0-100 /s.

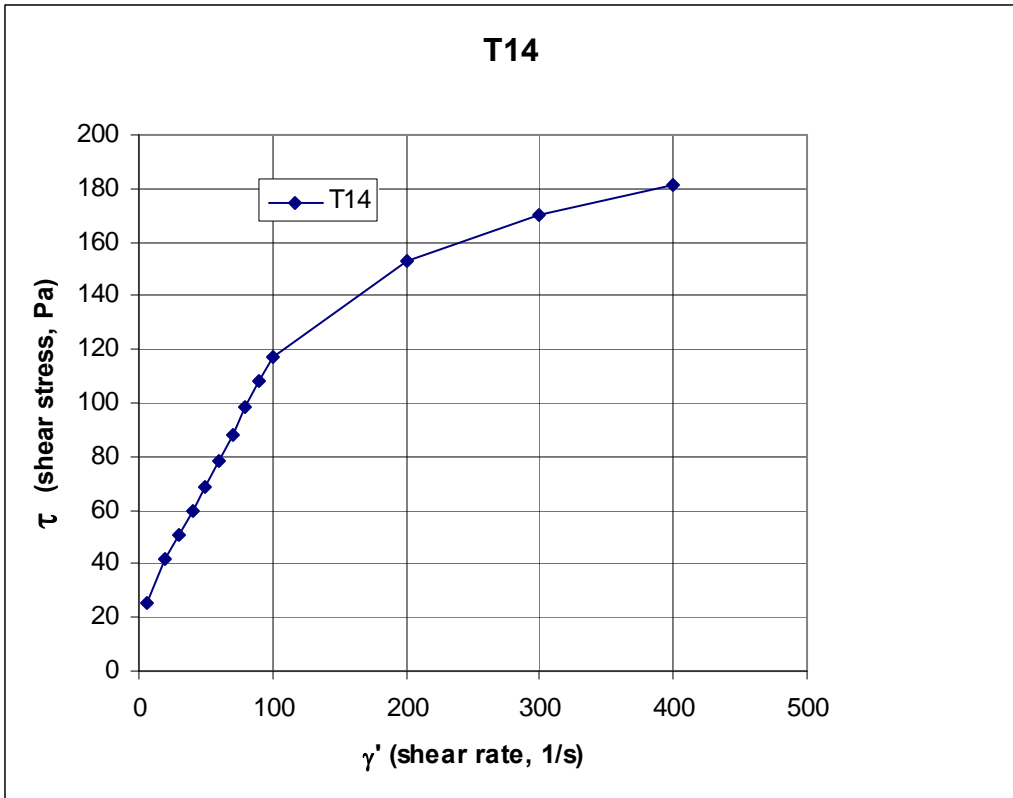


Figure B-28b Shear stress versus shear strain rate tests of T14 mix for shear rate range of 0-400 /s.

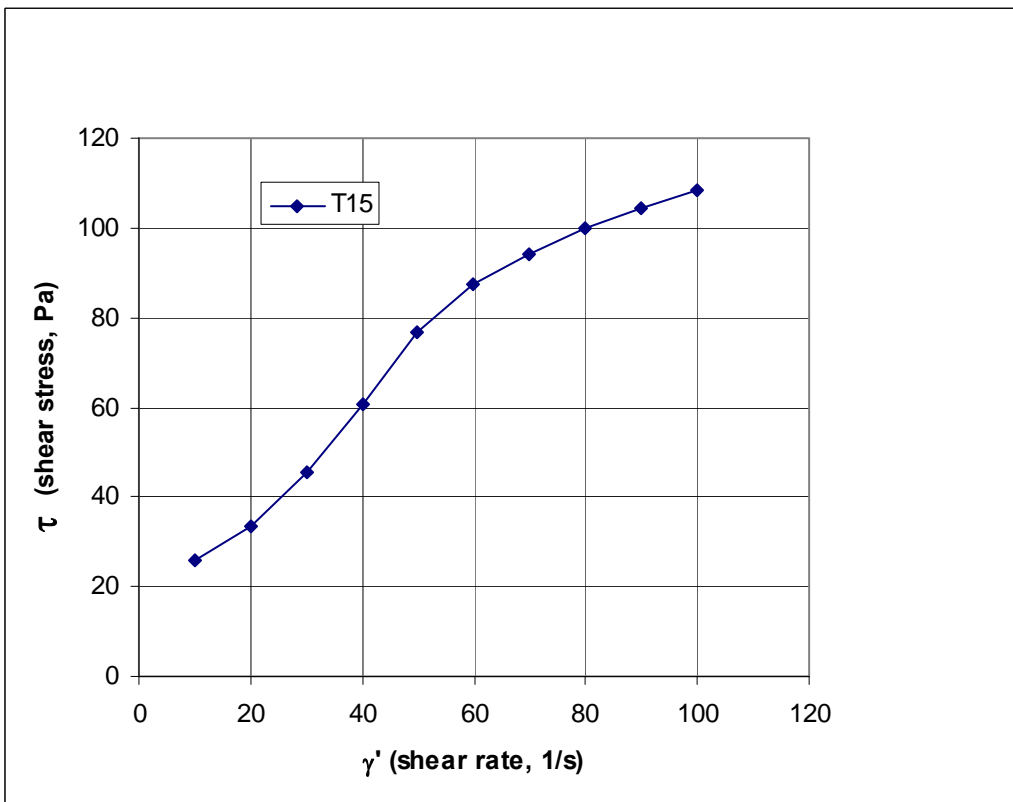


Figure B-29a Shear stress versus shear strain rate tests of T15 mix for shear rate range of 0-100 /s.

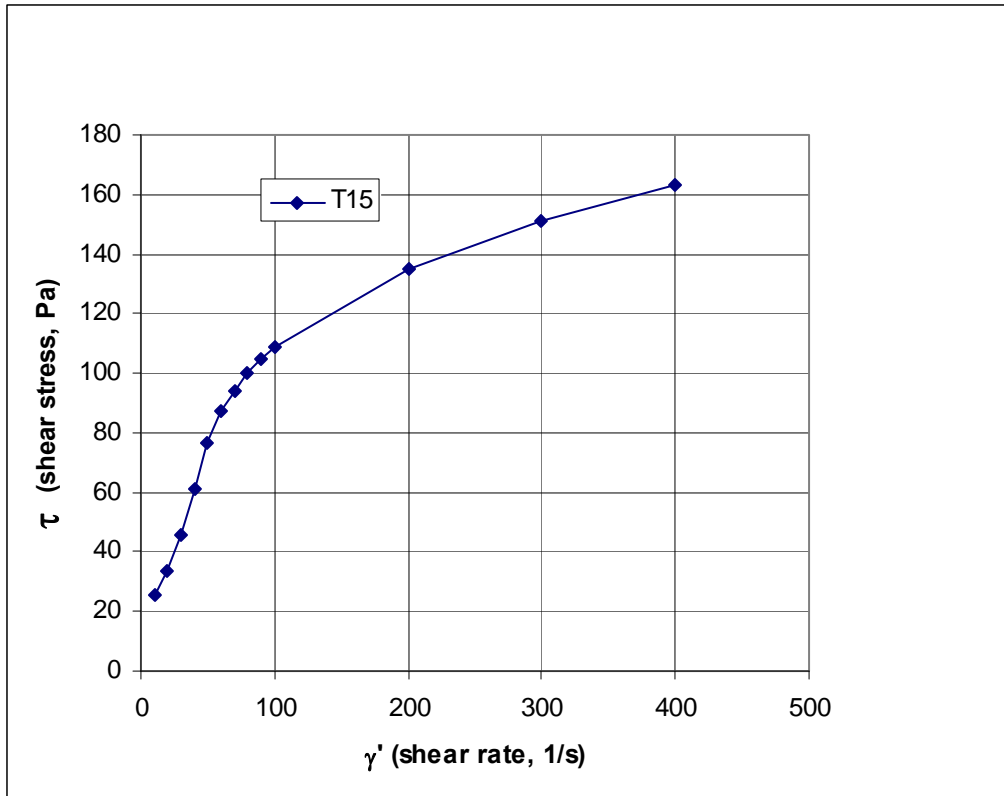


Figure B-29b Shear stress versus shear strain rate tests of T15 mix for shear rate range of 0-400 /s.

B.10 Summary of Viscosity Tests

Viscosity of fly ash is close to water, particularly at very low solid concentrations, however, it increases in orders of magnitude at high concentrations. When compared to all other coal washery mixed slurries, fly ash has proved to have the minimum shear resistance to flow and pump pressure both at low and high speeds.

The viscosity test becomes inapplicable and invalid at concentrations around 75% and larger, where it becomes more like a paste than slurry. A practical range of solid concentration for all grout handling, transporting and backfill operations is in the range of 50% to 60%. Therefore, selection of a pump meeting all the pump pressure and power requirements should be straightforward and not a great deal of technical problem.

B.11 Permeability (UQ)

Like silt, the piping or liquefaction capacity of fly ash is very high and hence can be triggered very easily by shaking or any dynamic loading. On the contrary, once consolidated, it becomes dense and much less permeable. From constant head and falling head permeability tests carried out on the hydraulic fill samples of various types of fly ash, fly ash permeability was measured to be in the range of 7 to 35 mm/h (2×10^{-6} to 1×10^{-5} m/s). According to one of the pioneers of paste technology, Robinsky (1999), virtually all mineral processing methodologies generate tailings amenable to paste production. When being transported either by gravity or through pumping, paste produces a plug flow, with the fine particles creating an outer

annulus, thereby reducing friction. The coarse particles are forced into the centre of the conduit with the finer fraction acting as the carrier. This allows for conveyance of very coarse fragments, the size of which is only limited by the pipe diameter. Very little free water is generated from paste. In addition, the permeability of a poorly sorted, run-of-mill paste is significantly lower than that of classified, well-sorted tailings. When placed underground, the paste may represent a hydraulic barrier to groundwater flow. The reduction in free water results from two characteristics of paste: (i) colloidal retention of water and (ii) reduced infiltration relative to traditional tailings.

Several processes may combine to create the behaviour unique to paste: (i) surface phenomena (electrostatic attraction between water and charged particle surfaces); (ii) chemical interaction between particles and water (e.g. hydrogen bonding); and (iii) physical interaction (water held under surface tension due to high capillary or matric tensile stresses). Since empirical observations have demonstrated that water retention and other paste characteristics, such as rheology, are related to the mineralogical composition of the tailings material, it appears that the chemical parameters of the tailings particles at least in part govern water-particle interaction.

Laboratory and field testing have demonstrated that the permeability of paste is generally approximately half an order of magnitude lower than that of the corresponding tailings slurry. This is primarily caused by the fact that paste is produced from run-of-mill tailings that have not undergone the particle size segregation commonly observed during tailings slurry deposition. Consequently, the paste maintains the full distribution of particle sizes, which results in the reduced permeability characteristic of poorly-sorted materials. In addition to the effect of grain size distribution, the tensile stresses in the tailings are responsible for reduced infiltration. This occurs because the gravitational downward pull on the liquid surrounding the tailings particles is countered by upward capillary suction (Robinsky, 1999). Ad mixture of small amounts (e.g. 1 to 2% by mass) of binder materials with pozzolanic and/or cementitious parameters may further decrease the permeability of the paste.

B.12 Suction Test

Since solid particles of fly ash are heavier than water by approximately 2 times, they settle down with time in a stationary hydrostatic slurry container, in which clear water stays on the top and solid particles deposit in the bottom of the container, as shown in Figure B-30 (top left photo). A suction tube was then applied to observe the effect of suction on the deposited sediment. As shown in the same figure (top right and bottom photos), the effect is highly local with minimum disturbance to far field sediment. The tube was penetrated into the deposit and it created a clear borehole of the same tube size. Figure B-31 shows what happens when the water inflow is put back into the suction hole.



Figure B-30 Suction test by siphoning water from a submerged fly ash sediment

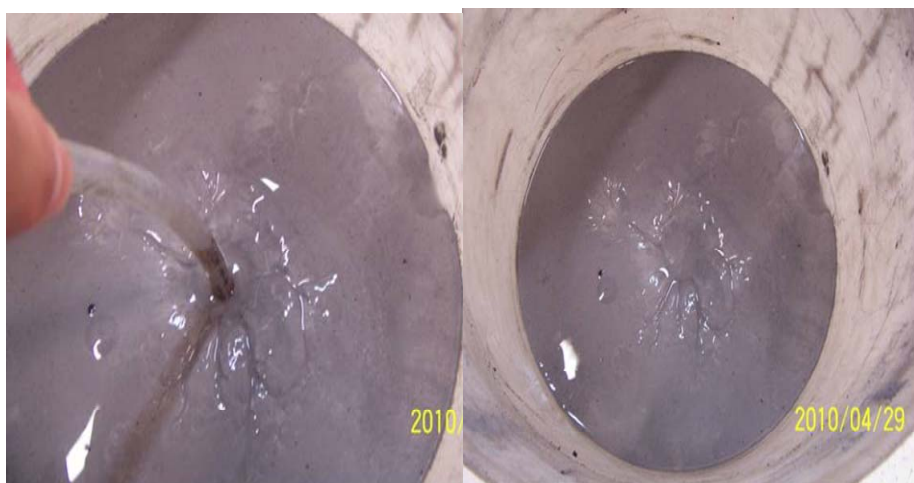


Figure B-31 Water backflow into fly ash by the same tube used for suction

B.13 Density Tests (UQ)

Like other soils, density of fly ash is a function of its moisture content, preloading and compaction and consolidation conditions. There is a strong correlation between fly ash strength and density. The specific gravity of Swanbank River fly ash is around 2, so that its saturated consolidated density, under 1.5 MPa and 3.0 MPa compressive loading, can reach a value between 1.5 and 2. It can also have a very low density, e.g. under natural moisture content of around 11% and loose and light condition its density is only around 0.81, which can reach above unity by either dry compaction or submerged consolidation.

Laboratory sedimentation testing has shown that hydraulic fill slurry settles to a dry density (g/cm^3) of 0.6 times the specific gravity (G_s) for a wide range of tailings with specific gravity values ranging from 2.8 to 4.4. This implies that all the hydraulic fills settled to a void ratio of 0.67 and porosity of 40%. Laboratory sedimentation testing verified this to some extent. A generic “rule of thumb” for the particle size distribution is for a minimum of 15% of the material to be finer than 20 mm, which ensures that the surface area of the particles is large enough to provide adequate surface tension to hold the water on the solid particles and provide a very thin, permanent lubricating film. Paste fill typically shows non-Newtonian Bingham plastic flow characteristics, resulting in plug flow (batches flow in solid slugs) characteristics of the paste.

Paste fill contains at least 15% of particles finer than 20 mm, and an effective size which 10% of particles pass (D_{10}) in the order of 5 mm. The 3 to 6% binder improves the strength and thus stability significantly. The large fines content of the paste fill enables most of the water to be held to the surface of the particles, and therefore drainage is not a concern on paste backfilling. High fly ash content flowable fill mixes are usually less dense than compacted natural soils, with wet densities ranging from 1.46 to 1.95 g/cm^3 (the first-placed material being densest). Low fly ash content flowable fill mixes have wet densities ranging from 1.79 to 2.19 g/cm^3 . Significant decreases in density (as low as 0.33 kg/m^3) have been achieved in high fly ash content flowable fill mixes by the use of foaming agents in proprietary mixtures for the purposes of load reduction.

Variations of density in different backfilling laboratory flume tests by UQ, summarised in Table B-5, highlights the potential sensitivity of density to field backfilling operational and environmental conditions. As shown in the table, by an increase in the slurry head, both the solid concentration and density of the fly ash deposit have increased, e.g. the dry density increased from about 1.0 g/cm^3 without an applied head to about 1.5 g/cm^3 with an applied head.

Table B-5 Initial and final average % solids, gravimetric moisture content and dry density on column settling, and on flume testing under a head of Swanbank fly ash slurry

% SOLIDS		GRAVIMETRIC MOISTURE CONTENT (%)		DRY DENSITY (g/cm ³)	
Initial	Final	Initial	Final	Initial	Final
On column settling (no excess head of fly ash slurry)					
55	64.9	81.8	54.2	0.771	0.980
50	66.7	100.0	50.0	0.676	1.022
45	68.0	122.2	47.1	0.588	1.053
35	72.2	185.7	38.6	0.428	1.157
Flume testing 50 mm void under high head of slurry @ 50% solids (initially 416 mm, finally 218 mm)					
50	88.4	100	13.1	0.676	1.641
Flume testing 50 mm void under high head of slurry @ 60% solids (initially 380 mm, finally 263 mm)					
60	82.1	66.7	21.8	0.873	1.436

B.14 Consolidation Tests (UQ)

Deposited fly ash particles should not only remain stable but also be able to have the required stiffness and strength to carry potential overburden loads, which can change with time, at minimum compressive deformations of the deposited fly ash. To check this property of the grout we have carried out a few consolidation tests (Figure B-32). A typical result is shown in Figure B-33, which shows the variation of consolidation deformation due to an increasing pressure on a saturated sample of 50mm diameter with 75% solids weight concentration. Under a total ultimate pressure of 2 MPa, a sample with an an initial height of 17.9mm deformed to a final height of 15.8mm, i.e. approximately 12% consolidation deformation took place.



Figure B-32 Water backflow into fly ash by the same tube used for suction

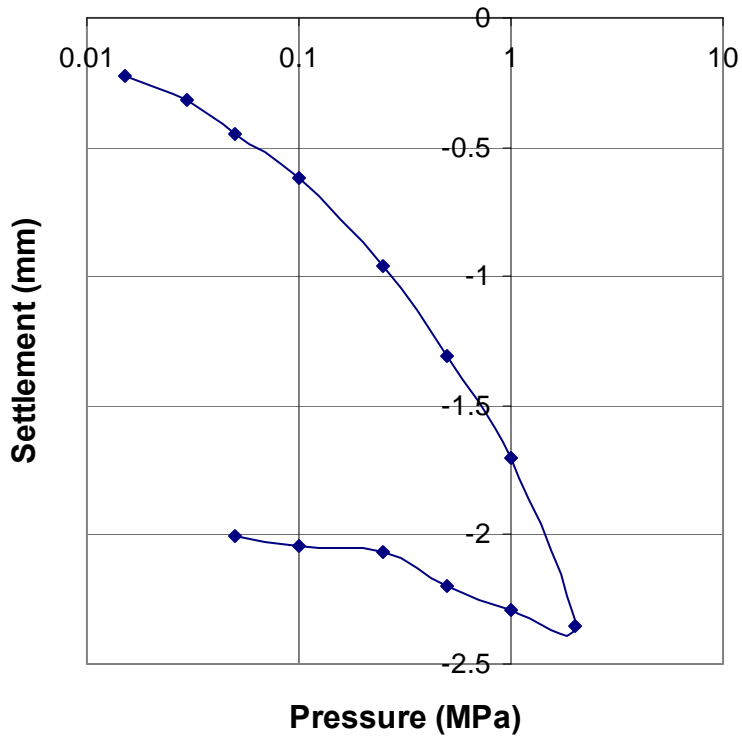


Figure B-33 Consolidation test of 75% non-cohesive fly ash slurry

The end-points of the oedometer test effective stress increments applied to Swanbank fly ash initially at 50% solids (initial void ratio e_0 of 2.09) are shown in Figure B-34, from which a Compression Index C_c of 0.0455 is calculated.

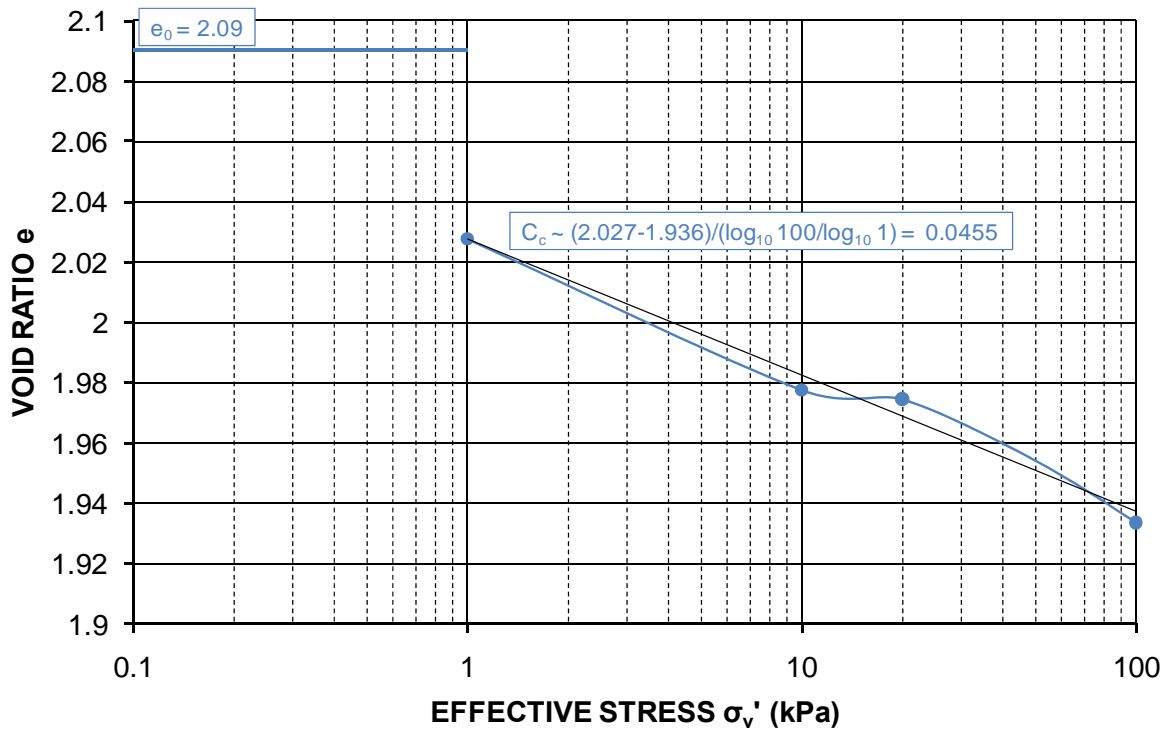


Figure B-34 Oedometer plot of Void ratio vs. Effective stress for settled Swanbank fly ash

A commonly-used approximation for calculating the Compression Index of clayey soils is:

$$C_c \sim 0.009 (LL-10) \quad (3)$$

where LL = Liquid Limit in %. For the measured average LL of Swanbank fly ash of 45.7% (**Appendix C**), Equation (1) suggests a C_c value of 0.32, and C_c values > 0.3 are typically quoted for soft clays.

The measured C_c value of 0.0455 for Swanbank fly ash is very much lower than typical values for soft clays, which may be explained by the high silt, sand and gravel-size fractions of Swanbank fly ash.

Coefficient of consolidation, c_v , in $m^2/year$, and Coefficient of volume decrease, m_v , for the Swanbank fly ash are obtained from the UQ oedometer tests. Table B-6 summarises the oedometer test parameters obtained for Swanbank fly ash.

The settlement-time data obtained for each effective stress increment are plotted in terms of \log_{10} (Time) in Figure B-35. From these plots and similar $\sqrt{\text{Time}}$ graph (**Appendix C**), the Coefficients of Consolidation c_v were estimated by graphical means. From the Settlement versus \log_{10} (Time) plot, c_v is given by:

$$c_v = 0.196 (d^2/t_{50}) = 3.91 \quad (4)$$

From the Settlement versus $\sqrt{\text{Time}}$ plot, c_v is given by:

$$c_v = (\pi/4) (d^2/t_1) = 33 \quad (5)$$

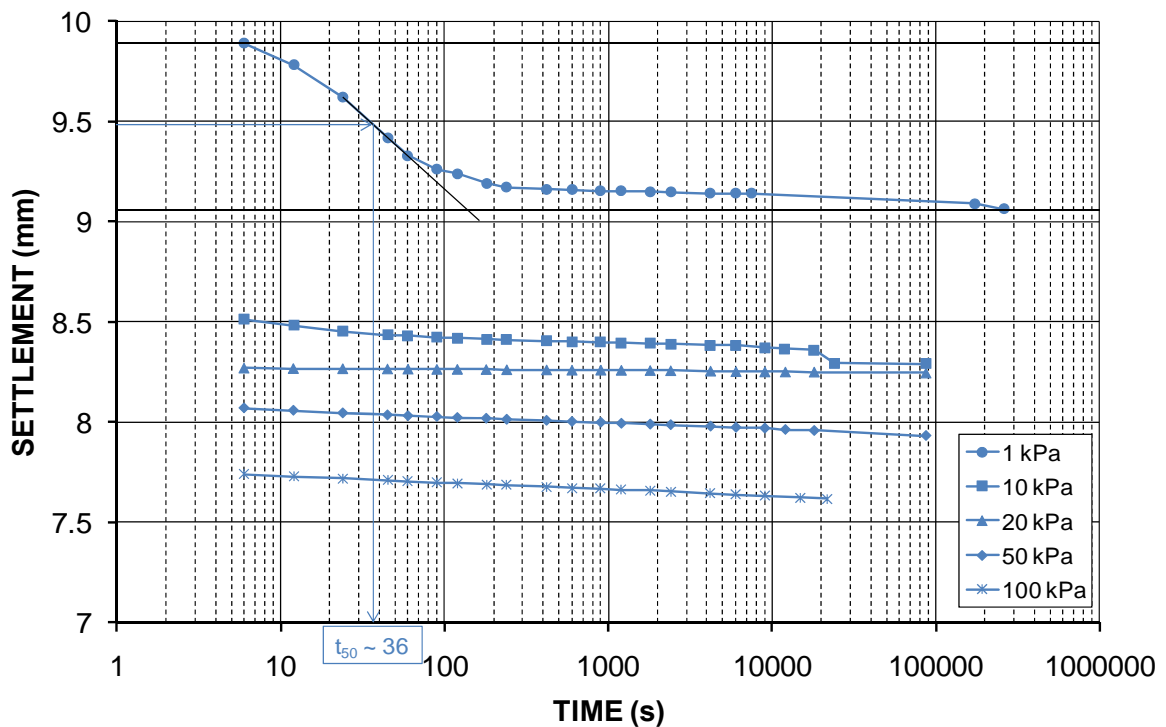


Figure B-35 Oedometer settlement vs. \log_{10} (Time) for settled Swanbank fly ash at various effective stresses

Table B-6 Oedometer test parameters

EFFECTIVE STRESS σ_v' (kPa)	VOID RATIO e	COEFFICIENT OF CONSOLIDATION c_v (m ² /year)		COEFFICIENT OF VOLUME DECREASE m_v (m ² /MN)	HYDRAULIC CONDUCTIVITY k (m/s)	
		Log ₁₀ Time	√Time		Log ₁₀ Time	√Time
0		-	-	-	-	-
1		3.91	5.64	6.537	7.95 x 10 ⁻⁹	1.15 x 10 ⁻⁸
10		-	42.8	0.665	-	8.85 x 10 ⁻⁹
20		-	47.0	0.333	-	4.87 x 10 ⁻⁹
50		-	45.9	0.134	-	1.91 x 10 ⁻⁹
100		-	23.4	0.068	-	4.91 x 10 ⁻⁹
Averages		3.91	33.0	1.547	7.95 x 10⁻⁹	5.52 x 10⁻⁹

B.15 Friction Angle

Friction angle of fly ash is a function of its density, void ratio, moisture content, degree of saturation, submergence and/or pore water pressure. Therefore, it is natural to expect that density, and hence friction angle, of a deposited layer of fly ash varies increasingly with depth. It is also evident from UQ direct shear tests that flyash dilates during the plastic shearing test. Under natural moisture content of around 11%, the repose or beach angle can reach to as high as 40-45 degrees, when it is measured from a pile of fly ash poured on a dry pile. However, when poured submerged, this can reduce to 1.5 to 2.2 degrees, as shown in Figure B-36. The reason for its very low friction angle is the effect of pore water in the porous medium inhibiting solid to solid contact between fly ash particles (low mix density). Once the pore water is drained either by consolidation or by drying, the higher values of friction come back again due to densification. An important phenomenon is the friction angle of the fly ash slurry reflected in the beach profile angle. Fly ash slurries with 50% to 60% solids weight concentrations usually maintain a "friction angle", or more precisely the angle of repose, or beach profile angle, in the range of 2-10 degrees depending on the solids weight concentration. This implies that the higher the concentration of the slurry, the closer the injection boreholes should be drilled to guarantee a perfect backfilling operation. It also becomes harder to fill behind constrictions and obstacles at higher solid concentrations.

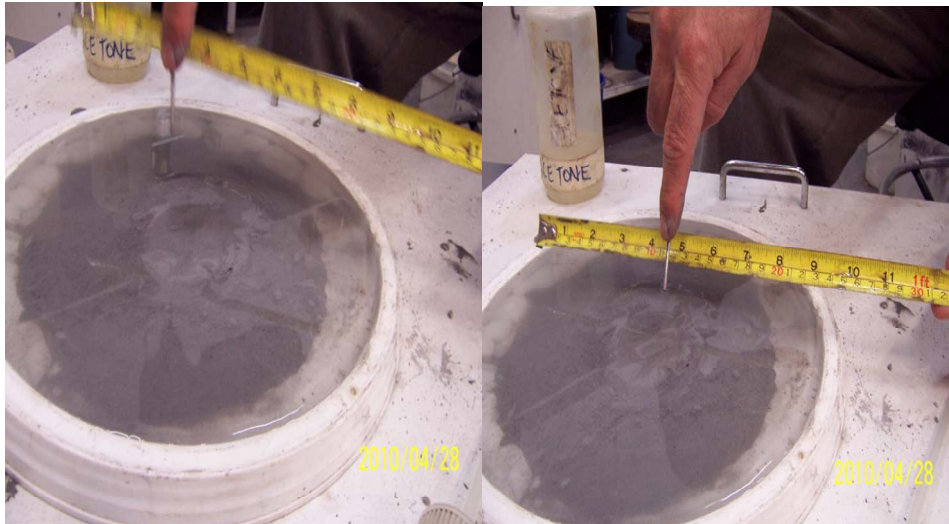


Figure B-36 Measuring angle of repose or friction angle of submerged fly ash.

B.16 Adhesion Test

Fly ash can stick to another material at remarkably high adhesion at a critical moisture content and density. Figure B-37 shows how a sticky remoulded paste of this material can be made, which can be tilt to even more than 40 degrees without becoming loose or unstable. However, it can easily be washed away by water flow, as shown in the bottom photos of the same figure.

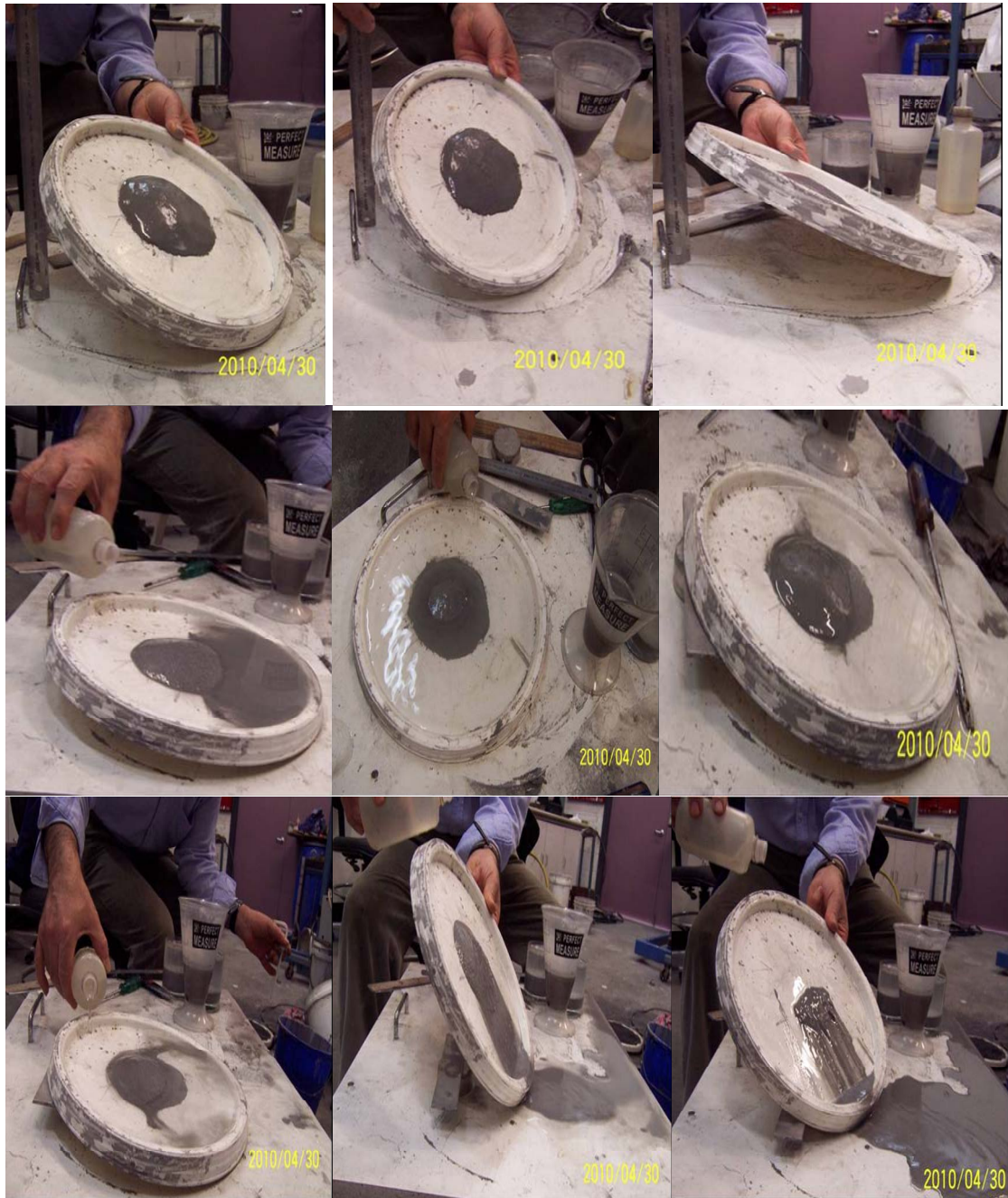


Figure B-37 Measuring adhesion and erosion of compacted fly ash on a plate

A.16.1 Disc grout tests

A.16.2 Single layer

A series of disc grout tests were conducted on Swanbank river fly ash (FA) both with and without cement. The testing gear consists of a disc of 1m diameter with an adjustable variable gap thickness, simulating a rock fracture opening, and a vertical pipe line at its centre, simulating an injection drilled borehole. The testing gear is shown in Figure B-38. As shown in the figure, the bottom disc plates can be pressurised by a separated oil chamber to balance and regulated the desired deflection of the bottom plate. Once slurry is injected through the vertical pipe, it

flows into the disc gap and flows radially. All parameters such as flow rate and pressure at key specified points can be measured. A pipe with an internal diameter of 4mm and a disc gap of 4mm thickness have been applied to all the fully-developed, single layer, disc grout tests discussed in this section. Notice that in some tests, rather than having a full free 360 degrees radial flow, the radial flow has been constricted to only a 90 degree section (e.g. Figure B-39). The major objective in these tests is to examine the flow-ability and the extension of the flow (radial distance) of the grout fluid through not only the 4mm disc gap but also any obstacles (resembling mine pillars) provided in front of its movement.

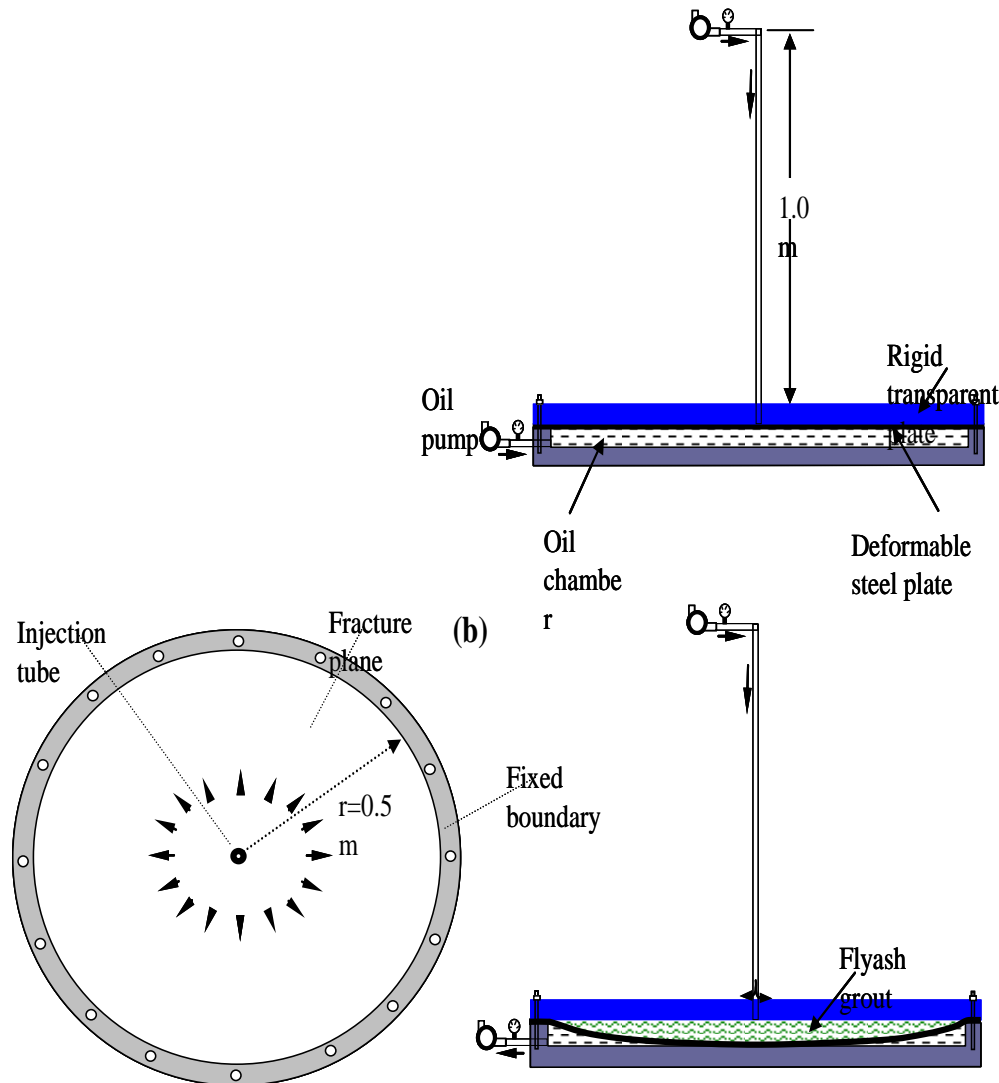


Figure B-38 Schematic of small scale laboratory grout injection testing gear simulating flow through rock cracks via a vertical pipe simulating grout injection borehole

Series of photos in Figure B-39 show flow of a fly ash grout at more than 50-70% solids weight concentration in a 90 degree section through a 4mm disc gap, and also through wide pillars and narrow curly path ways of 4mm height. There was no problem for various slurries fill these voids.



Figure B-39 Fly ash grout infill in a 4mm disc gap void (top left) and through wide voids and obstacles (top right and middle rows) and narrow curly paths (bottom row)

A.16.3 Double layers

Using several ring plates of 1mm thickness each, the disk gap thickness can be adjusted from 0 to 6mm. In a particular grout test shown in Figure B-29, first three rings were installed to provide a 3mm gap for slurry injection. The slurry grout (55% solids weight concentration) was injected successfully to cover the entire area of the disc. After two days, the top, thick, transparent lid was removed and another set of 3 rings were added to the previous rings to increase the total gap thickness to 6 mm. In other words, a net gap thickness of 3mm was left for the second layer grout injection experiment. As shown by the photos of Figure B-40, the behaviour of the flowing

slurry on a previous grout was not much different from the first layer experiment. The second layer filled the whole gap and covered the entire disc area successfully.

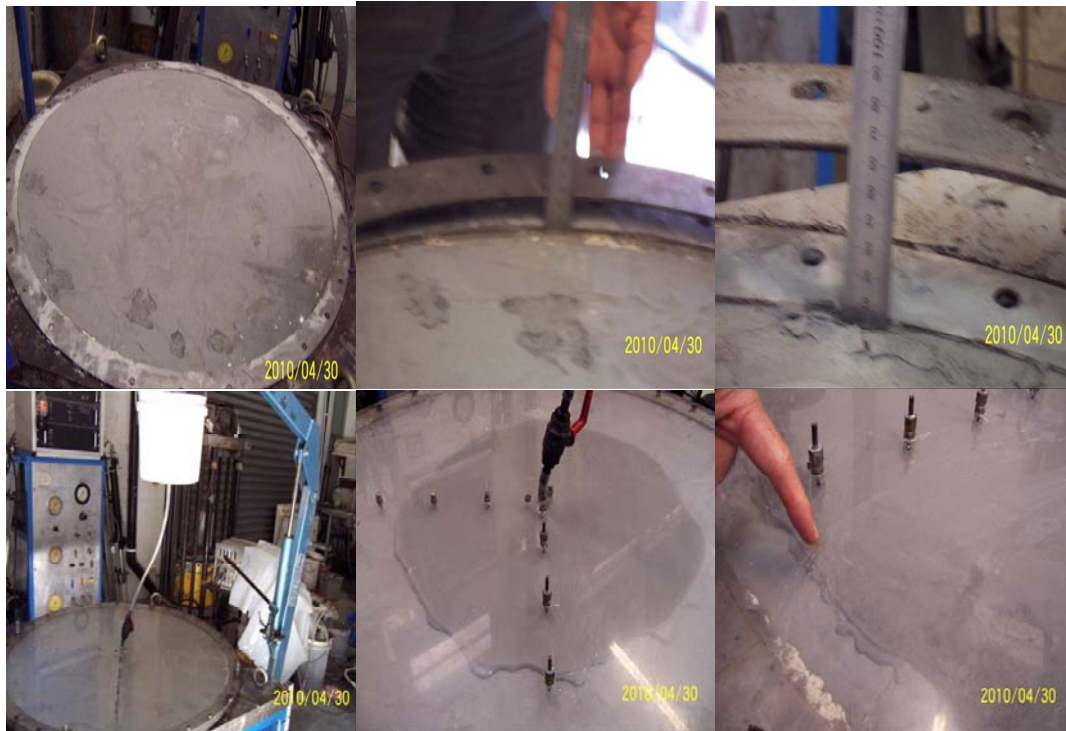


Figure B-40 Multiple grout layering and fly ash injection experiment in two 3mm gap thickness layers. First layer is shown in photos on top row and progress of second layer is shown in bottom row photos.

B.17 Pipeline transport tests

Fly ash slurries need be pumped through several pipes and bends to reach the target borehole destinations. Transportation of two phase slurries, in which solid particles are easily separated and deposited as sediments, is a challenging task, because blockage of the flowing slurry can occur, whenever the speed of suspended particles drops below a critical threshold velocity (Figure B-7). In this case, even injection of pure water, boosted by high pump pressures, may still be inadequate to solve the problem to reactivate the flow in a long pipe or sharp bend. Therefore, transportation characteristics of slurry need to be determined before any field injection trials. For such purposes, CSIRO conducts pipe-loop tests with both steel pipes, normally with diameters of 50 mm, 100 mm and 150 mm, and flexible pipes or hoses of different diameters. Here, only flexible rubber pipes of 20mm diameter were used for Swanbank fly ash slurry experiments, as shown in Figure A-41. The loop test results revealed the fact that fly ash slurry could successfully be pumped at all solids weight concentrations even up to 75% with no problem.

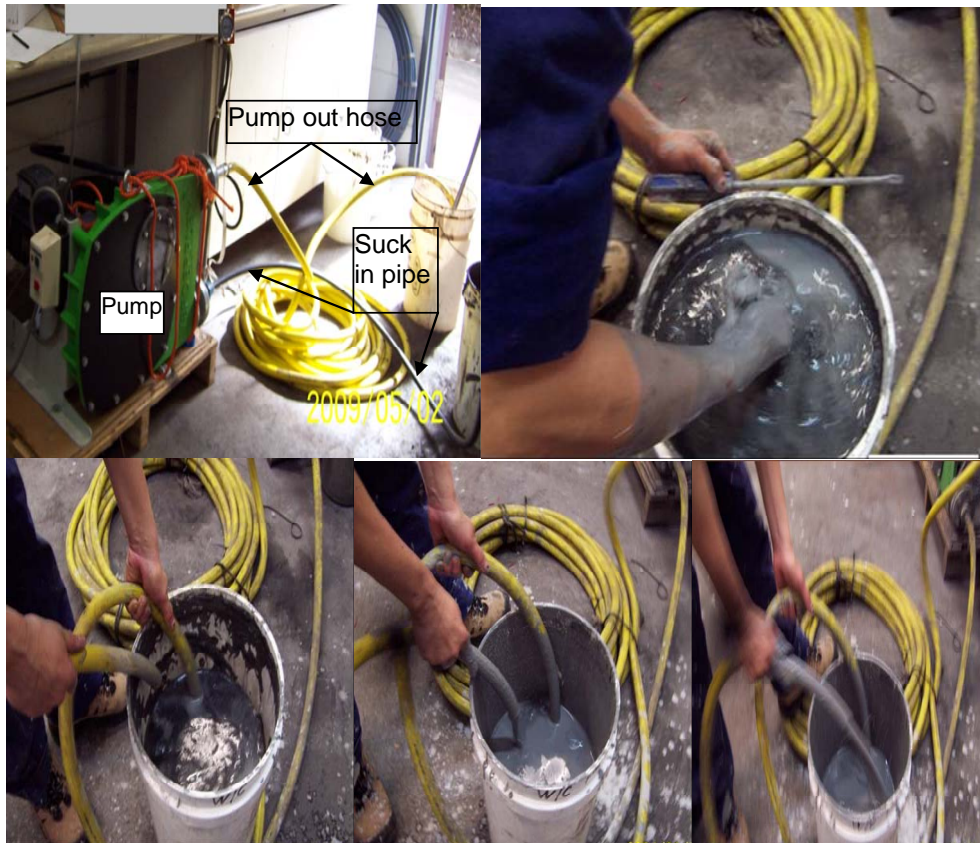


Figure B-41 Slurry transportation tests through 20mm rubber pipe of 20m length. Top left: CSIRO VERDERFLEX VF32 pump and flexible hose for slurry transportation tests. Top right: Fly ash slurry of 75% solids weight concentration before loop test. Bottom row: Loop or transport test of fly ash slurry at 75% solids weight concentration.

The principle of the peristaltic hose pump shown in Figure B-41 is based on moving the slurry through the hose, by alternately squeezing and releasing the hose. A smooth, flexible hose lies in the pump housing and is completely flattened against the wall of the housing by the action of two shoes mounted on a rotor. The rotating rotor causes the product to be moved through the hose at a constant volume and without any loss through leakage. This makes the pump suitable for dosage applications. After the hose is released, an almost complete vacuum arises, which ensures that the product is drawn into the hose. Its maximum possible pressure is 1.5 MPa, and its maximum possible flow rate is 4.2m³/hour, which implies a maximum possible flow velocity of 3.7 m/s in a 20mm pipe. All slurries of fly ash, including the cemented slurries, could be successfully pumped and circulated through all the commercial rubber pipes, even in their original curved, folded stack shape.

In the field, piston driven displacement concrete pumps seem to be quite appropriate for transportation of grout in the pipeline for all the thin and thick slurries tested here, provided their design operating power is adequate to provide the required pressure against the resisting shear and viscous frictional force. These slurry pipe tests emphasise the importance of the pump type and model required to inject slurry in long distances over surface ground, in the pipeline bends, in the injection borehole and finally in the radial direction in the underground void and to settle far enough from the borehole to provide a complete successful layer by layer backfilling of the void.

B.18 Flume Tests (UQ)

To simulate flooding effects on consolidated deposited fly ash, slurry flume tests were conducted at the Civil Engineering laboratory at the University of Queensland (UQ). The arrangement is shown in Figure B-42 and the complete UQ report on these tests is included in **Appendix C**.

The proposed testing was outlined in proposals dated 4 January and 2 June 2010, and focused on the beaching and settling of Swanbank fly ash at a range of % solids in a laboratory beaching flume measuring 2 m long, by 0.6 m wide by 0.6 m high (Figure B-42). Four series of tests was carried out in the flume: (i) sub-aerially (unflooded, no constriction) to simulate backfilling of a large, unflooded underground void, (ii) sub-aerially through a constriction to simulate backfilling of a narrow, unflooded underground void, (iii) under water (flooded, no constriction) to simulate backfilling of a large, flooded underground void, and (iv) under water and a head of fly ash slurry to simulate backfilling of a closed-ended, flooded underground void.

Characterisation testing of the Swanbank fly ash was also carried out, including particle size distribution analysis, Atterberg limit testing, specific gravity determination, Emerson crumb testing, total suction determination, and pH and Electrical conductivity testing. In addition, laboratory geotechnical parameter testing was carried out, including settling column testing, undrained vane shear and drained direct shear strength testing, and oedometer testing. By way of comparison, a drained and desiccated beach at Swanbank was profiled, sampled and characterised.

(a) Schematic

(b) Constricted, under water set-up

Figure B-42 UQ laboratory beaching flume

Figure B-43 summarises all of the open-ended beach profiles obtained for Swanbank fly ash tested at different % solids in the laboratory flume. Clearly, the higher the initial % solids, the steeper the beach profile, with $\leq 35\%$ solids producing an almost flat beach.

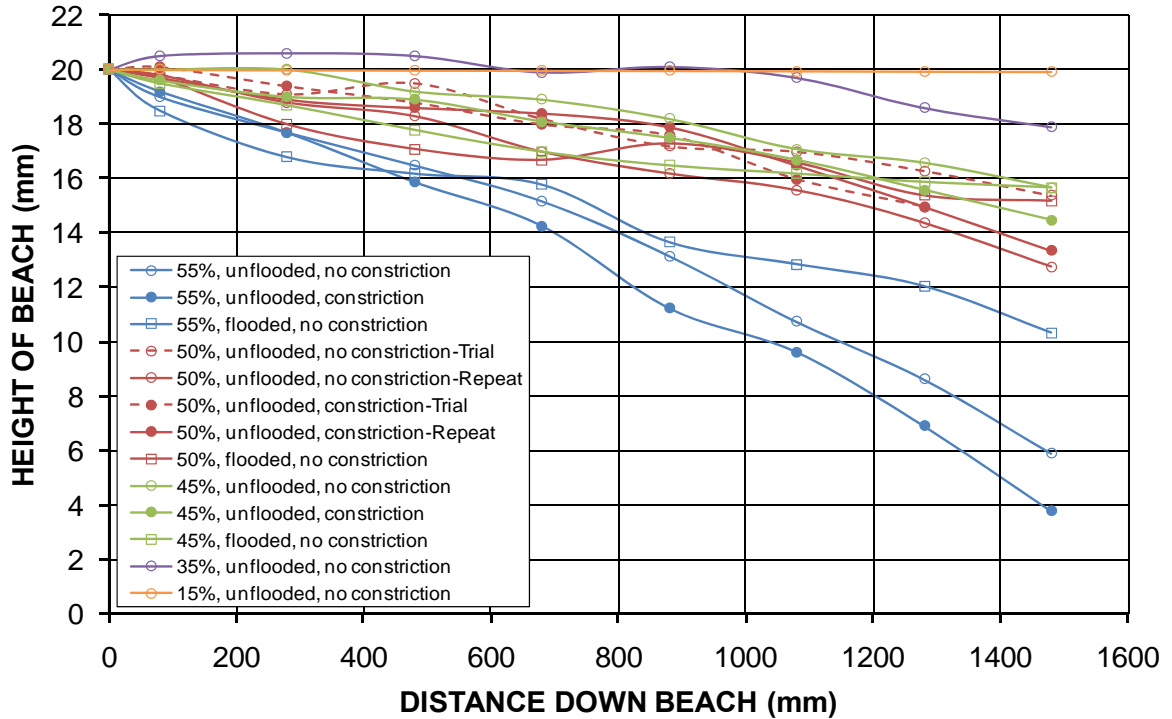


Figure B-43 Summary of open-ended laboratory flume beach profiles for Swanbank fly ash

Figures A-44, A-45 and A-46 show the open-ended beach profiles obtained for Swanbank fly ash tested at 55%, 50% and 45% solids, respectively, in the laboratory flume. At 55% solids, the steepest beach slope occurs due to a constriction, and the flattest beach slope occurs due to flooding. At $\leq 50\%$ solids, there is little distinction between beaches regardless of whether they are unflooded, flooded or constricted.

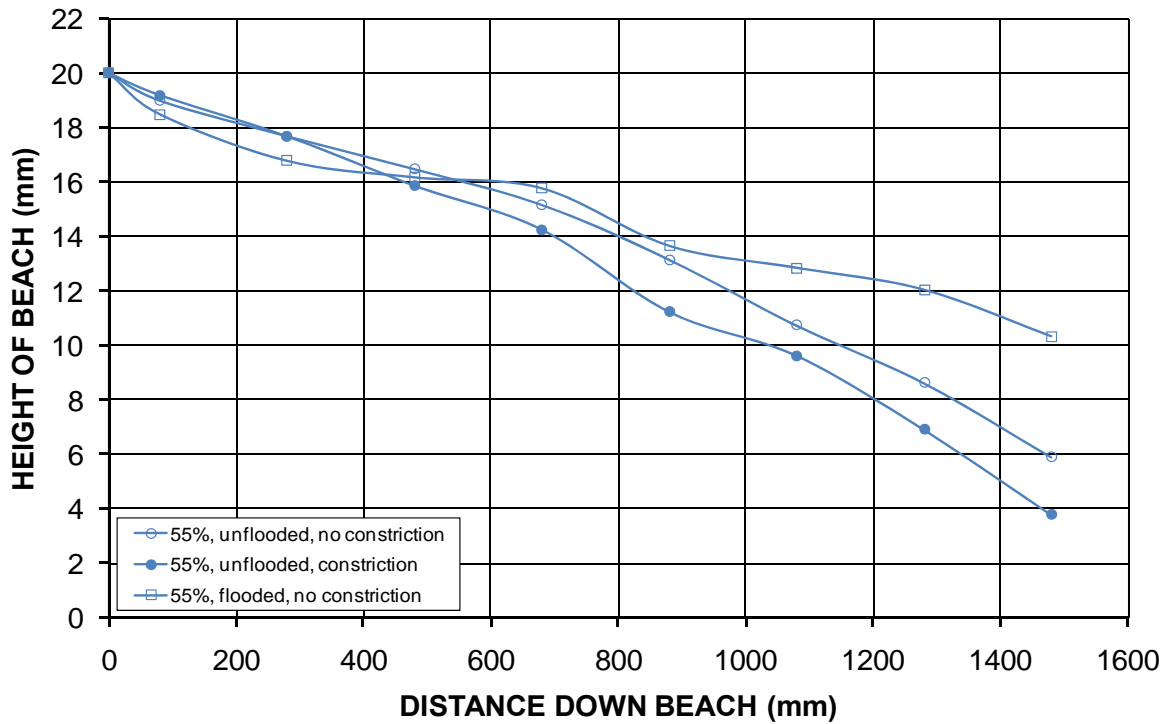


Figure B-44 Summary of open-ended laboratory flume beach profiles for Swanbank fly ash

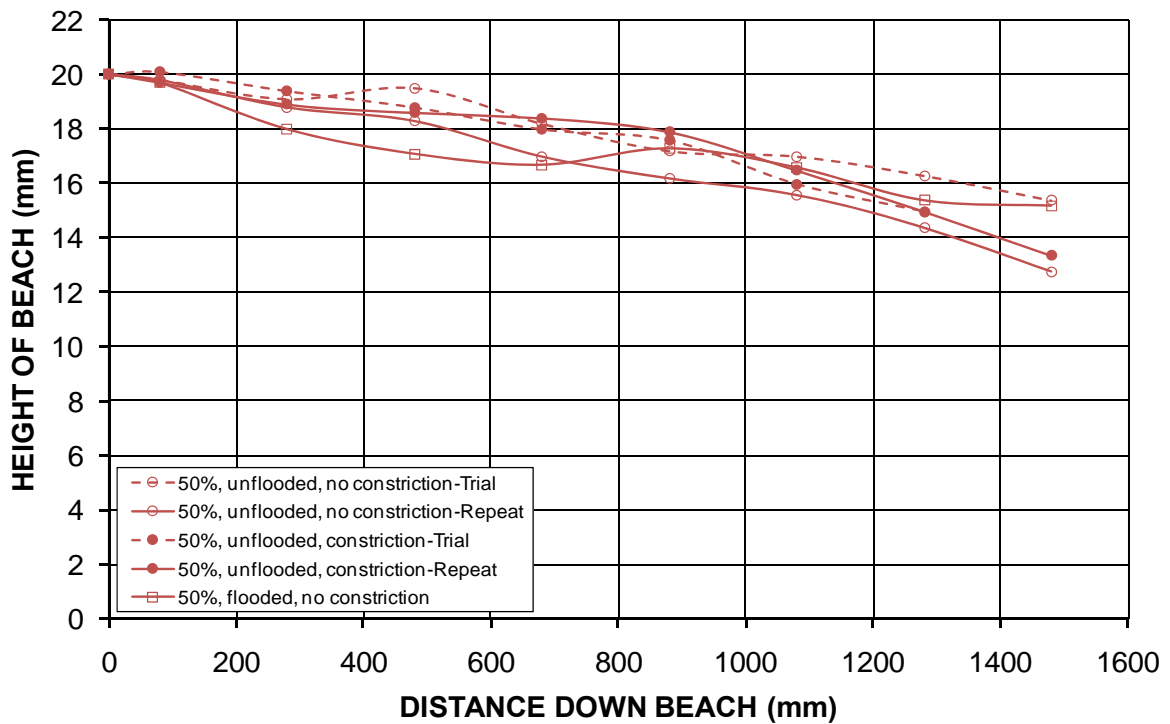


Figure B-45 Summary of open-ended laboratory flume beach profiles for Swanbank fly ash

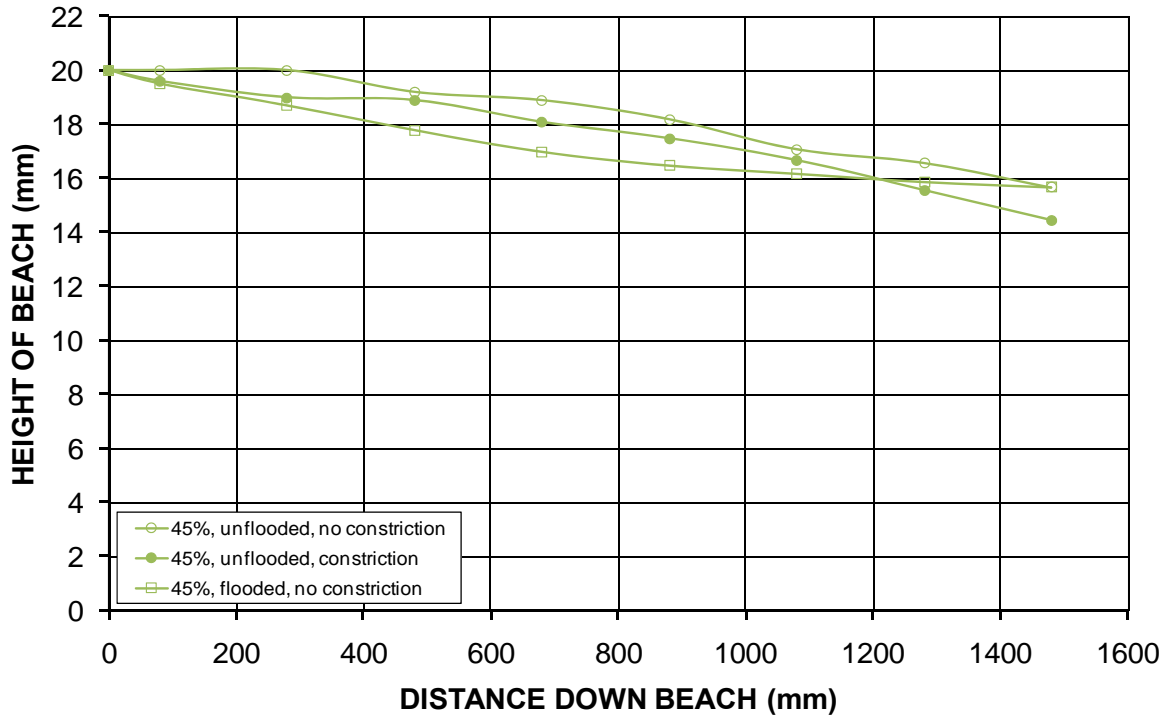


Figure B-46 Summary of open-ended laboratory flume beach profiles for Swanbank fly ash

Sub-Aerial, Unconstricted Beaching

Figure B-47 compares the open-ended, unflashed, unconstricted beach profiles obtained for Swanbank fly ash tested at different % solids in the laboratory flume, highlighting that the higher the initial % solids the steeper the beach profile.

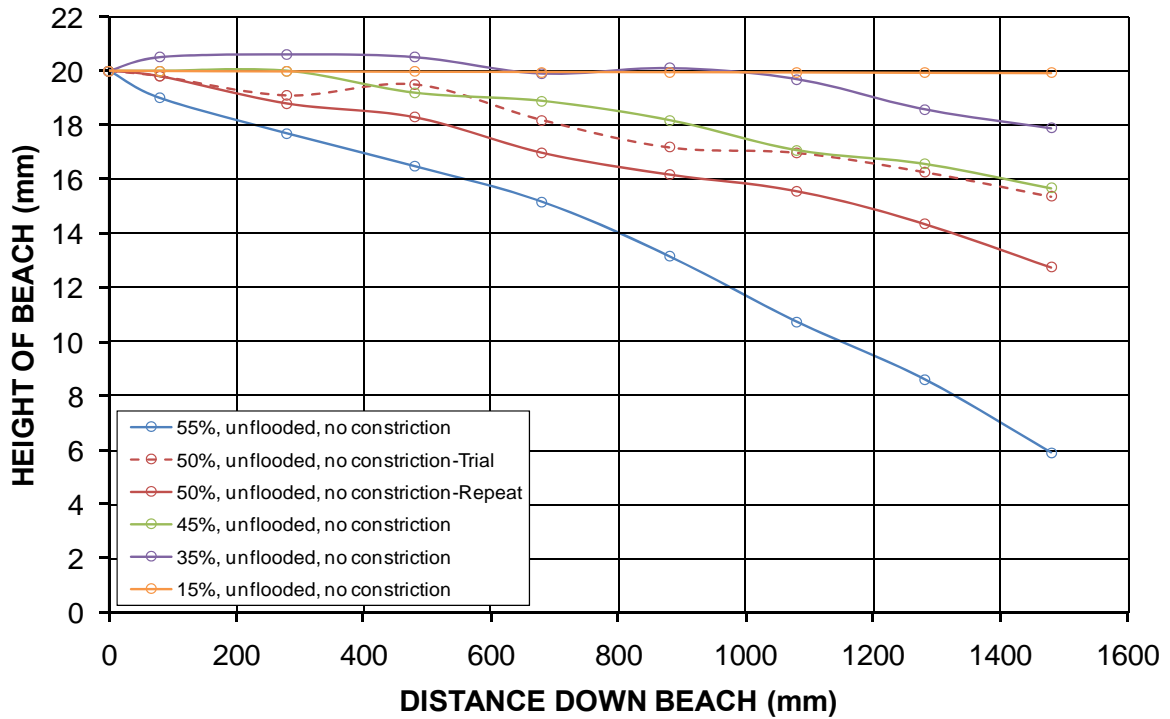


Figure B-47 Laboratory flume test beach profiles for unflooded, unconstricted deposition of Swanbank fly ash

Sub-Aerial, Constricted Beaching

Figure B-48 compares the open-ended, unflooded, constricted beach profiles obtained for Swanbank fly ash tested at different % solids in the laboratory flume, highlighting that only 55% solids produces a markedly steeper beach profile. The constriction has the effect of holding back the slurry, leading to a reduced beach slope before the constriction, and frees up the slurry flow beyond the constriction, leading to a steeper beach slope.

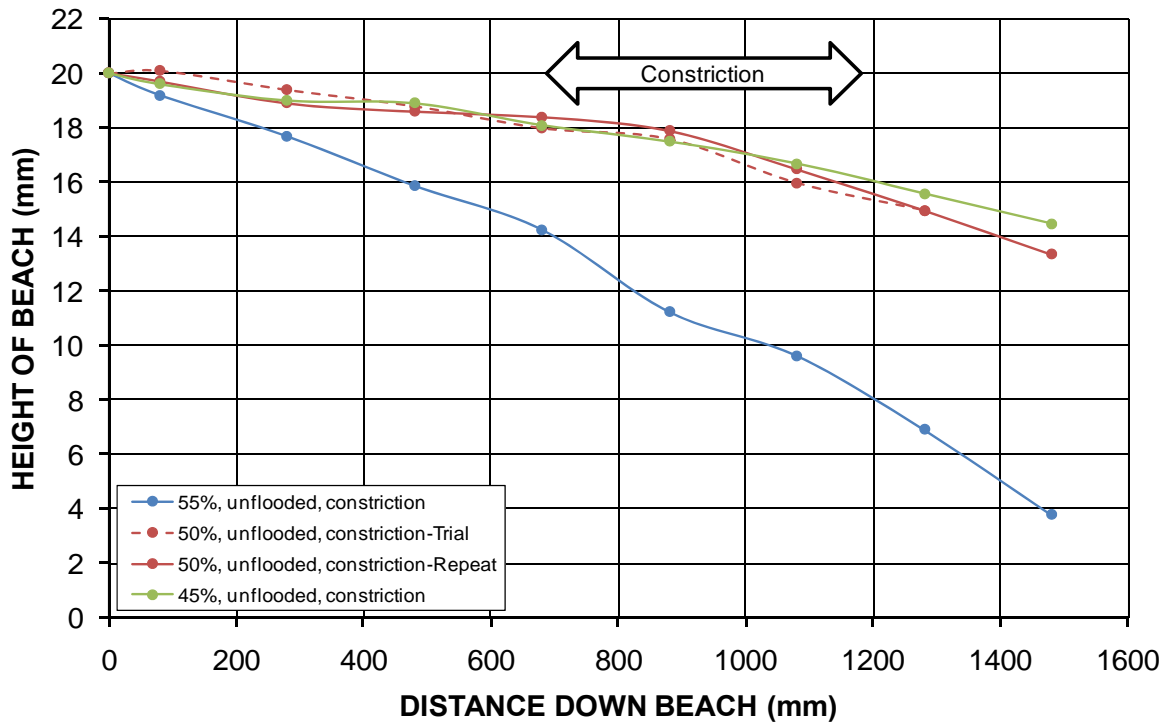


Figure B-48 Laboratory flume test beach profiles for unfllooded, constricted deposition of Swanbank fly ash

Under Water, Unconstricted Beaching

Figure B-49 compares the open-ended, fllooded, unconstricted beach profiles obtained for Swanbank fly ash tested at different % solids in the laboratory flume, highlighting that only 55% solids produces a markedly steeper beach profile.

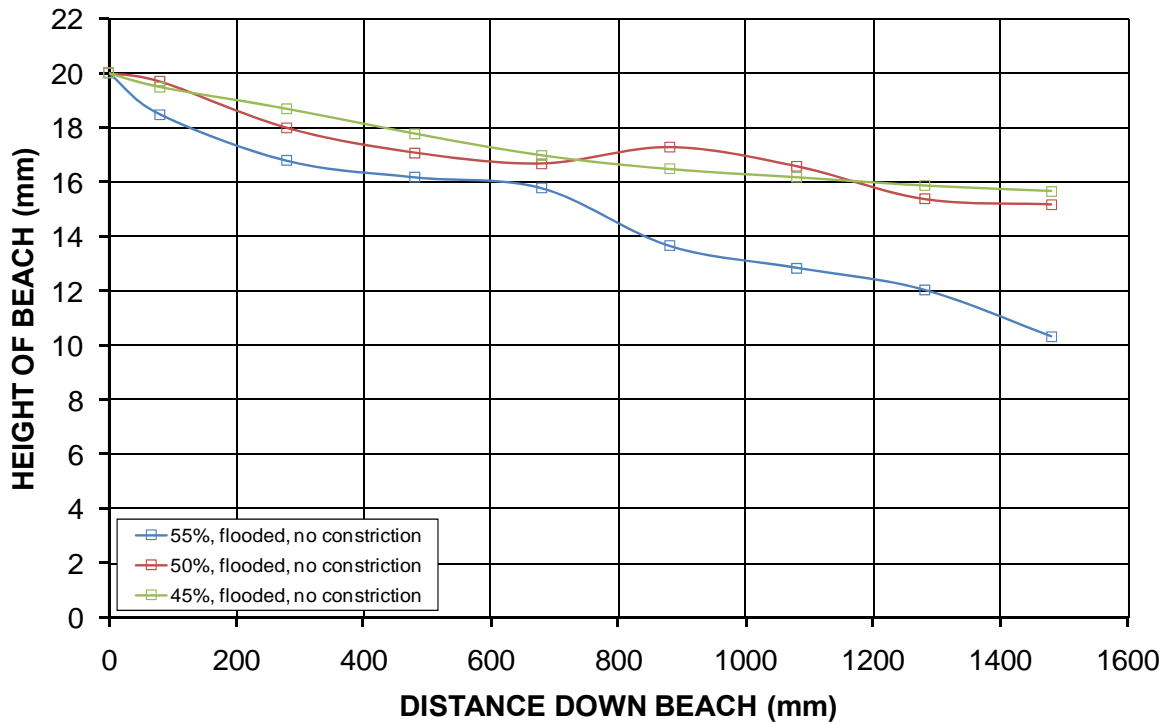


Figure B-49 Laboratory flume test beach profiles for flooded, unconstricted deposition of Swanbank fly ash

Constricted Backfilling, Under Water and a Head of Slurry

Figure B-50 shows the settled slurry profile resulting from flooded deposition of Swanbank slurry initially at 55% solids, under a low slurry head into a closed-ended constriction.

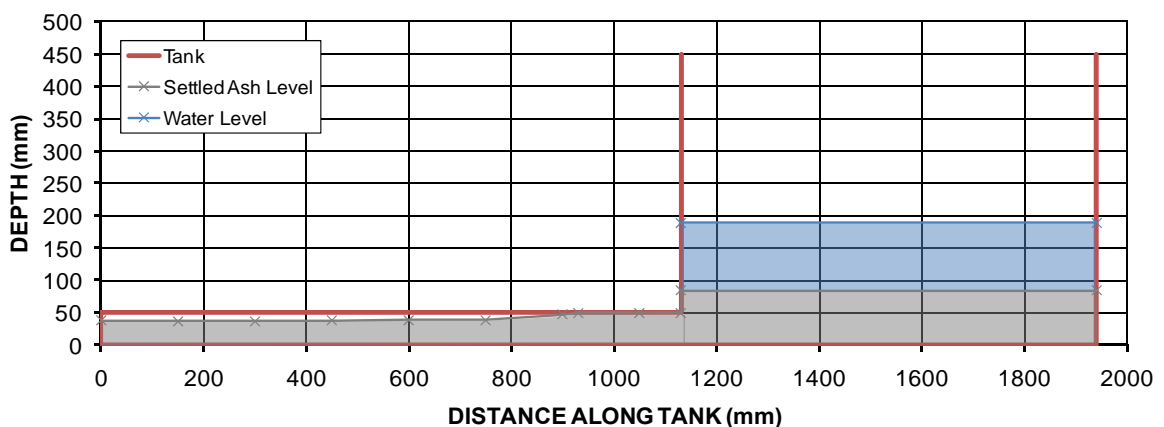


Figure B-50 Constricted backfilling, under water and a low head of Swanbank fly ash slurry, initially at 55% solids

Figure B-51 shows the settled slurry profile resulting from flooded deposition of Swanbank slurry initially at 60% solids, under a high slurry head into a closed-ended constriction.

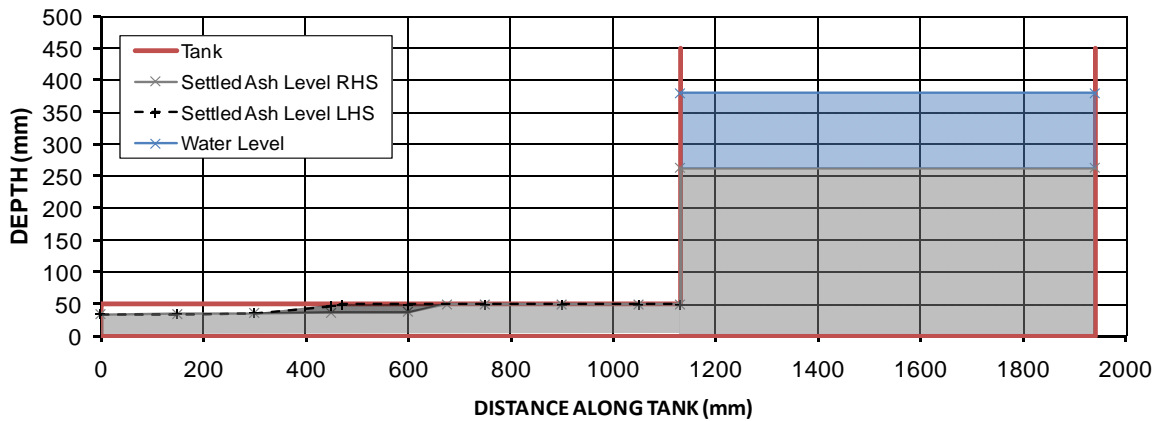


Figure B-51 **Constricted backfilling, under water and a high head of Swanbank fly ash slurry, initially at 60% solids**

Figure B-52 compares the average laboratory and field beach slopes obtained for Swanbank fly ash at different initial % solids, which highlights that for unflooded, unconstricted beaching the average beach slope is highest (at about 1%) for an initial % solids of 55%, lower but insensitive over the intermediate range of initial % solids, and flat for an initial % solids of 15%. The average field beach slope of 0.014% is similar to that obtained in the laboratory for an initial % solids of 15% (similar to the field initial % solids), and the non-dimensional beach profile is similar to that for the field profile.

For unflooded, constricted beaching the average beach slope is significantly greater at high initial % solids, and only slightly greater at intermediate initial % solids. Flooding generally has little effect on the average beach slope for unconstricted beaching.

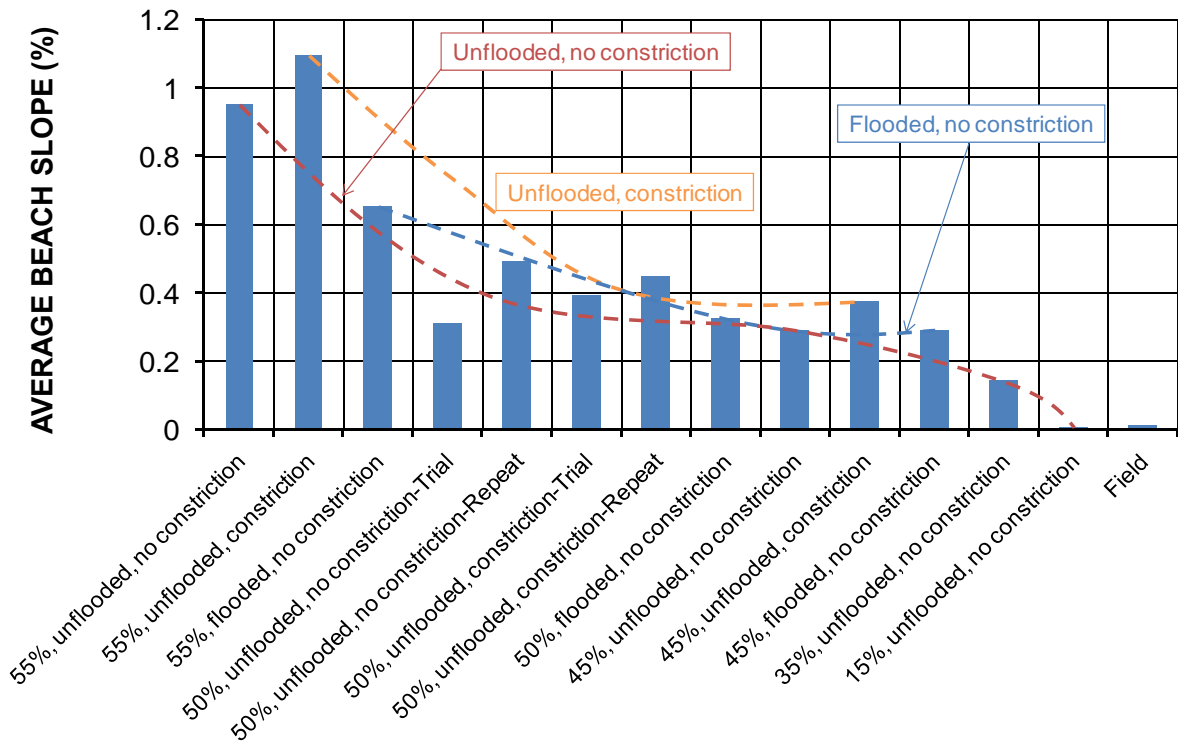


Figure B-52 **Comparison of average beach slopes of laboratory and field beach profiles for Swanbank fly ash**

Figure B-53 shows the field beach profile for Swanbank fly ash which is in reasonable agreement with the corresponding profile obtained in the laboratory (**Appendix C**).

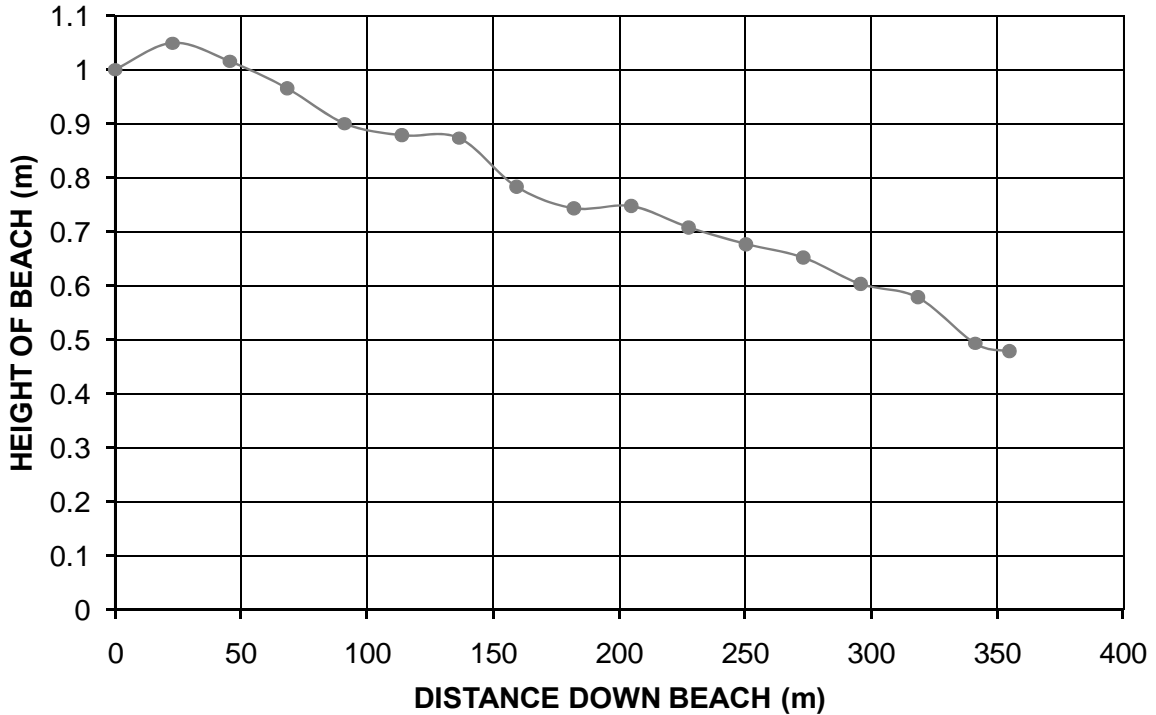


Figure B-53 **Field beach profile for sub-aerial, unconstricted deposition of Swanbank fly ash**

The open-ended laboratory flume testing has shown that the upper limit for the Swanbank fly ash to flow (without the application of an extra head of slurry) is about 55% solids, which may reduce to 50% solids at field scale under similar conditions. Testing at an initial % solids of 55% results in an average unconstricted laboratory beach slope of about 1% if unflooded, and about 0.6% if flooded. Lower initial % solids result in flatter beaches. The field fly ash beach (unflooded and unconstricted, but at much lower % solids) has an average slope of only 0.014%. Since higher initial % solids result in steeper beach profiles, underground voids would not fill as well, although the solids would settle less, leading to less residual void space. The poor filling of underground voids could be overcome to some extent by progressive filling, provided that the void slopes away from the delivery point.

At 50 to 60% solids, Swanbank fly ash deposited under an applied head of slurry will fill the void created by a closed-ended constriction, representing a blocked-off bord and pillar roadway and openings with fly ash slurry delivered via a borehole. It appears that complete filling of such a roadway is more effective for fly ash slurry at an initial % solids of 50% rather than 60%, since at the lower initial % solids the fly ash more readily fluidises, which facilitates filling of the void left as the fly ash solids settle, and a gain in dry density from about 1 g/cm³ with no applied head to about

1.5 g/cm³ with an applied head of slurry. Again, the void should slope away from the delivery point to facilitate filling through fluidisation.

B.19 CSIRO fly ash flow and backfill deposition tests

A series of slurry flow tests were conducted in a rectangular glass tank of 1.2m length, 400mm width and 600mm height. The grout flow rate was in the range of 10-30 litres per hour from a 12mm hose under simple gravity pressure for discharging into the tank, as shown schematically in Figure B-54. The tank is generally setup with an angle α with the horizon, representing coal seam floor dip angle. The angle in which the fly ash is deposited or piled up is shown by the angle β , which can be calculated by measuring the height of triangle, h , divided by the slurry deposition length, L ; i.e. $\tan(\beta) = h/L$. Typical glass tank tests are shown in the photos of Figure B-55 with typical measurements of these angles at different time of backfill in Table B-7 to Table B-10.

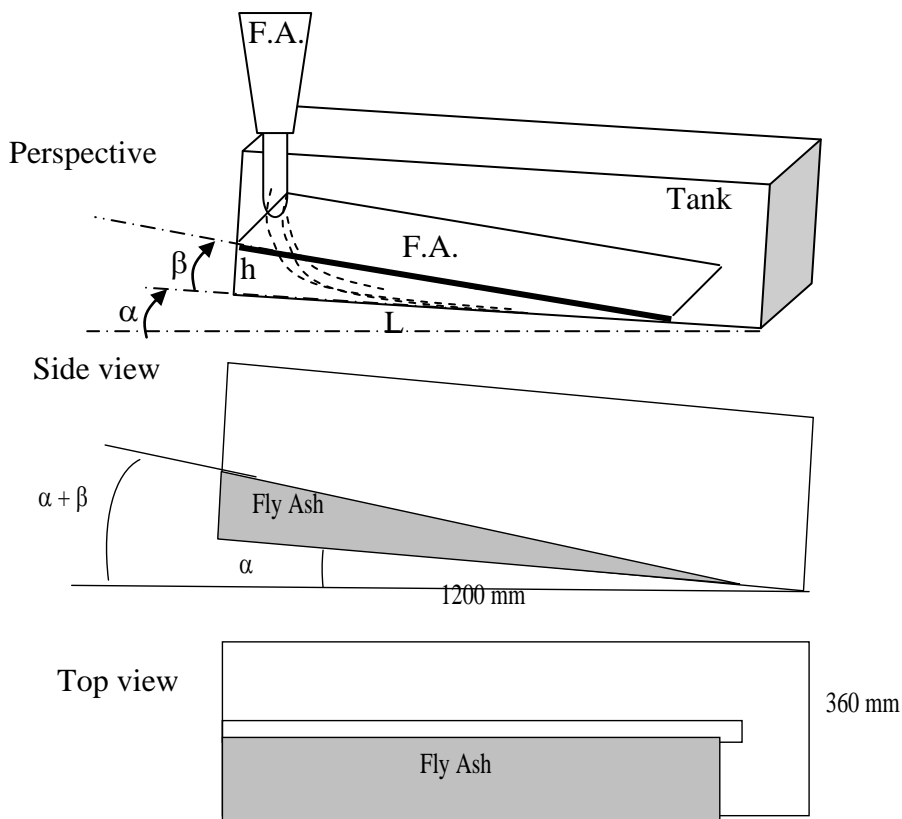


Figure B-54 Schematic of fly ash backfill angle once flown into tilted CSIRO glass tank

Figure B-55 shows photos of fly ash slurry backfilling into a glass tank under dry and submerged conditions on horizontal ground in a corrugated roof void situation. Figure B-56 shows backfilling of roof voids after formwork removal. Figure B-57 and Figure B-58 show similar corrugated roof voids backfilling test under submerged and dry conditions and the backfill condition and formwork removal after 40 hours of slurry consolidation. A surcharge load has been added to check the wall vertical stability in Figure B-58. Figure B-59 show similar results for a backfilling test of simulated roadways but under up-dip conditions.

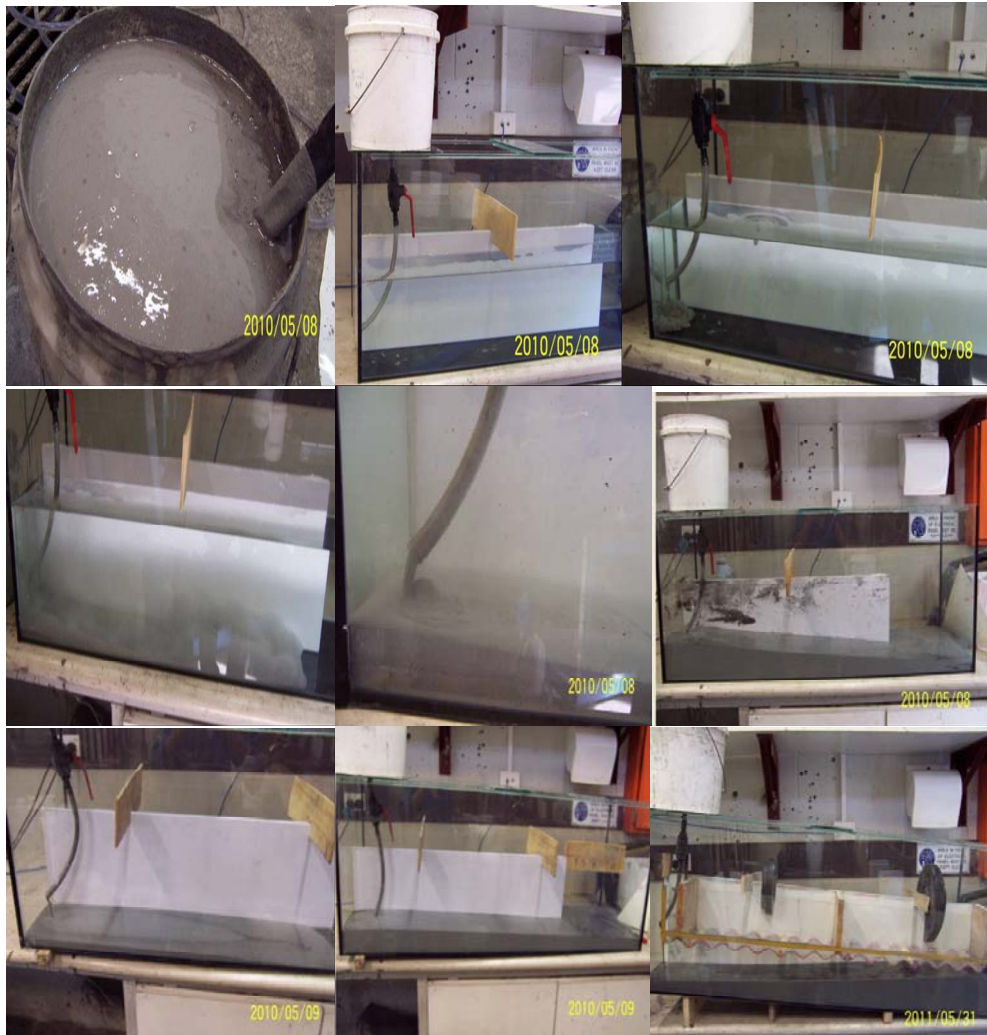


Figure B-55 Photos of fly ash slurry backfilling into a glass tank in different tests. Top row shows the fly ash slurry and the tank. Middle row photos show fly ash flow in submerged condition on horizontal ground. Also shown in the bottom right figure is a transparent colour bond roof cover simulating uneven mining roof conditions.

Table B-7 Glass tank deposition angles (air)

grout injection, not submerged, tilt angle = 0 degree

Hight	Length	ratio	absolute angle
26	390	0.066667	3.816009
41	740	0.055405	3.172862
46	940	0.048936	2.803022
53	1130	0.046903	2.686718
75	1200	0.0625	3.578148

Table B-8 Glass tank deposition angles (submerged)

Grout injection, submerged, tilt angle = 0 degree, density 1.336kg/l, solid content = 56.4%, flow rate=0.63l/min,

Hight	length	ratio	degree
45	420	0.107143	6.118605

70	500	0.14	7.973653
98	1130	0.086726	4.959127
102	1200	0.085	4.860927
76	1200	0.063333	3.625731

Table B-9 Glass tank deposition angles (submerged)

Grout injection, submerged, tilt angle = 1.6 degree, density 1.336kg/l, solid content = 56.4%.

Hight	Length	ratio	absolute angle ($\alpha+\beta$)
24	300	0.08	4.576241
40	470	0.085106	4.866982
49	820	0.059756	3.42144
78	1200	0.065	3.72088
83	1200	0.069167	3.958663

Table B-10 Glass tank deposition angles (air)

Grout injection, not submerged, tilt angle = 1.6 degree

Hight	length	ratio	degree
48	1000	0.048	2.749482
53	1150	0.046087	2.640059
57	1200	0.0475	2.720885
51	1200	0.0425	2.43484
66	1200	0.055	3.149693

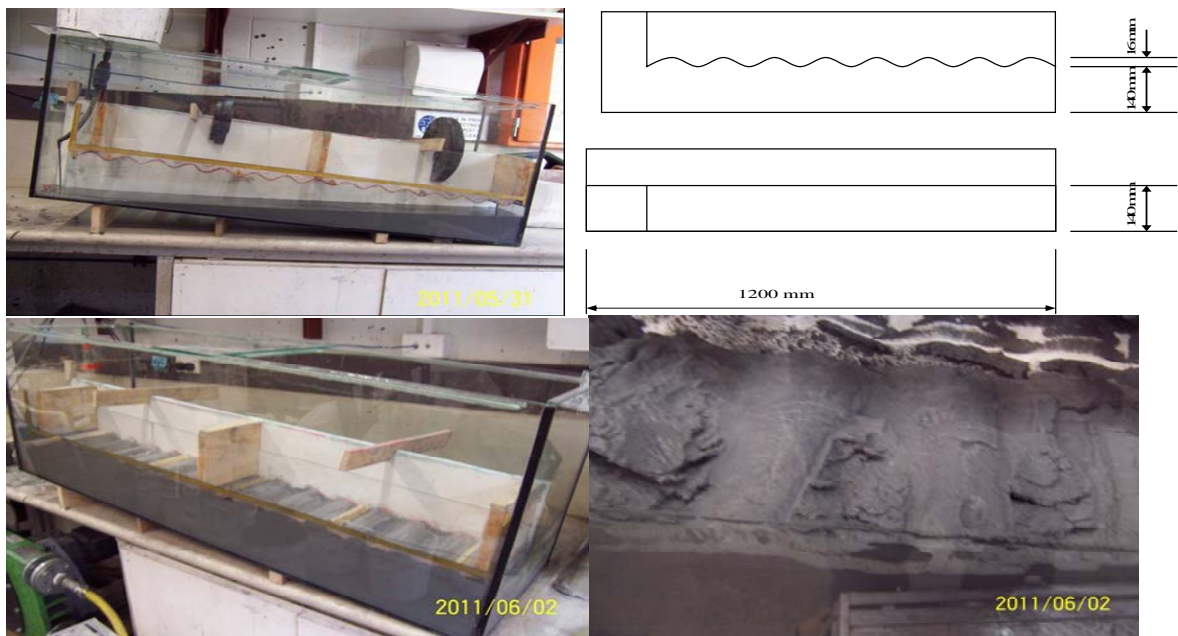


Figure B-56 Backfilling test of roadways with corrugated roofs in dry condition – Removal of corrugated roof form after 40 disclosed the backfill penetration into such voids



Figure B-57 Backfilling test of roadways with corrugated roofs under submerged condition – Drainage and removal of water and corrugated roof form after 40 hours resulted in a consolidated backfill and slurry penetration into roof



Figure B-58 Backfilling test of roadways with corrugated roofs – Under dry conditions still stable walls can remain even after formwork removal. A surcharge load has been added to check the wall vertical stability (middle photo)



Figure B-59 Backfilling test of roadways under up dip conditions

B.20 Strength tests on cohesive samples (T14 and T15)

Unconfined non-cohesive fly ash has zero cohesion, zero tensile and zero unconfined compressive strength. However, when confined, it gains its confined compressive strength through its frictional resistance, which is a direct increasing function of its friction angle. Under a fully, confined condition, a sample of consolidated fly ash having a friction angle of 40 degrees, can take a shear load up to 83% of its applied axial compressive load, or an axial stress 3.3 times the confining pressure.

Unconfined, hardened, cohesive fly ash mix has 0.1-0.3 MPa cohesion, 0.1 - 0.2 Brazilian tensile strength, and 1 – 1.5 MPa unconfined compressive strength (UCS). However, when confined, its compressive strength increases through its frictional resistance, which is a direct increasing function of its friction angle. Under a fully, confined condition, a solid sample of cohesive mix should take shear loads up to 83% of the applied axial compressive load plus the original 0.1 to 0.3 MPa cohesion, or an axial stress 3.3 times the confining pressure plus the 1 – 1.5 MPa unconfined compressive strength (UCS).

Figure B-60 shows photos of small diameter samples used for strength tests. In these experiments, the two weeks UCS strength of T14 and T15 were in the range of 1 to 1.5 MPa, while the values of Brazilian tensile strength (BTS) were in the range of 0.1 to 0.2 MPa.



Figure B-60 Samples of cohesive fly ash used in compressive UCS and tensile BTS strength tests

B.21 Chemical tests

A series of chemical tests on underground water and gas were organised during the drilling operations. The new results are consistent from the previous set of data.

Neither of the mine water samples are suitable for environmental purposes. The overall properties of the water indicate that the quality of water is worst at the borehole CP C005, medium in CP C009 and best in CP C004.

Referring to the high levels of Electrical conductivity (EC) and chlorine content of the water samples, the water can be classified as brackish. As an index for EC, we can expect freshwater to have 50-1000 microS/cm, industrial water would be 10,000 microS/cm and seawater about 50,000 microS/cm. At the given pH of about 7.5, total alkalinity and especially bicarbonate alkalinity of over 500mg/L is very high. We would expect this from groundwater from limestone rock or basalt landscapes. Next cause of concern would be very high level of sodium. Combined with this is greater

barium and boron (>1mg/L) concentrations. It would also be worthwhile to monitor the oxidation reduction potential (ORP) and nitrate in these waters.

Such water would require moderate treatment operation to make it environmentally acceptable. Intention to add flyash (which itself is alkaline) could offer limited assistance in terms of pollutant removal (metal adsorption). However, flyash itself would contain certain amount of toxic elements and so care must be taken in such application. The presence of sodium will also hinder removal process. Suitable treatment procedure for such waters must be selected. More verification tests of mixing of surface water with groundwater are needed. Preliminary chemical analysis of tested water indicates towards negative.

B.22 Conclusions

From several laboratory studies and economical considerations, CSIRO recommendation for backfilling a confined mine void structure (with no hazards from flooding and water or high seepage flow, which can cause liquefaction of fly ash particles) is a two phase ***non-cohesive slurry mixture*** of fly ash and water mix using 50 to 60 % solids weight concentration; i.e. 50%-60% of fly ash solid particles in the mix. The injected non-cohesive fly ash will consolidate with time and becomes stiffer and harder by gradual drainage and dissipation of its excess water accumulated in its pores. During the consolidation process, the friction angle of the confined consolidated fly ash will increase to near 40 degrees and its permeability will reduce to near 1 micron per second. A confined, consolidated fly ash will not only provide sufficient confinement to the previously failed pillars and prevent them from further failure and collapse, but also will minimise any further ground subsidence by filling more than 90% of the voids left in the current underground. However, in the lack of a closed or confined void structure, sealed barrier walls need to be built by the much more expensive cohesive slurry, in which cement and crush dust has to be added to the mix as well. These are similar to the cohesive mixes of T14 and T15 mixes, also considered in this study, which were used in the Ipswich motorway underground backfilling project.

B.23 Appendix References

Alehossein, H, A triangular caving subsidence model. Applied Earth Science: IMM Transactions Section B. 118 (1), pp. 1-4. 590, 2009

Alehossein, H., 2009. Viscous, cohesive, non-Newtonian, depositing, radial slurry flow. Int. J. Miner. Process. 93, 11–19.

Alehossein, H., Shen, B., Qin, Z. 2010. Viscous, cohesive, non-Newtonian, depositing, pipe slurry flow. Journal of Fluid Mechanics (under review).

Guo, H., Shen B. and Pala J. 2005a. Overburden grout injection project for targeted subsidence reduction at BHP Billiton Illawarra Coal Operations – A desk top study. CSIRO Exploration and Mining Report P2005/334

Guo, H., Shen, B and Chen, S. 2007. Investigation of overburden movement and a grout injection trial for mine subsidence control. In Eberhardt, Stead & Morrison (eds): Rock Mechanics: Meeting Society's Challenges and Demands. Proceedings of 1st Canada-U.S. Symposium, May 2007, Vancouver . Vol. 2, pp.1559-1566.

Guo, H., Shen, B., Chen, S. and Poole G. 2005b. Feasibility study of subsidence control using overburden grout injection technology - ACARP Project C12019 Final Report; CSIRO Exploration and Mining Report P2005/335

Robinsky, E.I. (1999). Thickened tailings disposal in the mining industry. *Robinsky Associates*, Toronto, 209 p (UQ Report to CSIRO, 2010).

Shen B., Alehossein H., Pousen B. and Waddington A, 2010. ACARP Project C16023 Final Report – Subsidence control using coal washery waste. CSIRO Earth Science and Resource Engineering Report P2010/65.

Shen, B. and Guo, H. 2007. A laboratory study of grout flow and settlement in open fractures. In Eberhardt, Stead & Morrison (eds): Rock Mechanics: Meeting Society's Challenges and Demands. Proceedings of 1st Canada-U.S. Symposium, May 2007, Vancouver . Vol. 1, pp.747-754.

Shen, B., Alehossein, H., Guo, H., Pala J., Armstrong, M., Poole, G., and Riley P. 2006. Overburden Grout Injection Project for Targeted Subsidence Reduction at BHP Billiton Illawarra Coal Operations - Phase 2 Site Investigation and System Design CSIRO Exploration and Mining Report P2006/118